ISTANBUL TECHNICAL UNIVERSITY ★ GRADUATE SCHOOL OF SCIENCE ENGINEERING AND TECHNOLOGY

PHYSIOLOGICAL ANALYSIS OF COBALT-RESISTANT *Rhodobacter sphaeroides* OBTAINED BY EVOLUTIONARY ENGINEERING

M.Sc. THESIS

Güneş ATAY

Department of Molecular Biology-Genetics & Biotechnology

Molecular Biology-Genetics & Biotechnology Programme

JANUARY 2015

ISTANBUL TECHNICAL UNIVERSITY ★ GRADUATE SCHOOL OF SCIENCE ENGINEERING AND TECHNOLOGY

PHYSIOLOGICAL ANALYSIS OF COBALT-RESISTANT *Rhodobacter sphaeroides* OBTAINED BY EVOLUTIONARY ENGINEERING

M.Sc. THESIS

Güneş ATAY
(521121139)

Department of Molecular Biology-Genetics & Biotechnology

Molecular Biology Genetics and Biotechnology Programme

Thesis Advisor: Prof. Dr. Zeynep Petek Çakar

23 JANUARY 2015

İSTANBUL TEKNİK ÜNİVERSİTESİ ★ FEN BİLİMLERİ ENSTİTÜSÜ

EVRİMSEL MÜHENDİSLİK YÖNTEMİ İLE ELDE EDİLEN KOBALTA DİRENÇLİ *Rhodobacter sphaeroides* BAKTERİSİNİN FİZYOLOJİK ANALİZİ

YÜKSEK LİSANS TEZİ

Güneş ATAY
(521121139)

Moleküler Biyoloji-Genetik ve Biyoteknoloji Ana Bilim Dalı

Moleküler Biyoloji Genetik ve Biyoteknoloji Programı

Tez Danışmanı: Prof. Dr. Zeynep Petek ÇAKAR

23 OCAK 2015

Güneş ATAY, a **M.Sc.** student of ITU **Institute of Science and Technology,** 521121139, successfully defended the **thesis/dissertation** entitled **" Physiological Analysis of Cobalt-Resistant *Rhodobacter sphaeroides* Obtained by Evolutionary Engineering",** which she prepared after fulfilling the requirements specified in the associated legislations, before the jury whose signatures are below.

Thesis Advisor : **Prof. Dr. Zeynep Petek ÇAKAR** .....
Istanbul Technical University

Jury Members : **Prof. Dr. Zeynep Petek ÇAKAR** .....
Istanbul Technical University

Assoc. Prof. Dr. Fatma Neşe KÖK .....
Istanbul Technical University

Prof. Dr. Kutlu ÜLGEN .....
Boğaziçi University

Date of Submission : 15 December 2014
Date of Defense : 23 January 2015

To my family,

FOREWORD

I would like to thank my supervisor Prof. Dr. Zeynep Petek ÇAKAR for not only giving me the opportunity to work in Yeast Research Group, but also for her guidance. I am thankful to her encouragements and critics throughout this study.

I would like to thank Dr. Massimo TROTTA (University of Bari, Italy) for providing the *Rhodobacter sphaeroides* reference strain.

I would like to express my gratitude to Ceren ALKIM for sharing her knowledge and experience with me. I would like to thank Burcu TURANLI YILDIZ for answering my every question and for her support.

I am grateful to Hanay KAMER for her contribution on this study. I also thank Cihan Erdinç GÜLSEV for DNA sequencing analysis.

I would like to thank to the members of the Yeast Research Group with my special thanks to Berrak Gülçin BALABAN for her support and encouragements. I also thank Mevlüt ARSLAN, Naciye DURMUŞ İŞLEYEN, Filiz DEMİR and Yusuf SÜRMELİ. It was a great pleasure to work in the same laboratory.

Finally, I would like to thank my family for their support during this study.

January 2015

Güneş ATAY
(Biochemist)

TABLE OF CONTENTS

Page

ABBREVIATIONS

AVG **:** Average
CDW **:** Cell dry weight
M27 **:** Medium 27
h **:** Hour
µg **:** Microgram
µL **:** Microliter
mL **:** Milliliter
mM **:** Micromolar
MPN **:** Most probable number
PHB **:** Polyhydroxybutyrate
RS **:** Reference strain

LIST OF TABLES

Page

LIST OF FIGURES

Page

PHYSIOLOGICAL ANALYSIS OF COBALT-RESISTANT *Rhodobacter sphaeroides* OBTAINED BY EVOLUTIONARY ENGINEERING

SUMMARY

Rhodobacter sphaeroides is a gram negative purple non-sulfur α-proteobacterium found in soil, mud, deep lakes and stagnate waters. It has metabolic diversity, as it is able to grow under photoheterotrophic, photoautotrophic, chemoheterotrophic and chemoautotrophic conditions. It can alter its metabolism according to the changing environmental conditions and nutrient deficiency. Due to its metabolic versality, sequenced genome and no requirement of unusual conditions for growth, it is commonly used in biotechnological applications. In response to harmful effects of plastic wastes on the environment, there has been great interest in the production and usage of biodegradable plastic materials. *R. sphaeroides* is capable of synthesizing and storing biodegradable and biocompatibile polyester polyhydroxybutyrate (PHB) as insoluble inclusion bodies in cytoplasm. Some of the other byproducts of *R.sphaeroides* in industry are 5-aminolevulinic acid, Coenzyme Q10, carotenoids, vitamin B12, indole terpenoids and plant hormones. Large scale H_2 production in a photobioreactor, ZnS nanoparticle production for medical purposes and potential usage in bioremediation are also reasons for biotechnological importance of *R. sphaeroides*.

There are different response mechanisms of microorganisms to metal exposure, such as intracellular and extracellular sequestration, metal exclusion by permeability barrier, active transport of the metal and enzymatic detoxification. *R. sphaeroides* has the ability to survive under changing stress conditions by modifying its cellular and genetic composition. For instance, oxidative stress causes down-regulation of the carotenoid genes, while heavy metal stress increases membrane integrity.

In another study, cobalt-resistant *R. sphaeroides* population was obtained under gradually increasing cobalt stress conditions, using evolutionary engineering approach. The last (64^{th}) population was able to survive 15 mM cobalt stress, with a survival rate of 21%. The last population was spread onto solid Luria Broth plate and eight colonies (called G1-G8) were selected from there. In this study, the selected individual mutants were phenotypically characterized. At the beginning, screening test was performed by optical density measurements at 535 nm and viable cell counting method, to determine the stress resistence of the reference strain, then spot assay and Most Probable Number tests were done to determine cobalt resistance of the mutant colonies. After that, cross-resistance tests were performed to determine potential resistance of the colonies against different stress types. Various concentrations of nickel (II) chloride (2mM, 2.2 mM, 2.4 mM), ethanol (8% v/v), sodium chloride (0.5 M), aluminum chloride (5 mM), copper (II) chloride (0.5 mM), magnesium chloride (500 mM, 750 mM, 1M), hydrogen peroxide (1 mM, 2 mM), iron (II) chloride (4 mM, 5 mM), manganese (II) chloride (10 mM), boric acid (30 mM, 50 mM), caffeine (20 mM), ammonium iron(II) sulfate (5 mM),

zinc chloride (1 mM) were used. As a result of the cross-resistance tests, the colonies G4, G6 and G7 were selected for further experiments. Besides, G7 showed significantly higher cross-resistance against nickel, boric acid, caffeine and magnesium stresses.

The genetic stability analyses of those three mutant colonies were then carried out. The main aim of these tests was to measure the persistence of $CoCl_2$ resistance of G4, G6 and G7 in the absence of $CoCl_2$ stress, and to find out if their resistance is permanent or not. It was shown that the selected mutants had genetically stable cobalt resistance characteristics. Finally, growth curves of the reference *R. sphaeroides* strain and the selected G7 were obtained and compared to each other.

EVRİMSEL MÜHENDİSLİK YÖNTEMİ İLE ELDE EDİLEN KOBALTA DİRENÇLİ *Rhodobacter sphaeroides* BAKTERİSİNİN FİZYOLOJİK ANALİZİ

ÖZET

Rhodobacter sphaeroides kükürtsüz, mor, α-proteobakteri grubuna ait gram negatif bir bakteridir. Metabolik olarak çok çeşitli reaksiyonlar gerçekleştirebilen *R. sphaeroides*; fotoheterotrofik, fotootrofik, kemoheterotrofik koşullarda yaşamını sürdürebilir; çamur, toprak, durgun sular, derin göller gibi çeşitli ortamlarda bulunabilir. Bulunduğu ortamdaki karbon kaynaklarının ve diğer besiyeri bileşenlerinin eksikliğinde, çeşitli çevresel stres koşulları altında gerekli metabolik yolakları aktive ederek canlılığını sürdürür. Sekanslanmış genomu, kompleks koşullara gereksinimi olmadan basit ortamlarda üreyebilme yeteneği ve en önemlisi sahip olduğu çok yönlü metabolizma, bu bakterinin biyoteknolojik açıdan oldukça ilgi çekici olmasının başlıca nedenlerindendir.

Günümüzde oldukça geniş kullanım alanına sahip plastikler, çoğunlukla petrolden elde edilir ve üretilen bu sentetik polimerler doğada uzun yıllar kalıntı bırakarak toksik madde birikimine neden olur. Bu yüzden sentetik polimerlere alternatif olarak günümüzde doğada çözünebilen, biyouyumlu, yenilenebilir biyoplastiklerin üretimi ve kullanımı önem kazanmaya başlamıştır. *R. sphaeroides*, biyolojik olarak parçalanabilen bir poliester olan polihidroksibütiratı (PHB) sentezleyebilme yeteneğine sahiptir. Hücre içi depo granülü olarak sentezlenen ve depolanan PHB'nin, *R. sphaeroides* tarafından büyük ölçekte üretilerek endüstriyel uygulamalarda kullanım potansiyeli vardır. PHB'nin yanısıra *R. sphaeroides* endüstriyel ve medikal öneme sahip bir çok ürün sentezleyebilir. Bunlara örnek; kalp hastalıklarının tedavisinde ve kozmetik endüstrisinde sıkça kullanılan koenzim Q10, kanserli hücrelerin takibini sağlayan 5-aminolevulinik asit, çeşitli ilaçların etken maddesi ya da besin katkı maddesi olarak kullanılabilen B12 vitamini, hayvan besin katkısı ya da gıda renklendirici olarak kullanılan karotenoidler, organik kirleticilerin ortamdan uzaklaştırılmasını sağlayan çinko sülfit nanopartiküller ve bitki hormonları verilebilir. Ayrıca, organik sübsratları kullanarak temiz ve yenilenebilir bir enerji kaynağı olan biyohidrojenin üretimini sağlayabilmektedir. Sentezleyebildiği yan ürünlere ek olarak, toksik metal birikimi olan çevrelerde biyoremediasyonu gerçekleştirebilmesi, *R. sphaeroides*'in biyoteknolojik önemini oldukça arttırmaktadır.

Mikroorganizmaların metal stresi altındayken canlı kalmak için aktive ettiği enzimatik detoksifikasyon, hücre dışında metalin tutulması ya da daha az toksik forma çevrilmesi, hücre içinde metalin proteinlere bağlanarak tutulması veya hücre dışına aktif metal taşınımı gibi çeşitli direnç mekanizmaları vardır. *R. sphaeroides*, metabolizmasındaki çeşitlilik sayesinde gerektiğinde uygun metabolik yolakları aktive edip, hücresel ve genetik yapısında değişiklikler geçirerek çok farklı stres koşullarına direç sağlayabilmektedir. Bu değişikliklere örnek, ağır metallere maruz

kalan *R. sphaeroides* hücrelerinin membran bütünlüğünün arttırılması ya da oksidatif stres altındaki hücrelerde karotenoid sentezinden sorumlu genlerin regülasyonunun azalması verilebilir.

Kobalt, organizmaların metabolik aktiviteleri gerçekleştirebilmeleri ve yapısal organizasyonu sağlayabilmeleri için gerekli olan, eksikliğinde ya da fazlalığında toksik etkilere yol açan esansiyel bir iz elementtir. Kobalt, B12 vitamininin yapısında bulunur, ayrıca transkarboksilaz ve aminido aspartaz gibi bazı enzimlerinin çalışabilmesi için gereklidir. Fakat yüksek konsantrasyonlarda hücresel solunumu ve sitrik asit çevriminde görevli enzimleri inhibe ederek hücreler için toksik etki yapar. Bakterilerde yüksek kobalt konsantrasyonu oksidatif stresi arttırarak ya da iyon geçişinin modifikasyonuna neden olarak bazı makromoleküler özelliklerin düzeltilmesini engeller. *R. sphaeroides* çok yönlü metabolizması sayesinde yüksek kobalt konsantrasyonunda kobaltı hücre yüzeyinde biriktirerek yaşamını sürdürebilir.

Bu tez çalışmasında kullanılan *R. sphaeroides* bakterisi, evrimsel mühendislik çalışmasıyla elde edilmiş olup, kobalt konsantrasyonu aşama aşama arttırılarak kobalta dirençli hale getirilmiştir. Başlangıçta uygulanan $CoCl_2$ konsantrasyonu 0.1 mM iken, 64. popülasyonda 15 mM stres uygulanmıştır. Bu sayede referans suşun hayatta kalamadığı kobalt konsantrasyonunda yaşayabilen bir popülasyon elde edilmiştir. 64. popülasyonun hayatta kalma yüzdesi % 21 gibi yüksek bir değer olmasına rağmen, artan konsantrasyonlarda kobaltın çökerek birikim yapması nedeniyle spektrofotometrik ölçüm yapılması zorlaşmıştır. Bu yüzden bu popülasyon son popülasyon olmuştur ve seyreltilip katı LB besiyerine ekilerek bu besiyerinden 8 koloni seçilmiştir. Kırmızı rengin farklı tonlarına sahip koloniler; G1, G2, G3, G4, G5, G6, G7 ve G8 olarak isimlendirilmiş ve çeşitli metodlarla bu mutant bireylerin fizyolojik analizleri gerçekleştirilmiştir.

Referans suş için tarama testi, referans suşun hayatta kalabildiği en yüksek kobalt seviyesini belirleyebilmek için, optik yoğunluğun 535 nanometrede ölçümü ve ölçümler sırasında hücrelerin katı besiyerine üçlü tekrarlar halinde ekilmesi ile hücre sayımı yapılarak gerçekleştirilmiştir. Yüksek kobalt konsantrasyonunda çalışılırken kobalt çöktüğünden dolayı, optik yoğunluk ölçümleri çok doğru sonuç vermese de, hücrelerin katı besiyerinden ekimleri sonucunda alınan veriler grafiğe dökülerek 5 mM kobalt konsantrasyonunda hücrelerin hayatta kalma oranının en yüksek seviyede olduğu saptanmıştır. Ayrıca 12.5 mM $CoCl_2$ konsantrasyonunda bile çok düşük olsa da yaşayabilen hücrelerin varlığı tespit edilmiştir.

Seçilen sekiz mutant bireyin kobalt stresine karşı direncini ölçmek için Most Probable Number (MPN) ve damlatma (spot) testleri gerçekleştirilmiştir. *R. sphaeroides* bakterisi çok kolay kontaminasyona uğradığından, G2'nin katı besiyerine ekim sonucuna göre kontaminasyona uğramış olabileceği şüphesinden dolayı G2 sonraki deneylerde yer almamıştır. MPN sonuçlarına göre mutant bireylerin en iyi ürediği kobalt konsantrasyonu 4 mM'dır. Damlatma testine göre, 1 mM $CoCl_2$ konsantrasyonu içeren katı LB besiyerlerinde tüm mutant bireyler ve referans suşu aynı oranda büyüyebilmekte iken, 2 mM'dan itibaren referans suş kobalta direnç gösterememeye başlamıştır ve 3.5 mM ile üzerindeki konsantrasyonlarda hiç üreyememiştir.

Çapraz direnç testinde, kobalta direnç geliştirmiş olan bireylerin başka hangi stres türlerine karşı direnç kazanmış olabilecekleri incelenerek karşılaştırma yapılmıştır. Bunun için; nikel (II) klorür (2 mM, 2.2 mM, 2.4 mM), etanol (8% v/v), sodyum klorür (0.5 M), alüminyum klorür (5 mM), bakır (II) klorür (0.5 mM), magnezyum

klorür (500 mM, 750 mM, 1M), hidrojen peroksit (1 mM, 2 mM), demir (II) klörür (4 mM, 5 mM), mangan (II) klorür (10 mM), borik asit (30 mM, 50 mM), kafein (20 mM), amonyum demir (II) sülfat (5 mM) ve çinko klorür (1 mM) kullanılmıştır. Testin sonucuna göre, direnç dereceleri diğer kolonilere göre daha yüksek olan G4, G6 ve G7 bireyleri, sonraki deneylerde incelenmek üzere seçilmiştir. Bunun yanı sıra, G7'nin nikel, borik asit, kafein ve magnezyum stresine karşı gösterdiği yüksek direnç kapasitesi, çapraz direnç testinin en önemli bulgularındandır.

Genetik kararlılık testinde; G4, G6 ve G7'nin kobalta karşı kazandığı direncin geçici olup olmadığı MPN yöntemiyle araştırılmıştır. On gün boyunca hücrelerin strese karşı direnç düzeyleri MPN ile incelenmiştir, fakat *R. sphaeroides* için bu yöntem çok güvenilir olmadığından, deneyin sonuçlarına göre bireyler gün geçtikçe kobalta karşı dirençlerini kaybetmişlerdir. Sonuçlar tatmin edici olmadığından, stabilite düzeylerinin incelenmesi amacıyla koloniler 5 gün boyunca 4 mM $CoCl_2$ içeren sıvı ortamda büyütülmüş, ardından 5 gün boyunca taze M27 sıvı besiyerine aktarılarak her günün sonunda katı LB besiyerine damlatma testi uygulanmıştır. İlk gün ve son günün katı besiyerlerine bakıldığında, artan kobalt konsantrasyonlarında bile ilk ve son gün üreyebilen kolonilerin dilüsyon dereceleri aynıdır. Damlatma tekniğinde alınan gözle görünen sonuçlar güvenilir olduğundan, bu test bitiminde kolonilerin kobalt stresine karşı geliştirdiği direncin kalıcı bir direnç olduğu sonucuna varılmıştır.

Son olarak, referans suşun ve G7'nin 4 mM $CoCl_2$ varlığında ve kobaltsız ortamlarda optik yoğunluklarının 535 nanometre dalga boyunda belli aralıklarla ölçümü ve hücre kuru ağırlıklarının tartımı sonucu büyüme eğrileri çizilerek birbiriyle karşılaştırılmıştır.

1. INTRODUCTION

1.1 General Information About *Rhodobacter sphaeroides*

1.1.1 General properties

Rhodobacter sphaeroides is a purple, gram negative bacterium. Purple bacteria are able to perform photosynthesis and are divided into two groups: purple sulfur bacteria and purple non-sulfur bacteria. Different from other purple non-sulfur bacteria, *R. sphaeroides* is capable of growing in the presence and absence of light.

R. sphaeroides is a member of alpha subgroup of proteobacteria (Table 1.1). Proteobacteria, the most diverse bacterial phyla, are divided into six sections according to the ribosomal RNA sequences. Like all proteobacteria species, *R. sphaeroides* contains lipopolysaccharides on the outer membrane.

Table 1.1: Taxonomic classification of *R. sphaeroides.*

Kingdom	Bacteria
Phylum	Proteobacteria
Class	Alphaproteobacteria
Order	Rhodobacterales
Family	Rhodobacteraceae
Genus	*Rhodobacter*
Species	*Rhodobacter sphaeroides*

1.1.2 Flagellum

R. sphaeroides has the ability to perform taxis, propelled by a single flagellum (Figure 1.1). It can swim in response to different stimulants including pH, light intensity, oxygen and various concentrations of organic chemicals. Direction changes

by switching the flagellar rotation. Bacterial flagellum is composed of three parts: a flagellar filament, hook and a motor. The filament is joint to the motor with the hook. The flagellar motor rotates the cell and changes the orientation in one direction, and stops randomly (Berry and Armitage, 2000). Energy source of the flagellum in *R. sphaeroides* is the proton motive force. Flagellum is an important structure because of its roles in biofilm production and quorum-sensing.

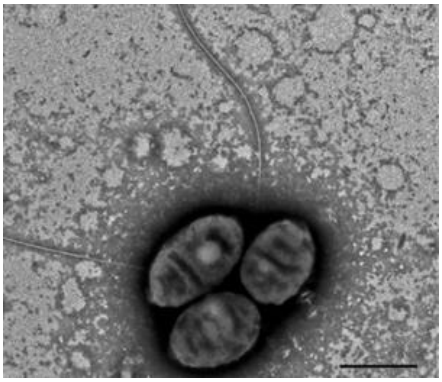

Figure 1.1 Electron micrograph of the flagellar filaments of wild type *Rhodobacter sphaeroides.* Bar = 1 μm. (Fabela et al., 2013).

1.1.3 Growth

R. sphaeroides is found in various habitats like freshwater, soil, mud, sludge and in anoxic zones of water where dissolved oxygen is depleted. It is referred as facultative anaerob due to its ability to live in both aerobic and anaerobic environments.

1.2 Genome Structure

The *R. sphaeroides* genome is 460 million bp long and contains 4370 predicted genes. The genome of *R. sphaeroides* was sequenced in 2001 and according to this sequence analysis, it is widely accepted that this photosynthetic bacterium consists of two circular chromosomes (I and II), one nearly 3 Mbp long and one nearly 0.9 Mbp long, and five endogenous plasmids (A, B, C, D, E). Size of chromosome I (CI) is similar in many *R. sphaeroides* strains, while size of chromosome II (CII) changes. Optical mapping by Choudhary et al. revealed that CII of *R. sphaeroides* strains consisted of 0.94, 1.23 and 0.91 Mb of DNA (Choudhary et al., 2007).

It was found that a wide variety of housekeeping genes and essential genes are located on CI and CII. Gene duplication gives rise to metabolic capabilities, in addition, it contributes to biodiversity. Duplicated sequences represent approximately

2.7 % of the chromosomal DNA of the *R. sphaeroides*. CI and CII contains 3106 and 874 open reading frames, respectively (Choudhary et al., 2004).

1.3 Metabolism of *R. sphaeroides*

R. sphaeroides has various metabolic capabilities; it is capable of doing aerobic, anaerobic respiration, fermentation and anaerobic photosynthesis (Figure 1.2). Imam et al. (2011) have identified metabolic capabilities of *R. sphaeroides* by a genome-scale metabolic network model. According to their study, *R. sphaeroides* consists of 1095 genes, 796 metabolites and 1158 reactions. Additionally, reactions related to transport metabolism have the highest proportion of all reactions (Figure 1.3) (Imam et al., 2011).

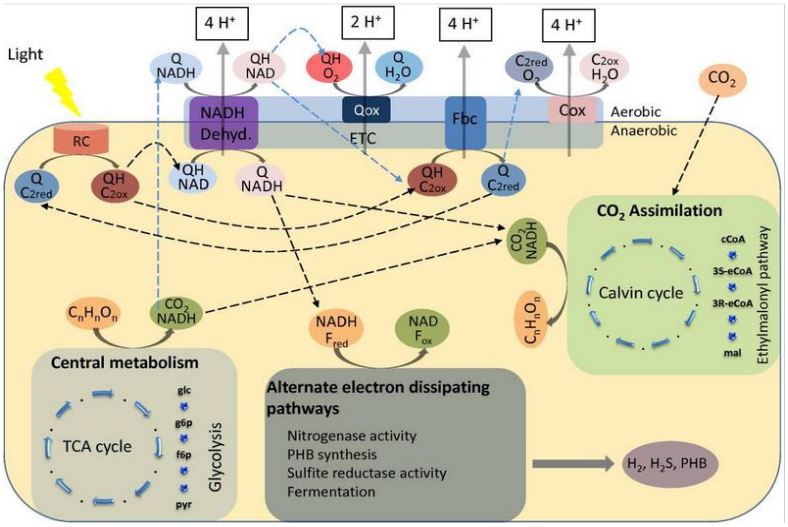

Figure 1.2: Metabolic pathways of *R. sphaeroides*. Light-blue dashed arrows represent electrons flow in aerobic growth and black dashed arrows represent flow of electrons in photosynthetic growth. Electrons flow through electron transport chain (ETC) during anaerobic growth, in addition, protons are pumped into the periplasm. However, protons are pumped across the cytoplasmic membrane during aerobic growth. Excess reducing power is utilized by a wide variety of pathways such as sulfite reductase reaction, which results in H_2S production, ethylmalonyl pathway, PHB synthesis and H_2 production reaction (Imam et al., 2011).

The presence of oxygen affects structural changes in bacteria. Cells grown aerobically have no photosynthetic apparatus like other Gram-negative members of the proteobacteria class. Photosynthetic complex production completely stops under high oxygen tension. In contrast, under anaerobic conditions or limited oxygen in the environment in the light or dark, electron transfer and light-harvesting components

are synthesized by *R. sphaeroides*. These components of the photosynthetic apparatus are then inserted into intracytoplasmic membranes (ICM). In this condition, bacteria uses dimethyl sulfoxide (DMSO), trimethyl amine-N-oxide and other terminal electron acceptors. Also, cellular morphology of *R. sphaeroides* changes in the presence of oxygen. Cells that are grown under aerobic conditions are rod-shaped, while those grown photoheterotrophically are coccobacillus shaped (Slovak et al., 2005).

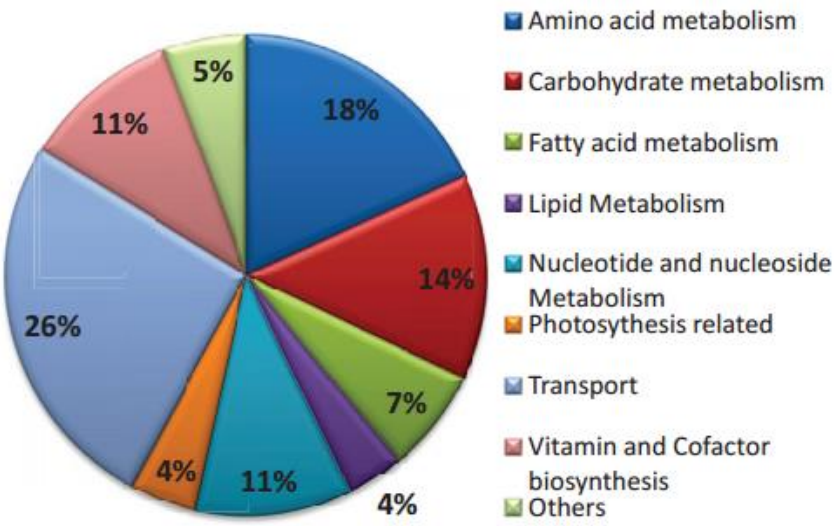

Figure 1.3: The pie chart of the reactions that take place in *R. sphaeroides*. Reactions about aminoacids, carbohydrate and nucleotide mechanism have the highest percentage, however, only a low percentage of the reactions are related to photosynthesis (Imam et al., 2011).

1.4 Photosynthesis

1.4.1 Reaction center (RC)

Photosynthesis is the primary option for *R. sphaeroides* under anaerobic conditions (Tosques et al., 1997). The reaction center (RC) in *R. sphaeroides* is a stable integral membrane protein-pigment complex that carries out light-induced electron transfer (Chang et al., 1991). RC is a potential model system for understanding protein-cofactor interactions and protein functions in electron transfer. It consists of three protein subunits, the L, M and H and cofactors such as bacteriochlorophyll dimer, bacteriochlorophyll monomers, two bacteriopheophytin monomers, two ubiquinones and a nonheme iron ion (Figure 1.4).

R. sphaeroides uses bacteriochlorophyll (BChl) a in its light absorbing complex and reaction centers (Canniffe and Hunter et al., 2014). The difference between BChl *b*

and BChl *a* is BChl *b* contains ethylidene group instead of an ethyl group at the C8 position.

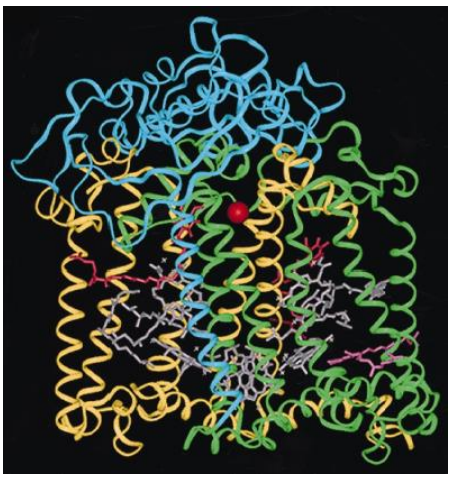

Figure 1.4: Reaction center of *R. sphaeroides*. Yellow, green and blue ribbons are respectively symbolized L, M, H subunits. Bacteriochloropyll and bacteriapheophytin are represented as grey chains, whereas primary and secondary ubiquinone are shown as red chain. The pink chain is carotenoid molecule and the red sphere in the central symbolized the iron atom (Verméglio et al., 1999).

1.4.2 Photoinduced cyclic electron transfer chain

Energy transduction in *R. sphaeroides* includes light-induced transfer of an electron from bacteriochlorophyll molecules to a ubiquinone molecule.

Multimeric transmembrane protein complexes, including light-harvesting complexes (LHCs), the reaction center (RC) and the cytochrome (cyt) bc1 complex, are the components of the photosynthetic apparatus. Two types of light-harvesting complexes are found in *R. sphaeroides* like the other purple bacteria, termed B875 (LH1) and B800-850 (LH2). B875 and B800-850 names are derived from their near-bacteriochlorophyll infrared absorption maxima (Kiley and Kaplan, 1988).

Light-harvesting protein complexes are responsible for collecting light during electron-transfer chain. LH1 and LH2 absorb a photon and transfer it to the reaction center (RC) and charge separation is performed in the RC. An electron is transferred from the bacteriochlorophyll dimer to the secondary acceptor (Q_B) by bacteriopheophytin and the primary quinone (Q_A). In the second cycle, Q_B picks up two protons from the cytoplasmic territory and quinol (QH_2) is constructed. QH_2 formation reaction is catalyzed by the bc_1 complex and this reaction oxidized by a periplasmic protein termed cyt c_2. As a result, two protons are released to the

periplasm. The photoinduced cyclic electron-transfer chain reaction finishes with photooxidized primary electron donor reduction by cyt c_2 (Vermeglio and Joliot, 1999), (Figure 1.5).

Photosynthetic apparatus formation depends on environmental conditions like light and oxygen. Low oxygen tension enhances photosynthetic complex formation in the dark, whereas high oxygen tension halts the photosynthetic apparatus production.

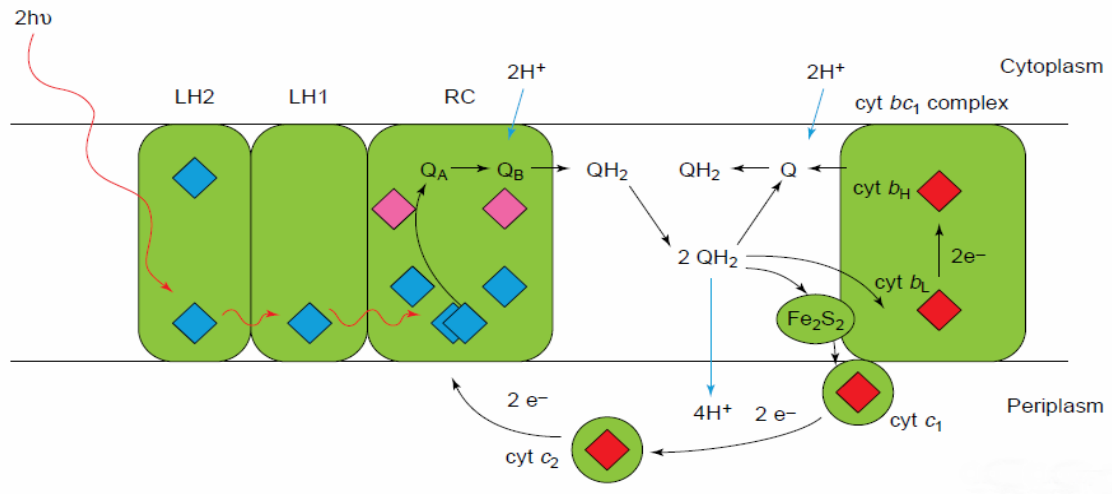

Figure 1.5: Light-induced electron transfer in *R.sphaeroides*. Blue diamonds symbolize bacteriochlorophyll molecules, pink diamonds represent bacteriophytins, and red diamonds indicate hemes. Excitation transfer is represented by red arrows and the black and blue arrows demonstrate, respectively, electron and proton transfer (Vermeglio and Joliot, 1999).

1.5 Pigmentation

1.5.1 Carotenoids

Isoprenoids are organic compounds that include five-carbon isoprene units organized in a specific order. Functional chemical groups, like hydroxyl group or carbonyl group, attached to the carbon skeleton cause the variety of isoprenoids such as monoterpenes, sesquiterpenes, diterpenes, triterpenes, tetraterpenes or polyterpenes.

Carotenoid is a member of the tetraterpene class that absorbs light between 450 nm and 550 nm, and is found in all photosynthetic organisms. Carotenoids are crucial components of the light-harvesting complexes (LHCs), especially LH2, in purple bacteria because of the roles in harvesting light energy, exciton transfer and photoprotection process under photo-oxidative stress (Glaeser and Klug, 2005).

There are two excited states of carotenoids , S1 and S2, and in LH2 complex these states act as energy donors (Šlouf et al., 2012).

Photooxidative stress, defined as accumulation of destructive reactive oxygen species (ROS), is caused by excess light absorption. Carotenoids hinder the damage of singlet oxygen by quenching. Singlet oxygen kills various cells quickly by targeting DNA, proteins and lipids. The effectiveness of singlet oxygen quenching depends on carotenoid concentrations, functional groups and length of the conjugated systems (Glaeser and Klug, 2005).

Zeller et al. (2005) reported that carotenoid-deficient mutant of *R. sphaeroides* could not grow under aerobic conditions while oxygen is present since oxygen has damaging effect on DNA, lipids, proteins of the cell (Zahiri et al., 2006).

The carotenoid-biosynthesis genes (*crt*) are clustered in *R. sphaeroides* and located between *bch* genes which encode enzymes involved in bacteriochlorophyll biosynthesis. Borders of *bch* genes are *puhA* and *puf* operon. The *puf* operon contains genes that encode for L and M subunits of the reaction centre (RC) and the LH1 α- and β- polypeptides. The *puhA* gene encodes the H subunit of the RC. The *pucBA* genes encoding the LH2 α- and β- polypeptides are located in the *puc* operon which was mapped 18 kb downstream of *puhA* gene (Figure 1.6) (Hunter et al., 1994).

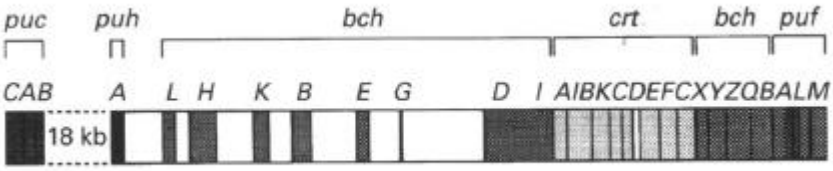

Figure 1.6: Clustered carotenoid-biosynthesis genes in *R. sphaeroides* (Lang and Hunter, 1994).

1.5.2 Spheroidene (SE) and spheroidenone (SO)

Spheroidene (SE) and spheroidenone (SO) are two main carotenoids synthesized by *R. sphaeroides* grown aerobically or anaerobically (Figure 1.7). Under aerobic conditions or during photosynthesis at high light illumination, SO is synthesized and SE is the major carotenoid synthesized in the absence of oxygen (Yeliseev and Kaplan, 1997). SO gives red brown colour to the phototrophic *R. sphaeroides* cultures (Takaichi et al., 2001).

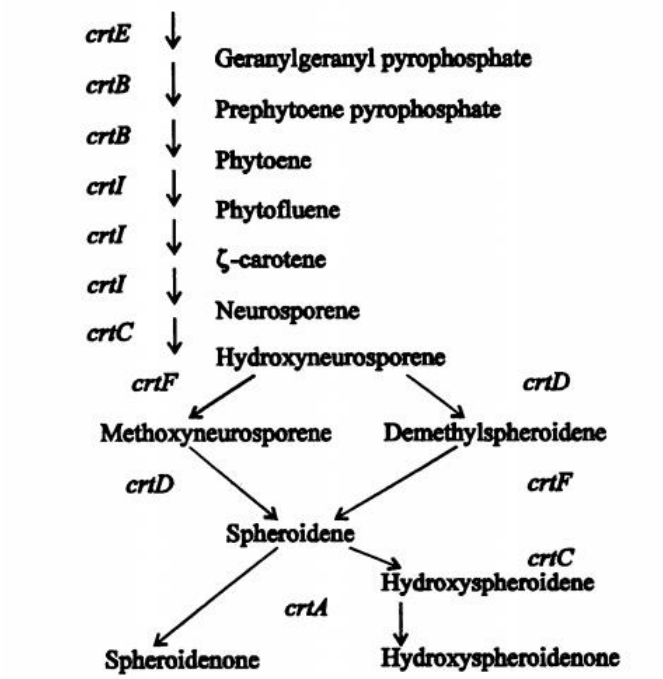

Figure 1.7: The carotenoid-biosynthetic pathway of *R. sphaeroides* (Lang and Hunter, 1994).

1.6 Biotechnological Importance

R. sphaeroides is an important organism for environmental applications because of its ability to survive under high concentrations of metal ions. It can change its metabolism under strict circumstances and can easily adapt to new environmental conditions. Investigation of its unique metabolism may elucidate the mechanism of bacterial stress response and bacterial metal adaptation.

1.6.1 Hydrogen production

Hydrogen (H_2) is a clean, renewable and environment-friendly fuel produced by photosynthetic organisms such as green algae, cyanobacteria and purple bacteria using light as energy source. Purple non-sulfur bacteria produce hydrogen by photo-fermentation process in which organic substrate is converted to biohydrogen and carbondioxide in the presence of light under anaerobic conditions. Additionally, purple bacteria can produce hydrogen by anoxygenic photosynthesis, which involves capturing light and converting to ATP without oxygen production.

Two enzymes are crucial in hydrogen production process by *R. sphaeroides*. The first one is [Mo-Fe]-nitrogenase enzyme that is responsible for nitrogen fixation (reducing N_2 to NH_3) and reduction of H^+ to H_2. The second one, [Ni-Fe]-

hydrogenase, provides hydrogen uptake under photo-fermentative conditions in the absence of oxygen (Gabrielyan et al., 2014).

Akroum-Amrouche et al. (2011) have shown that duration of hydrogen production was decreased after enhancement of light intensity, however, light intensity was not directly related to total hydrogen volume and final concentration of the biomass. Additionally, *R. sphaeroides* can produce hydrogen during the logarithmic and stationary growth phase, and production rate is higher in stationary phase than in logarithmic phase. Composition of the growth medium, cultivation conditions like pH, light intensity, temperature, and reactor design can also affect the hydrogen production efficiency (Levin et al., 2004).

R. sphaeroides is an advantageous choice for large-scale hydrogen production because of its high activity in the absence of oxygen and its ability to use different substrates. Even though various substrates can be used for the growth of *R. sphaeroides,* not all of them are appropriate for H_2 production (Akroum-Amrouche et al., 2011). H_2 production is generally accomplished in a medium with poor nitrogen source to repress nitrogenase activity. The highest H_2 yield and production rate is achieved by glutamate usage as the nitrogen source (Tao et al., 2012).

1.6.2 Polyhydroxybutyrate (PHB) production

Polyhydroxyalkanoates (PHAs) are prokaryotic carbon, energy and storage compounds. Polyhydroxy butyrate (PHB) is the most common PHA that is produced by microorganisms in response to stress conditions like nitrogen, phosphorus, sulphur or oxygen depletion in the presence of carbon source in the media (Çetin et al., 2006). Therefore, PHB synthesis increases in nutrient-depleted environments because of its usage as energy and carbon source after its degradation (Yang et al., 2006). In a study of Suzuki et al. (1995), PHB synthesis was performed under nitrogen limitation in *R. sphaeroides* and cells grown in that media had PHB content higher than 40% of cell dry weight. Also, it was observed that pH affects the PHB accumulation; in the pH range of 8.0-8.5, PHB content of cells was higher rather than in the optimal pH 7.5 (Suzuki et al., 1995).

PHB synthesis begins with condensation of two molecules of acetyl-CoA to form acetoacetyl-CoA. This reaction is catalyzed by the PHA-specific β-ketothiolase enzyme, encoded by *phbA*. In the second step, acetoacetyl-CoA is reduced to β-

hydroxybutyryl-CoA by acetoacetyl-CoA reductase, encoded by *phbB*. β-hydroxybutyryl-CoA is polymerized by PHB synthase in the last step, and high molecular weight PHB, encoded by *phbC*, is formed (Yang et al., 2006).

Due to biodegradable, nontoxic, biocompatible characteristics of the PHB , it can be used in various applicaitons in medical, domestic, agricultural and industrial fields.

1.6.3 Coenzyme Q10 (CoQ10) production

Coenzyme Q10 (ubiquinone) is a lipid-soluble antioxidant with a quinone head and a tail composed of ten isoprene units. CoQ homologues differ by the number of the isoprenoid units in the side chain, for instance 10 in the CoQ10 refers to 10 isoprenyl groups in tail, and 9 in CoQ9 means there are 9 isoprenyl groups in the side chain. Both CoQ9 and CoQ10 are present in human plasma (Molyneux et al., 2008). The CoQ10 can be present in different redox states: completely oxidized, semiquinone and completely reduced forms referred as ubiquinone, ubisemiquinone and ubiquinol, respectively.

CoQ10 exists in the inner mitochondrial membrane of the eukaryotes and in the plasma membrane of the prokaryotes. It is responsible for preventing formation of the free radicals and DNA, lipid, protein modification. In addition, it plays a crucial role in aerobic respiration by generating energy in the form of ATP and acts as an electron carrier in the electron transfer system. Regulation of gene expression and NAD^+/NADH ratio control are other important roles of CoQ10 (Zahiri et al., 2006).

Some microorganisms are capable of producing CoQ10 such as *Agrobacterium tumefaciens* and *Paracoccus denitrificans*. Additionally, *R. sphaeroides* is a good candidate for CoQ10 production because of its ability to grow under various conditions. Yen and Shih (2009) have reported that minimized dissolved oxygen concentration is necessary for maximized CoQ10 production by *R. sphaeroides* (Yen and Shih, 2009).

1.6.4 5-aminolevulinic acid (ALA)

5-aminolevulinic acid (ALA) is the precursor of tetrapyrolles which is used in heme, vitamin B12 and bacteriochlorophyll synthesis. Nonphotosynthetic eukaryotes and α-proteobacteria synthesize ALA by Shemin pathway, while in higher plants it is formed by C-5 pathway. There has been significant interest in biological ALA synthesis because of the requirements of various difficult steps in chemical ALA

synthesis. It was observed that addition of levulinic acid in the growth media of *R. sphaeroides* caused extracellular ALA accumulation in large amounts. ALA has various applications in agriculture as an herbicide, an insecticide and growth-promoting factor. In addition, it can be applied in medicine for cancer treatment and tumor diagnosis (Sasaki et al., 2002).

1.6.5 Denitrification

Denitrification is generally used for removal of nitrogen from wastewater and sewage, also it can be used in riparian zones and wetlands for removing nitrate from groundwater and wetlands (Mulvaney et al., 1997). *Rhodobacter sphaeroides* f. sp. *denitrificans* is a photosynthetic denitrifying bacterium able to carry out diverse metabolic reactions including denitrification.

Denitrification process takes place where oxygen is depleted and carried out by bacteria using nitrate and nitrogen oxides as alternative electron acceptors. This process involves reduction of nitrate (NO_3^-) to nitrite (NO_2^-), nitric oxide (NO), nitrous oxide (N_2O) and dinitrogen (N_2) catalyzed by nitrate reductase, nitrite reductase, nitric oxide reductase and nitrous oxide reductase (Tosques et al., 1996). There are two different types of nitrite reductase enzymes in denitrifying bacteria, they differ from each other based on the molecule found in redox active center: a copper ion is localized as redox-active transition metal, or *c*-type and *d*-type heme as the redox active centers. *R. sphaeroides* strains contain a copper-type nitrite reductase enzyme (Tosques et al., 1997). Nitrate, nitrite and nitrous oxide reductases are located in the periplasmic space, while nitric oxide reductase is localized in the membrane (Sabaty et al., 1994).

1.7 Metal Resistance of Microorganisms

The bioremediation of metal-contaminated areas using metal-resistant bacteria is a very important tool for environmental biotechnology. Microorganisms have the ability to change the metal chemistry through accumulation, mobilization, immobilization and reduction (Stephen et al., 1998). Heavy metals have a harmful effect on microbial growth resulting in change of biochemical activities and morphology (Panwichian et al., 2011). According to the study by Feris et al. (2003), soils experimentally contaminated with heavy metals support microbial population with declined fungus/bacterium ratios, decreased archaeal abundance, decreased

metabolic potential and enhanced levels of metal tolerance (Feris et al., 2003). Also, Sandaa et al. (1999) have shown that bacterial biomass decreases with increasing metal concentrations in the environment. They reported that bacteria in soil contaminated with Cu, Pb, Ni or Zn have similar G+C% base profiles (Sandaa et al., 1999).

There are two uptake systems for heavy metal ions in microorganisms: the first one is used by different subsrates, it is fast, unspecific and driven only by the chemiosmotic gradient which is across the membrane. However, the second one takes up specific substrates, is slower than the first one, and frequently uses ATP as the energy source, sometimes in addition to the chemiosmotic gradient (Nies, 1999).

Gram negative bacteria, archaea and yeast accumulate Ni^{2+}, Co^{2+}, Zn^{2+} and Mn^{2+} by unspecific CorA magnesium uptake system. Also, there are ATP-binding cassette (ABC) transporters for Mn^{2+}, Zn^{2+} and Ni^{2+}, and specific chemiosmotic transporters of the HoxN family for Co^{2+} and Ni^{2+} in bacteria (Figure 1.8), (Nies, 1999).

Phase variation is a method resulted in reversible variations in bacterial genome due to bacterial adaptation to changing environmental conditions. *R. sphaeroides* has phase variation abilities and R and M phase variants were investigated in a study by Mil'ko et al. (2014). These variants exhibit different colony morphology. Despite this, their growth rate, stress response to chemical and physical factors and pigmentation characteristics differed from each other. The growth rate of R variant under aerobic or anaerobic conditions in the light, at high temperature, under aeration and UV irradiation was higher than that of the M variant (Ivanovskii et al., 2013). However, the M variant grew better in the dark aerobically or at increased NaCl concentrations compared to the R variant (Mil'ko et al, 2014).

Family	Direction of transport	Energy	Metal ions
ABC	Uptake	ATP	Mn^{2+}, Zn^{2+}, Ni^{2+}, Fe^{2+}
	Efflux	ATP	–
P-type	Both	ATP	Mg^{2+}, Mn^{2+}, Ca^{2+}, K^{+}, Cu^{2+}, Zn^{2+}, Cd^{2+}, Pb^{2+}, Ag^{+}
A-type	Efflux	ATP	Arsenite
RND	Efflux	Proton gradient	Co^{2+}, Zn^{2+}, Cd^{2+}, Ni^{2+}, Cu^{2+}?, Ag^{+}?
HoxN	Uptake	Chemiosmotic	Co^{2+}, Ni^{2+}
CHR	Antiport?	Chemiosmotic	Chromate
MIT	Uptake	Chemiosmotic	Most cations
CDF	Efflux	Chemiosmotic	Zn^{2+}, Cd^{2+}, Co^{2+}, Fe^{2+}?

Figure 1.8: Different protein families responsible for heavy metal removal in microorganisms (ABC: ATP-binding cassette, RND resistance, nodulation, cell division, CHR: chromate transport, MIT: metal inorganic transport , CDF: cation-diffusion facilitators) (Nies, 1999).

1.7.1 Metal resistance of *R. sphaeroides*

R. sphaeroides is resistant to tellurite and other toxic rare-earth oxyanions such as arsenate, periodate, stannate, tungstate, vanadate, and some oxoacids of molybdenum, rhodium, selenium and silicon (Moore and Kaplan, 1992). According to the biochemical and physiological analyses, it is found that tellurite affects viability of the cells and superoxide dismutase enzyme activity under oxidative stress conditions in some *Rhodobacter* species (Borsetti et al., 2005).

Giotta et al. (2005) have reported that *R. sphaeroides* was more tolerant to heavy metals compared to *E. coli*. The protonable residues on outer membrane affect heavy metal resistance by accumulating divalent cations like Co^{2+}. Tolerance towards heavy metals allows *R. sphaeroides* to be extensively studied for its bioremediation potential in metal contaminated environments (Giotta et al., 2005).

1.7.2 Heavy metal removal of *R. sphaeroides*

Biosorption is a process defined as adsorption of metal ions onto the surface of the cell without energy demand. Purple non-sulfur bacteria (PNSB) are able to survive under various heavy metal stress conditions, PNSB also carry out bioremediation by accumulating heavy metals in their cells. *R. sphaeroides* is capable of removing heavy metals from contaminated areas under both aerobic dark and micro-aerobic light conditions. Due to this ability, it has been widely used for wastewater treatment for metal recovery from contaminated aquatic environments by biosorption

(Panwichian et al., 2011). *R. sphaeroides* growing in contaminated environments undergoes adaptation to survive by changing its molecular mechanisms.

Cu^{2+} and Zn^{2+} ions change the cellular morphology and they are accumulated in the cell wall, cytoplasm and cell membrane of *R. sphaeroides* (Panwichian et al., 2010). Cu^{2+} is an essential active part of the enzymes like oxygenases, for this reason bacteria can tolerate high Cu^{2+} concentrations compared to other heavy metals. In addition to Cu^{2+}, Zn^{2+} is a crucial trace element for bacteria too; it is a cofactor of some enzymes and forms enzyme complexes (Panwichian et al., 2011).

1.7.3 Stress response

R. sphaeroides is able to operate metabolic reactions and activate the alternative pathways in response to changing environmental conditions such as nutrient starvation or temperature changes. Heat shock response allows cells to resist to various types of environmental stresses, additionally heat shock proteins are upregulated as a response to stress (Karls et al., 1998).

Heat shock proteins chaperonin 60 and chaperonin 10 are stress proteins that are found in *R. sphaeroides*, and their concentration is increased by stress factors. These stress proteins resemble the chaperonin proteins of *E. coli* in their N-terminal amino acid sequence (Nepple and Bachofen, 1997).

1.8 Cobalt

Cobalt is a necessary ion for metabolic processes of bacteria, whereas high concentrations of cobalt has detrimental effects. Cobalt stress causes oxidative stress in cells, however, *R. sphaeroides* can survive under high cobalt concentrations and accumulate it on the cell surface. Cobalt binds to carboxylate on the photosynthetic membrane of the cell and sulfolipid formation is a response for high cobalt stress

Cobalt affects the growth of *R. sphaeroides* more negatively under aerobic conditions, the growth rate declines by 80%. Cobalt exposure causes upregulation of enzymes that have a role in protein and DNA degradation. Proteomics studies by Pisani et al. (2009) showed that cobalt stress causes overexpression of glucose-1-phosphatethymidylyltransferase involved in cell wall lipopolysaccharide biosynthesis in *R. sphaeroides* (Pisani et al., 2009). However, enzymes that take part in ammonia assimilation, protein biosynthesis and DNA replication are downregulated under

cobalt stress. In addition, cobalt downregulates expression of two enzymes related to bacteriochlorophyll biosynthesis: aconitate hydratase and porphobilinogen deaminase (Italiano et al., 2008). Aconitate hydratase catalyses isomerization of citrate to isocitrate, and porphobilinogen deaminase catalyses the formation of hydroxymethylbilane from four porphobiliogen molecules while four ammonia molecules are released.

Divalent metal cations carry a double positive charge and have similar structure: Mn^{2+}, Fe^{2+}, Co^{2+}, Ni^{2+}, Cu^{2+} and Zn^{2+} have ionic diameters between 138 pm and 160 pm. Related to the similarities, in Gram-negative bacteria, Zn^{2+}, Ni^{2+}, Co^{2+} and Cd^{2+} resistance is based on the action of proton-cation antiporters, which are members of a RND protein family responsible for metal resistance/nodulation of legumes/cell division (Nies and Silver, 1995). Also, Ni^{2+} and Co^{2+} have a similar damaging effect on bacteriochlorophyll synthesis because of the possibility of sharing binding sites and membrane transport systems. However, the inhibitory effect of nickel is stronger than that of cobalt in *R. sphaeroides* (Italiano et al., 2009).

1.9 Evolutionary Engineering

Evolutionary engineering is an approach based on obtaining desired phenotypes by taking the benefits of natural evolution. This technique consists of two strategies: random mutation is applied initially, and phenotypes with mutated genes that express products with desired properties are obtained under selective conditions. Evolutionary engineering is advantageous, because of the possibility of obtaining and developing phenotypes that synthesize industrially important products that are not produced naturally. A disadvantage of this method is that mutants obtained may have gained resistance under selective conditions, but their growth rate may be lower than that of the reference strain (Çakar et al., 2012).

In this thesis study, a mutant *R. sphaeroides* population that can survive high levels of cobalt stress was used, and eight colonies were selected randomly for physiological analysis. There are several evolutionary engineering studies beginning with chemical mutagenesis or UV-light exposure. However, in this study, random mutagenesis was not used, as it may negatively affect pigment production.

1.10 The Aim of the Study

The aim of the study presented in this thesis was to perform physiological analysis of eight mutant individuals selected from the $CoCl_2$-resistant *R. sphaeroides* final population obtained by evolutionary engineering. Stress resistance levels of the mutant individuals were estimated by various techniques such as Most Probable Number (MPN) method, cross resistance tests, and spot assay. Additionaly, genetic stability tests were also applied to mutant individuals. Diluted cultures were spread on solid LB plates to observe changes in time required for colony formation, pigmentation characteristics, colony phenotypes and detect possible contaminations. To ensure that the mutant cultures were not contaminated, 16S rRNA-based sequence analysis was performed.

2. MATERIALS AND METHODS

2.1 Materials

2.1.1 Strain

The *Rhodobacter sphaeroides* R-26 reference strain (RS) was provided by Dr. Massimo Trotta (University of Bari, Italy). *R. sphaeroides* reference strain was previously exposed to gradually increasing cobalt stress levels and cobalt resistant populations were obtained (Kamer, 2015). Eight mutant individuals with varying red pigmentation intensities were chosen from the last 64^{th} population of selection. The mutants were then compared to each other, according to their resistance levels.

2.1.2 Cultivation of *R. sphaeroides*

100 µL of the stock culture of *R. sphaeroides* was inoculated into 10 mL Medium 27 (M27) at 30°C with shaking at 150 rpm overnight. Inoculation was performed in dark and semi-aerobic conditions.

2.1.3 Stock culture preparation

Stock cultures of each population and mutant individuals were prepared during the experiments. 1.5 mL of overnight culture containing exponentially growing phase cells were inoculated to a 1.5 mL microfuge tube, and pelleted by centrifugation at 13,000 rpm (revolutions per minute) for 5 minutes. This step was repeated and 3 mL of the cell pellet was resuspended in 1 mL M27 to remove $CoCl_2$ residues from the environment. After centrifugation at 13,000 rpm for 5 minutes, the supernatant was removed and the pellet was dissolved in 1 mL of 30% (v/v) glycerol. The sample was homogenized by vortexing for 30 seconds. This procedure was carried out for all colonies, and prepared stock cultures were kept at -80°C for long-term storage.

2.1.4 Culture media and solid plate compositions

2.1.4.1 Preparation of growth media (Medium 27)

Medium 27 was used in this study. Medium 27 (M27) of the DSMZ was prepared by adding the macronutrients, as indicated in Table 2.1 (Italiano et al., 2009). The pH of the medium was adjusted to 6.8 after macronutrients were dissolved in deionized

water and autoclaved at 121°C, 1 atm pressure for 15 min. Micronutrients were filtered through 0.22 μm Spritzen- / Syringe-Filter, and then added to sterilized M27. The medium was stored at 4 °C.

Table 2.1: Ingredients of M27 of the DSMZ

Micronutrients	**Amount**
$ZnSO_4$	100 mg
$MnCl_2 \cdot 4H_2O$	30 mg
H_3BO_3	300 mg
$CoCl_2 \cdot 6H_2O$	200 mg
$CuCl_2 \cdot 2H_2O$	10 mg
$NiCl_2 \cdot 6H_2O$	20 mg
$Na_2MoO_4 \cdot H_2O$	30 mg
Macronutrients	**Amount**
KH_2PO_4	500 mg
$MgSO_4 \cdot 7H_2O$	800 mg
NaCl	400 mg
NH_4Cl	400 mg
$CaCl_2 \cdot 2H_2O$	50 mg
D-L malic acid	1500 mg
Yeast extract	2000 mg
Water	**to 1 L**

2.1.4.2 Preparation of solid Luria Broth (LB) plates

Solid LB medium was prepared as indicated in Table 2.2. The medium was autoclaved at 121°C and 1 atm pressure for 15 min. The medium was poured to Petri dishes and after solidification, they were stored at 4°C.

Cells were cultivated on LB solid medium in order to test for potential contamination (Bertani, 1951), (Table 2.2).

Table 2.2: Chemical composition of LB

Chemical	Amount
NaCl	10 g
Tryptone	10 g
Yeast extract	5 g
Agar	20 g
Water	**to 1 L**

2.1.5 Laboratory equipment

Laboratory equipment used in this study is listed in Table 2.3.

Table 2.3: Laboratory equipment used in this study.

Equipment	Supplier	Country
Autoclaves	Tommy SX700E	China
	Tuttnauer Systec Autoclave 2540ml-2870ELVC	Switzerland
Balance	Precisa BJ 610C	Switzerland
Benchtop Centrifuge	Eppendorf 5424	Germany
Deep-freezer	-80°C Sanyo Ultra Low MDT-U40865	Japan
Desiccator	Finemech Bola-Star Vitrium Desiccator	USA
Refrigerators and Deep-freezers	-20°C Arçelik 3011 NY	Turkey
	+4°C Arçelik	Turkey
Incubator	Nüve EN400-EN500	Turkey
Laminar Flow Hood	Biolab Faster BH-EU 2003	Italy
Light Microscope	Olympus CH30	Japan
Magnetic Stirrer	Labworld	Germany
Microbalance	Precisa 620C SCS	Switzerland
Microfuge	Eppendorf Microcentrifuge-5424	Germany
Micropipettes	Eppendorf	Germany

Table 2.3 (continued): Laboratory equipment used in this study.

Equipment	Supplier	Country
pH meter	Mettler Toledo MP220	Switzerland
Orbital Shaker Incubators	Certomat S-2 Sartorius	Germany
Shaker	Thermo Scientific Orbital Shaker	USA
Ultrapure Water System	TKA	Germany
UV Visible Spectrophotometer	Shimadzu UV-1700	Japan
Vortex Mixer	Nüve NM 110	Turkey

2.1.6 Chemicals

The chemicals and enzymes/kits used in this study are shown in Tables 2.4 and 2.5, respectively.

Table 2.4: Chemicals that are used in this study.

Chemical	Supplier	Country
6x Loading Dye	Fermentas	Lithuania
Acetone, C_3H_6O	MERCK KGaA	Germany
Agar	BD Difco™	USA
Agarose	Applichem	Germany
Aluminium chloride hexahydrate, $AlCl_3 6H_2O$	MERCK	Germany
p-amino benzoic acid, $C_7H_7NO_2$	Fluka	USA
Ammonium chloride, NH_4Cl	Sigma ALDRICH	USA
Ammonium iron (II) sulfate hexahydrate, $(NH_4)_2 Fe(SO_4)_2 \cdot 6H_2O$	MERCK	Germany
Benzoic acid, $C_7H_6O_2$	Fluka	USA
Boric acid, H_3BO_3	MERCK KGaA	Germany
Calcium chloride dehydrate, $CaCl_2 \cdot 2H_2O$	Carlo Erba	Italy

Table 2.4 (continued): Chemicals that are used in this study.

Chemical	**Supplier**	**Country**
Cobalt chloride hexahydrate, $CoCl_2 \cdot 6H_2O$	Fluka	USA
Copper chloride dihydrate, $CuCl_2 \cdot 2H_2O$	Sigma ALDRICH	USA
Copper (II) sulfate pentahydrate, $CuSO_4 \cdot 5H_2O$	Sigma ALDRICH	USA
DNA Markers	Fermentas	Lithuania
Ethanol, C_2H_6O	J.T. Baker	The Netherlands
Ferrous chloride tetrahydrate, $FeCl_2 \cdot 4H_2O$	Fluka Biochemika	Switzerland
Glycerol, $C_3H_8O_3$	Duchefa Bochemie	The Netherlands
Hydrogene peroxide, H_2O_2	MERCK	Germany
Iron (II) chloride, $FeCl_2$	Sigma ALDRICH	USA
Iron (II) citrate, $C_6H_6FeO_7$	Sigma ALDRICH	USA
Isopropanol	MasterPure™	USA
Lambda DNA/*Eco*RI+*Hind*III Marker	Thermo Scientific	USA
Magnesium sulfite heptahydrate, $MgSO_4 \cdot 7H_2O$	MERCK	Germany
Magnesium chloride hexahydrate, $MgCl_2 \cdot 6H_2O$	MERCK	Germany
D,L malic acid	MERCK	Germany
Manganase (II) chloride tetrahydrate, $MnCl_2 \cdot 4H_2O$	MERCK	Germany
MasterPure Complete (MCP) Protein Precipitation Reagent	MasterPure™	USA
Nickel chloride hexahydrate, $NiCl_2 \cdot 6H_2O$	MERCK	Germany
Sodium chloride, NaCl	MERCK	Germany
Sodium hydroxide, NaOH	MERCK	Germany
Sodium molybdate, $Na_2Mo_4 \cdot 2H_2O$	MERCK	Germany
SYBR Gold	Roche SYBR Gold Gel Stain	Switzerland

Table 2.4 (continued): Chemicals that are used in this study.

Chemical	**Supplier**	**Country**
Tryptone	MERCK	Germany
Yeast extract	MERCK	Germany
Zinc chloride, $ZnCl_2$	Carlo Erba	Italy
Zinc sulfate heptahydrate, $ZnSO_4 \cdot 7H_2O$	MERCK	Germany

Table 2.5: Kits and enzymes used in this study.

Kits and Enzymes	**Company**	**Country**
iTaq DNA Polymerase (5U/µL)	Intron Biotechnology	Korea
MasterPure™ DNA Purification Kit	Epicentre Biotechnologies, No. MCD85201	USA
Proteinase K	MasterPure™	USA
RNase A	MasterPure™	USA

2.1.7 Sequence of the primers

Forward and reverse primers used in Polymerase Chain Reaction (PCR) are shown in Table 2.6.

Table 2.6: Sequences of the primers used in PCR.

Primer	**Sequence**	**Melting Temperature**
16sRNA_seq1_forw	5'- GCCTAACACATGCAAGTCGAGC -3'	56.7 °C
16sRNA_seq1_rev	5'- TTCCACTCACCTCTCTCGACC -3'	56.3 °C
16sRNA_seq2_forw	5'- TGACGGTACCACCAGAAGAAGC -3'	56.7 °C
16sRNA_seq2_rev	5'- ATCTCACGACACGAGCTGACG -3'	56.3 °C
16sRNA_seq3_forw	5'- ATTCGAAGCAACGCGCAGAAC -3'	54.4 °C
16sRNA_seq3_rev	5'- ACGACTTCACCCCAGTCACTG -3'	56.3 °C

2.2 Methods

2.2.1 Obtaining cobalt resistant individual mutants through evolutionary engineering

Cobalt resistant mutants were chosen from the last (64^{th}) population obtained by evolutionary engineering method, based on continuous cobalt exposure. A brief description of the evolutionary engineering procedure is described below (Kamer, 2015):

To determine the initial $CoCl_2$ concentration, reference strain (RS) was incubated in M27 with 0.25 mM, 0.5 mM, 1 mM, 2.5 mM and 5 mM $CoCl_2$. After overnight cultivation at 30°C, 150 rpm under semi-aerobic conditions in 50 mL test tubes containing 15 mL M27, optical density values at 535 nm were measured. Survival rates of the cultures were determined by dividing OD_{535} of stress cultures under different $CoCl_2$ concentrations to that of the control culture without stress. According to the survival rate values, 0.1 mM $CoCl_2$ was chosen as the initial stress concentration for selection. The RS inoculated into 15 mL of M27 with 0.1 mM $CoCl_2$ was incubated overnight at 30°C, 150 rpm and this stress-treated culture was named as the first population of selection.

$CoCl_2$ concentration was increased by 0.05 mM between 1-13^{th} populations, by 0.1 mM between 13-16^{th} populations, by 0.2 mM between 16-49^{th} populations, and by 0.5 mM between 49-64^{th} populations. The last (64^{th}) population was plated on solid LB media and eight mutant individuals were randomly picked to investigate their stress resistance.

2.2.2 Estimation of stress resistance

2.2.2.1 Most Probable Number (MPN) method

Cobalt resistance levels of eight selected mutant individuals from the 64^{th} population were compared via Most Probable Number (MPN) method**.** MPN is used for estimating cell density of a sample due to positive/negative turbidity differences.

100 µL of the colonies from frozen stock cultures were inoculated into 10 mL M27, incubated overnight at 30°C, and 150 rpm. The next day, while cells were at the exponential growth phase, cultures were inoculated into 10 mL M27 at a starting OD_{535} of 0.2 and incubated at 30°C, 150 rpm. After about 5 hours, the cultures reached an OD_{535} of 1.2, 1 OD_{535} units were harvested and centrifuged at 13,000 rpm

for 5 min. 100 µL M27 was dropped on cell pellets and the pellets were homogenized by vortexing. Twenty µL of the cultures from these samples were added on 180 µL M27 in 96-well plates.

In control plate, without any $CoCl_2$ stress, mutant individuals were diluted 10^{-1} to 10^{-12}, because of the ability of *R. sphaeroides* cells to grow better at higher dilutions. In plates containing 2 mM, 4 mM, 6 mM, 8 mM and 15 mM $CoCl_2$, mutants were diluted 10^{-1} to 10^{-8}. After incubation at 30°C for four days, the number of surviving cells at different cobalt concentrations was estimated by using the MPN table, based on the Poisson regression (Rowe et al., 1977).

2.2.2.2 Spot assay

Mutant individuals' resistance levels were generally different from each other. Comparison of the mutants was carried out by spot assay. Seven individual mutants (G1, G3, G4, G5, G6, G7, G8) and the reference strain (RS) and were prepared, by incubating 100 µL of the stock cultures into 10 mL fresh M27 overnight at 30°C and shaking at 150 rpm. During exponential growth phase of the cells, cultures were inoculated at a starting OD_{535} of 0.2 into 10 mL M27 and incubated at 30°C, 150 rpm. When the cultures reached the OD_{535} of 1.2, OD_{535} units of 5 were harvested and centrifuged at 13,000 rpm for 5 min. Pellets were resuspended in 1 mL M27 and all dilutions of colonies were placed on solid LB plates with 1 mM, 2mM, 3 mM, 3.5 mM, 4 mM and 5 mM $CoCl_2$, including the control plate, which did not contain any $CoCl_2$. After four days of incubation, more resistant individuals were determined.

2.2.3 Cross-resistance

Each mutant was tested for its ability to grow on solid LB media containing different stress factors. Seven individual mutants, RS and the 64^{th} population were prepared by incubating 100 µL of the frozen stock cultures in 10 mL M27 overnight at 30°C and 150 rpm. During exponential growth phase of the cells, cultures were taken and inoculated at a starting OD_{535} of 0.2 into 10 mL M27, and incubated at 30°C, 150 rpm. When the cultures reached the OD_{535} of 1.2, 5 OD_{535} units were harvested and centrifuged at 13,000 rpm for 5 min. Pellets were resuspended in 1 mL M27 and the cultures were inoculated at different dilution factors, ranging from 10^{-1} to 10^{-8}. After

four days of incubation, more resistant mutants were determined and selected for further analysis.

In cross-resistance test, serial dilutions of mutant individuals and RS cultures were incubated at various concentrations of ethanol (8% v/v), sodium chloride (0.5 M), aluminum chloride (5 mM), copper (II) chloride (0.5 mM), nickel (II) chloride (2mM, 2.2 mM, 2.4 mM), magnesium chloride (500 mM, 750 mM, 1M), hydrogen peroxide (1 mM, 2 mM), iron (II) chloride (4 mM, 5 mM), manganese (II) chloride (10 mM), boric acid (30 mM, 50 mM), caffeine (20 mM), ammonium iron(II) sulfate (5 mM), and zinc chloride (1 mM). According to spot assay results, mutants with higher survival rates under various stress conditions were chosen for further tests.

2.2.4 Genetic stability test

The aim of the genetic stability test was to determine the genetic stability of cobalt resistance of the mutants by repeated cultivation under non-selective conditions and testing for cobalt resistance.

100 µL of frozen stock cultures of the selected mutant individuals and the RS were incubated in fresh medium (M27) at 30°C and 150 rpm. Each day, optical density was set as 0.25 and when OD_{535} reached 1.5, MPN test was performed with 4 mM, 8 mM, 12 mM $CoCl_2$ in 96-well plates with five replicates and serially diluted up to 10^8-fold dilution for five days. MPN was continued with 4 mM and 8 mM $CoCl_2$ for the remaining ten days of the experiment. For every day of the ten day-period, frozen-stocks were prepared; 3 mL of cultures was centrifuged at 13,000 rpm for 5 min. Supernatant was removed and 1 mL of 30% glycerol (v/v) was added. Stock cultures were stored at -80°C. 96^{th} hour MPN scores of colonies under 4 mM, 8 mM and 12 mM $CuCl_2$ stress conditions were read and the number of cells/mL were calculated to find potential changes in survival rates in ten days.

Genetic stability was also tested by spot assay, as described in Section 2.2.5.

2.2.5 Continuous $CoCl_2$ stress exposure

At the beginning, 100 µL of frozen stock cultures of the mutant individuals, and the RS were inoculated into fresh 10 mL M27. For five days, initial OD_{535} was set as 0.25 and cultures were inoculated into 10 mL M27 containing 4 mM $CoCl_2$. Cultures were cultivated overnight at 30°C at a shaking speed of 150 rpm. Spot assay was then performed. Each culture was serially diluted to 10^{-8}. Each dilution of the

selected colony was spotted onto solid Luria Broth (LB) plates containing 1 mM, 2 mM, 3 mM, 4 mM, 5 mM and 7 mM $CoCl_2$. Plates were incubated at 30°C for four days.

2.2.6 Obtaining growth curves of RS and G7

Preculture of a mutant individual and RS were obtained by inoculating 100 µL of 80°C stock cultures into 10 mL M27. After overnight incubation at 30°C and at 150 rpm, cultures were inoculated into 500 mL flasks including 100 mL M27 without stress condition and with 4 mM $CoCl_2$ at an initial OD_{535} value of 0.2. Every 2 hours, OD_{535} values were measured during 83 hours of incubation. As a result, growth curves of the mutant individual and RS without stress and in the presence of 4 mM $CoCl_2$ were obtained.

2.2.7 Measurement of cell dry weight (CDW)

Cell dry weight analysis was performed during the growth curve experiment. Before beginning the analysis, 1.5 mL microfuge tubes were dried in oven at 80° C for 48 hours, placed in desiccator for 3 hours, then weighed. Throughout the OD_{535} measurements, 2 mL of the samples were taken and centrifuged at 14,000 rpm for 5 minutes. Supernatants were discarded and pellets were placed in oven at 80°C to dry. After 48 hours, tubes were weighted again. The cell dry weight was calculated by subtracting the first weight from the second weight.

2.2.8 Sequence analysis

Sequencing was done to detect potential contamination. The bacterial 16S rRNA gene regions of the mutant individuals were amplified for sequencing, to confirm the purity of the cultures.

2.2.8.1 DNA extraction

Epicentre Biotechnologies (USA) MasterPure™ DNA Purification Kit (Cat. No. MCD85201) was used for DNA extraction.

500 µL (20 ng/µL) of the reference *R. sphaeroides* strain, and overnight cultures of the mutant individuals were transferred to microfuge tubes and centrifuged at 13,000 rpm for 5 min. The supernatants of cultures were discarded and after 10 seconds of vortex, 300 µL of Tissue and Cell Lysis Solution containing 1 µL of Proteinase K (50µg/µ) was added to the remaining pellets and mixed. Microfuge tubes were

incubated at 65°C for 15 min by vortexing every five minutes. After that, samples were cooled down to 37°C and 0.5 µL of RNase A (10 µg/µL) was added. Tubes were then incubated at 37°C for 30 min, and placed on ice for 3-5 min. After cooling of samples, 150 µL of MCP Protein Precipitation Buffer was added to 300 µL of the lysed sample. Tubes were vortexed for 10 seconds and centrifuged for 10 min at 10,000xg. Pellets were discarded and supernatants were transferred to new microfuge tubes and 500 µL of isopropanol was added to each sample. Contents were mixed by inverting the tubes for 30 times. Samples were centrifuged for 10 min at 10,000xg and the supernatants were discarded. 70 % (v/v) ethanol wash was performed twice without moving the pellet. Tubes were incubated at 37°C to remove the ethanol. Extracted DNAs were resuspended in 35 µL of TE Buffer, and concentrations were measured using NanoDrop (Thermo SCIENTIFIC, USA), before performing the PCR.

2.2.8.2 Polymerase Chain Reaction (PCR)

Two gene fragments for each colony and the reference strain from isolated DNA samples were amplified by PCR to be used in sequence analysis. PCR reaction was performed using 1 µL template DNA (20 ng/µL), 2 µL of dNTP (10 mM), 2 µL of 10xPCR Buffer, 1 µL forward primer (2.5 µM), 1 µL of reverse primer (2.5 µM) and 0.5 µL of iTaq DNA Polymerase (5 U/µL), and 12.5 µL distilled water for each sample. The PCR conditions are shown in Table 2.7.

Table 2.7: PCR reaction conditions.

Step	Temperature (°C)	Duration	Number of cycles
Initial denaturation	95	3 min	1
Denaturation	94	20 sec	34
Annealing	51	30 sec	
Extension	72	1 min	
Final extension	72	5 min	1
Hold	+5	∞	

PCR products were analyzed on 1 % agarose gel, electrophoresis was performed at 110 V for 40 minutes.

2.2.8.3 DNA sequence analysis

Sequence analysis of the amplified gene regions was performed by GENOMED AG Laboratories.

3. RESULTS

3.1 Evolutionary Engineering Strategy to Obtain $CoCl_2$-Resistant Population and Selection of Individual Mutant Colonies

Reference *R. sphaeroides* strain was subjected to cultivation in the presence of increasing cobalt concentrations (0.1 mM to 15 mM). The last population that survived under 15 mM $CoCl_2$ stress referred as the "64^{th} population" (Kamer, 2015). 10^6-fold dilution of the 64^{th} population was then spread on solid LB plate and eight colonies (G1, G2, G3, G4, G5, G6, G7, G8) were picked from the plate at varying red pigmentation intensities: G1, G2 and G3 had pink colour, G4 and G5 were red, G6, G7 and G8 were dark red.

3.2 Stress Resistance Analysis by Most Probable Number (MPN) Method

Resistance to different $CoCl_2$ stress levels of eight mutant individuals were determined by Most Probable Number (MPN) method during constant stress exposure. Mutants were cultivated in 96-well plates with 2 mM, 4 mM, 6 mM, 8 mM, 10 mM, 15 mM $CoCl_2$, and without $CoCl_2$ stress for control.

The number of viable cells of the selected mutants was determined by MPN assay after four days of incubation at 30°C, and cell numbers was determined by using the MPN table. Also, the survival rate values were calculated by dividing cell numbers of stress treated cells to that of the non-treated control cells.

Table 3.1: Viable cell numbers of the mutants and the RS under 2 mM, 4 mM, 6 mM, 8 mM, 15 mM $CoCl_2$ stress application and without stress.

Individual number	Number of cells (cell/mL)					
	0 mM	**2 mM**	**4 mM**	**6 mM**	**8 mM**	**15 mM**
1	$5.4x10^9$	$7.0x10^7$	$9.2x10^8$	$1.6x10^5$	$2.4x10^6$	23
2	$2.4x10^9$	$2.2x10^8$	$1.7x10^8$	$2.4x10^6$	$2.4x10^6$	23
3	$1.7x10^9$	$4.6x10^8$	$1.7x10^8$	$2.4x10^5$	$2.4x10^6$	23

Table 3.1 (continued): Viable cell numbers of the mutants and the RS under 2 mM, 4 mM, 6 mM, 8 mM, 15 mM $CoCl_2$ stress application and without stress.

Individual number	Number of cells (cell/mL)					
	0 mM	2 mM	4 mM	6 mM	8 mM	15 mM
4	$1.7x10^9$	$2.4x10^8$	$1.1x10^8$	$1.6x10^7$	$1.6x10^8$	33
5	$1.6x10^{10}$	$5.4x10^8$	$1.6x10^8$	$1.1x0^7$	$1.1x10^8$	23
6	$7.0x10^8$	$9.2x10^7$	$5.4x10^8$	$1.6x10^8$	$7.0x10^7$	23
7	$1.7x10^9$	$1.7x10^8$	$1.6x10^9$	$1.6x10^8$	$1.6x10^8$	23
8	$2.2x10^9$	$9.2x10^8$	$1.7x10^9$	$2.8x10^6$	$2.4x10^7$	23
RS	$1.6x10^9$	23	23	23	23	23

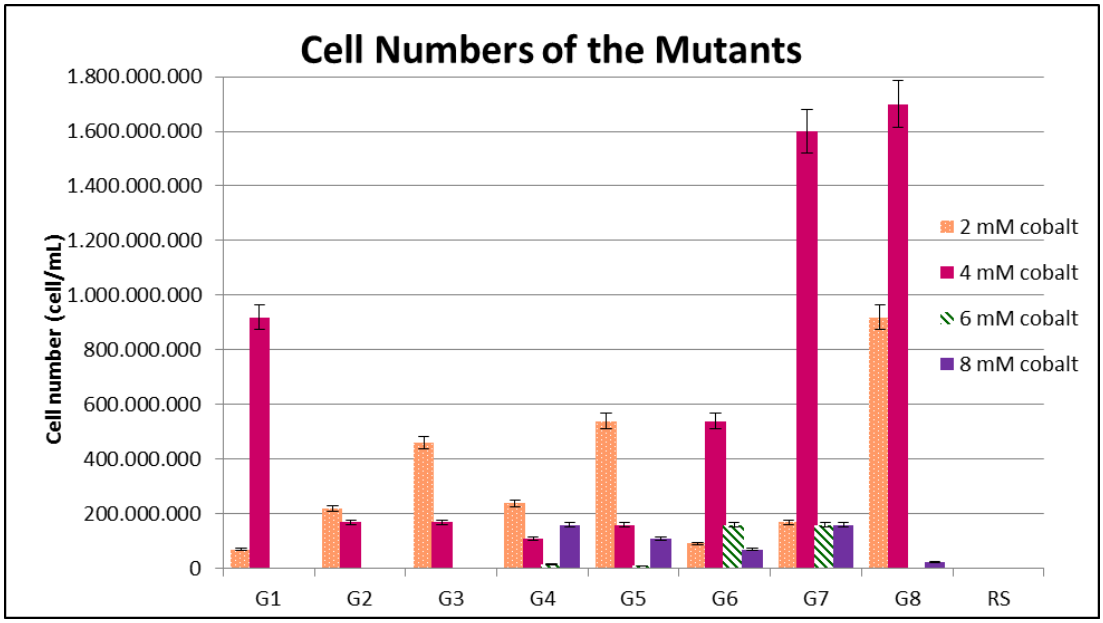

Figure 3.1: Comparison of the numbers of the individuals at 2 mM, 4 mM, 6 mM and 8 mM $CoCl_2$ stress application after four days of incubation.

MPN method demonstrated that the mutant individuals managed to grow at low $CoCl_2$ concentrations than the RS. Colonies that were cultured in M27 containing 4 mM $CoCl_2$ had the highest cell number when compared to mutants exposed to other $CoCl_2$ concentrations. Also, they seem to be significantly resistant to cobalt under 4 mM $CoCl_2$ stress, when compared to RS. Percent survival results were obtained by dividing the number of stress applied cells to that of the non-treated cells (Table 3.2).

Table 3.2: $CoCl_2$ resistance levels of the individuals after four days of incubation.

Individual number	% Survival Rate			
	2 mM	4 mM	6 mM	8 mM
1	1.30	17.04	0.00	0.04
2	9.17	7.08	0.10	0.10
3	27.06	10.00	0.01	0.14
4	14.12	6.47	0.94	9.41
5	3.38	1.00	0.07	0.69
6	13.14	77.14	22.86	10.00
7	10.00	94.12	9.41	9.41
8	41.82	77.27	0.13	1.09

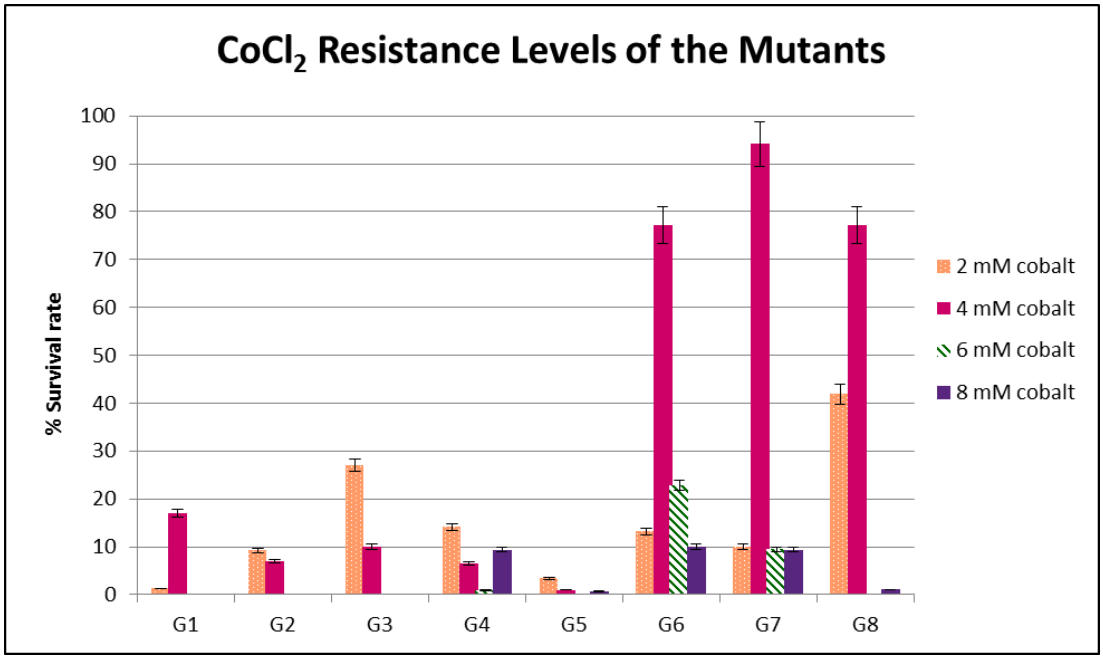

Figure 3.2: Percent survival results of the mutant individuals due to MPN method.

Table 3.3: Mutant individuals' survival rates as fold of RS values.

Individual number	Cell number (cell/mL) of colony / cell number (cell/mL) of RS				
	0 mM	2 mM	4 mM	6 mM	8 mM
1	3.38	538462	7076923	6957	104348
2	1.50	1692308	1307692	104348	104348
3	1.06	3538462	1307692	10435	104348

Table 3.3 (continued): Mutant individuals' survival rates as fold of RS values.

Individual number	Cell number (cell/mL) of colony / cell number (cell/mL) of RS				
	0 mM	**2 mM**	**4 mM**	**6 mM**	**8 mM**
4	1.06	1846154	846154	695652	6956522
5	10	4153846	1230769	478261	4782609
6	0.44	707692	4153846	6956522	3043478
7	1.06	1307692	12307692	6956522	6956522
8	1.38	7076923	13076923	121739	1043478

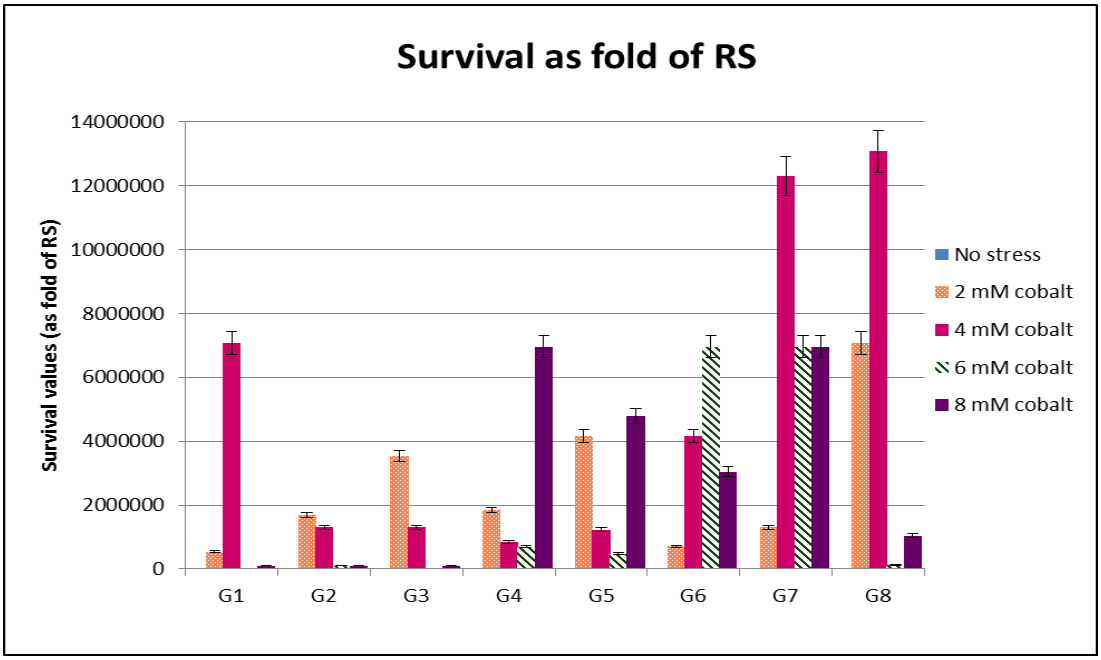

Figure 3.3: Survival of the mutants in M27 with different $CoCl_2$ concentrations.

3.3 Analysis of $CoCl_2$ Stress Resistances Through Spot Assay

The stress resistance levels of selected mutants were determined by spotting cultures on LB plates containing stress factors. Serial dilutions of the RS and the mutants were inoculated onto LB plates containing 1 mM, 2 mM, 3 mM, 3.5 mM, 4 mM and 5 mM $CoCl_2$ concentrations. After incubation at 30°C for four days, plate images were taken.

3.3.1 Control plate

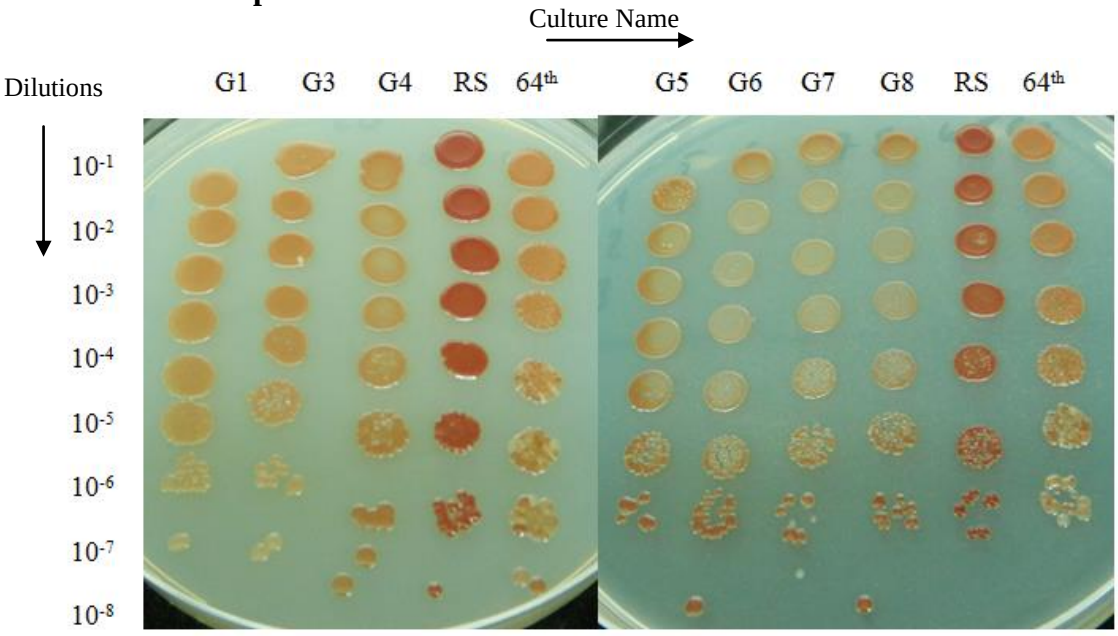

Figure 3.4: Mutant individuals, 64th population and the RS on control LB plate after four days of incubation.

3.3.2 1 mM $CoCl_2$

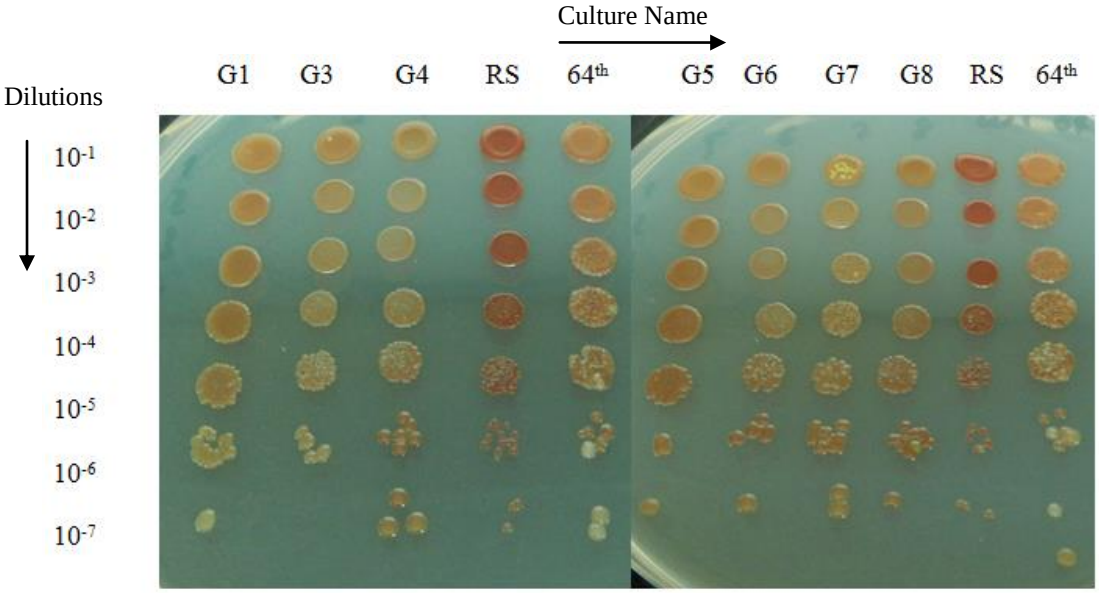

Figure 3.5: Mutant individuals, 64th population and the RS on LB plate containing 1 mM $CoCl_2$.

According to the Figure 3.5, mutant individuals' resistance levels were the same as RS at 1 mM $CoCl_2$ concentration.

3.3.3 2 mM $CoCl_2$

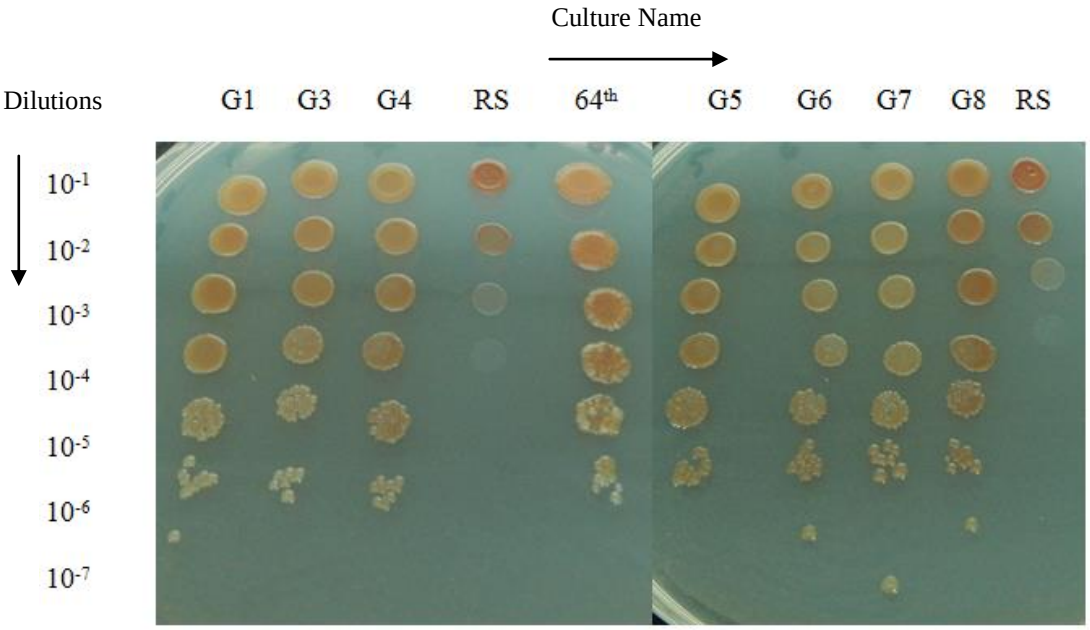

Figure 3.6: Mutant individuals, 64th population and the RS spotted on LB plate with 2 mM $CoCl_2$.

It is obvious that 10^6-fold diluted individuals could grow under 2 mM $CoCl_2$ stress, while RS was barely survived at this concentration.

3.3.4 3 mM $CoCl_2$

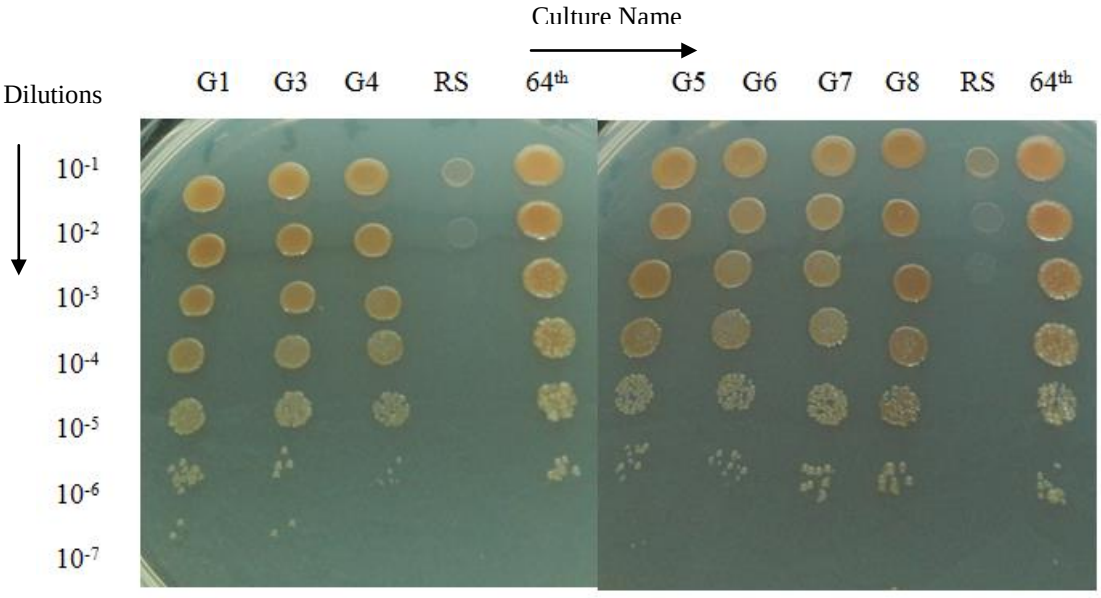

Figure 3.7: Mutant individuals, 64th population and the RS on LB plate containing 3 mM $CoCl_2$ after four days of incubation.

3.3.5 3.5 mM $CoCl_2$

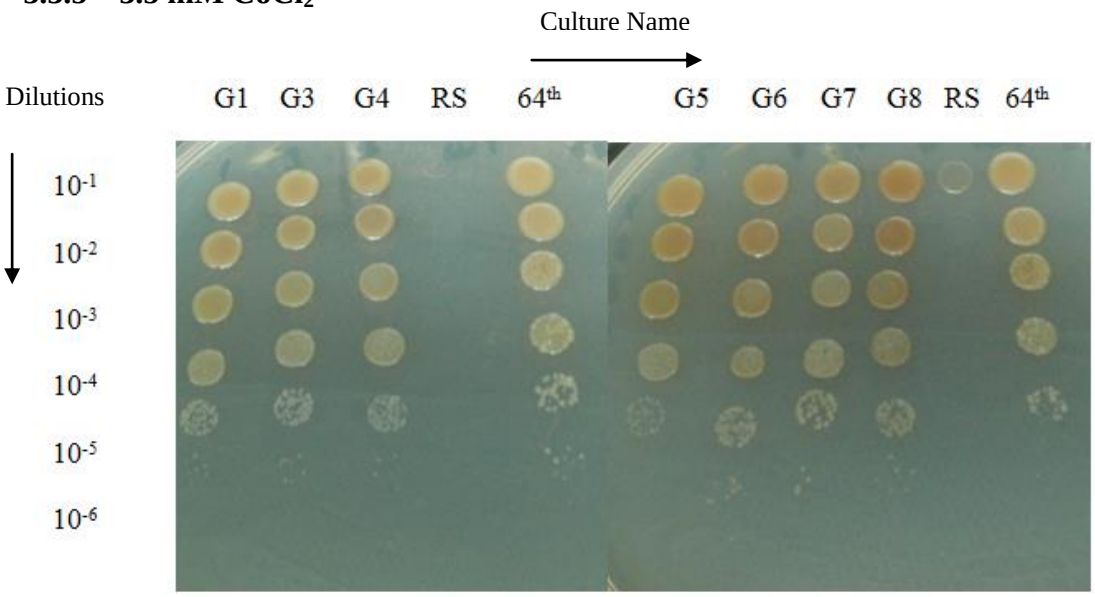

Figure 3.8: Mutant individuals and the RS on LB plate with 3.5 mM $CoCl_2$ after four days.

According to the Figure 3.8, solid LB plate containing 3.5 mM $CoCl_2$ had detrimental effect on RS.

3.3.6 4 mM $CoCl_2$

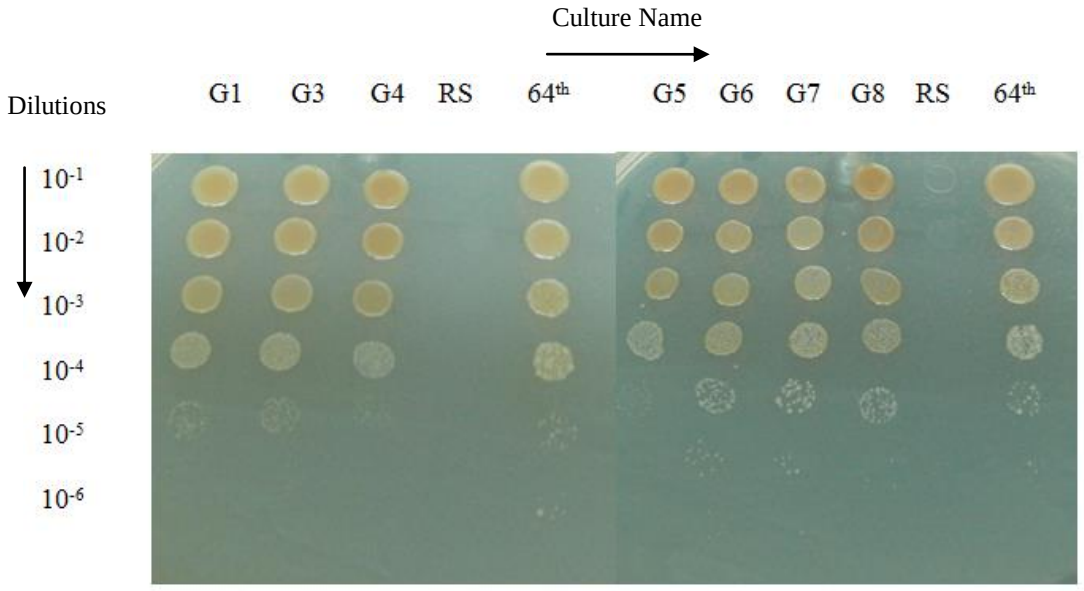

Figure 3.9: Mutant individuals and the RS on LB plate with 4 mM $CoCl_2$ after four days.

3.3.7 5 mM $CoCl_2$

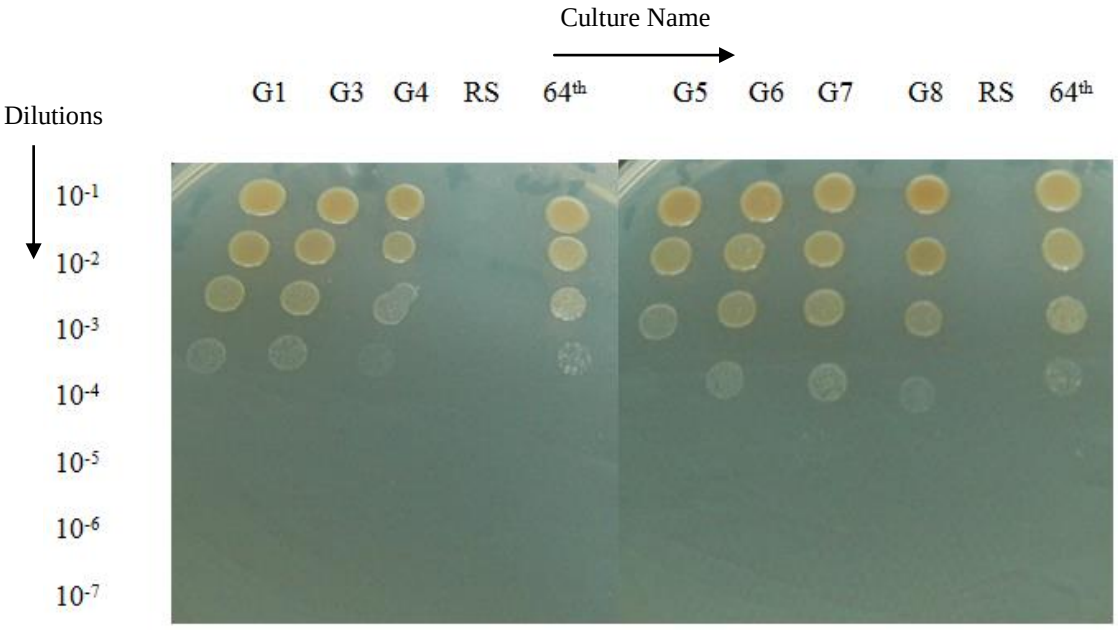

Figure 3.10: Mutant individuals, 64th population and the RS on LB plate containing 5 mM $CoCl_2$ after four days of incubation.

The RS and individuals were shown similar growth in control plate and LB containing 1 mM $CoCl_2$ stress. At 3.5 mM concentration, growth of RS is drastically inhibited. Also, 4 mM $CoCl_2$ and above that concentration had detrimental effect on growth of RS. However, it was observed that G1, G3, G4, G6, G7 and G8 survived better at higher concentrations when compared to G5, which shows that their resistance is stronger than G5.

3.4 Cross-Resistance Test

Mutant individuals and the RS were incubated in solid LB plates containing various stress factors. Growth was monitored after four, five or eight days of incubation at 30°C and images of the colonies were taken.

3.4.1 Control plate

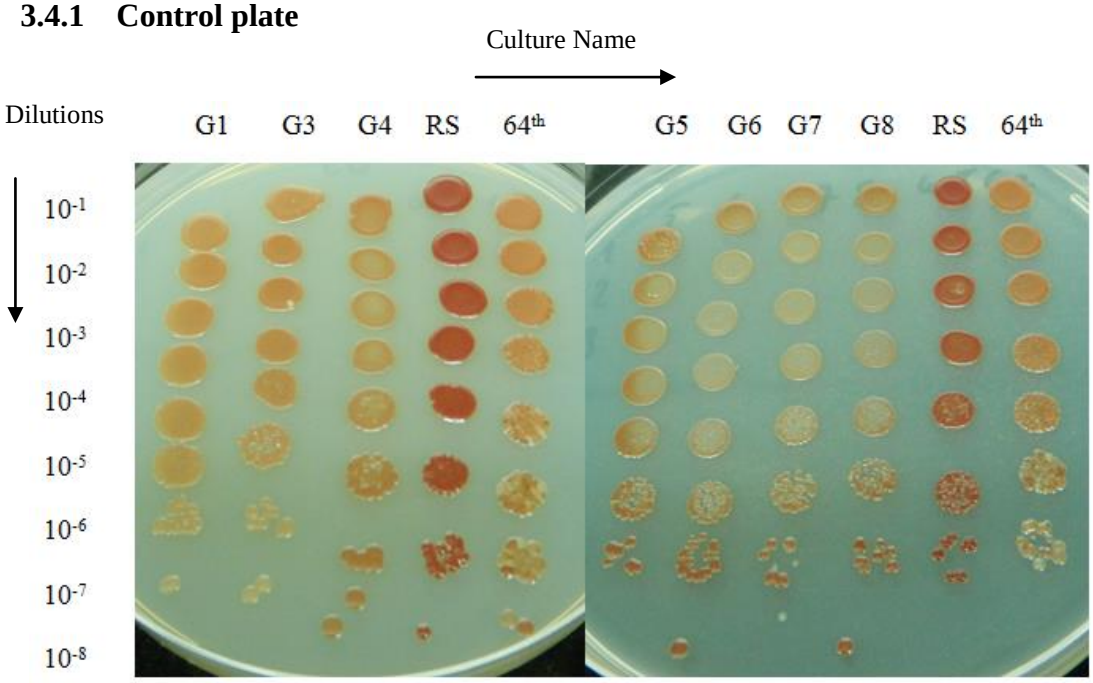

Figure 3.11: Mutant individuals (G1, G3, G4, G5, G6, G7, G8), 64th population and the RS on control LB plate after four days of incubation.

3.4.2 8% (v/v) ethanol

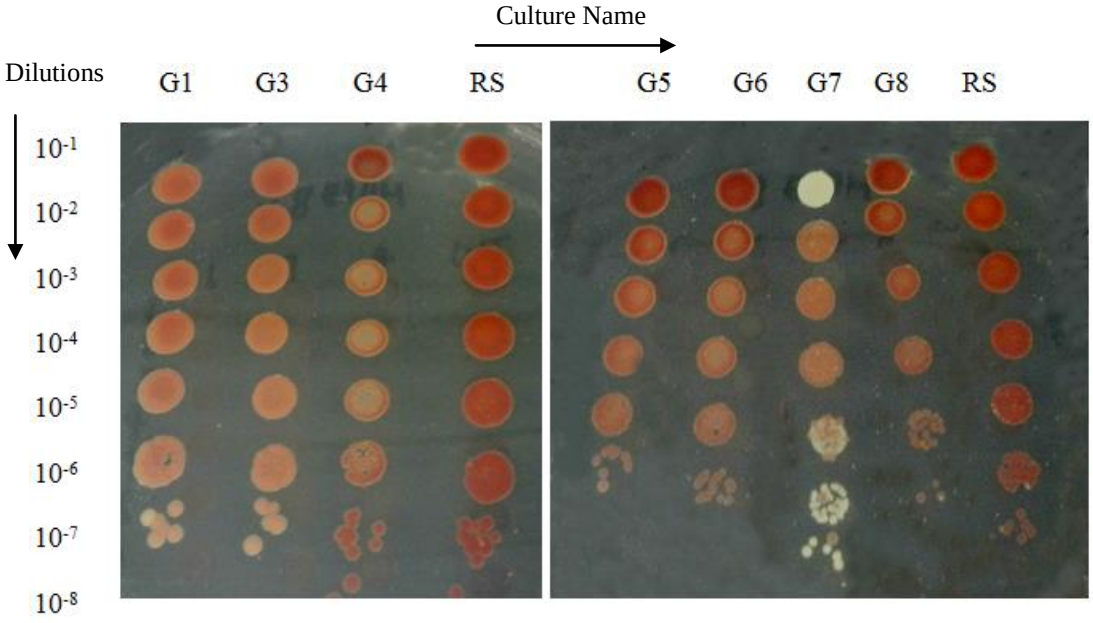

Figure 3.12: Mutant individuals and the RS on LB plate with 8% ethanol after four days of incubation.

It was interesting to observe that while all dilutions of G7 were white three days after incubation, and some dilutions became reddish on the fourth day.

3.4.3 0.5 M NaCl

Figure 3.13: Mutant individuals on 0.5 M NaCl after four days of incubation.

Figure 3.13 shows the resistance of G7 on LB plate with 0.5 M NaCl, while only 10^1-fold diluted individuals could grow under this stress condition.

3.4.4 5 mM $AlCl_3$

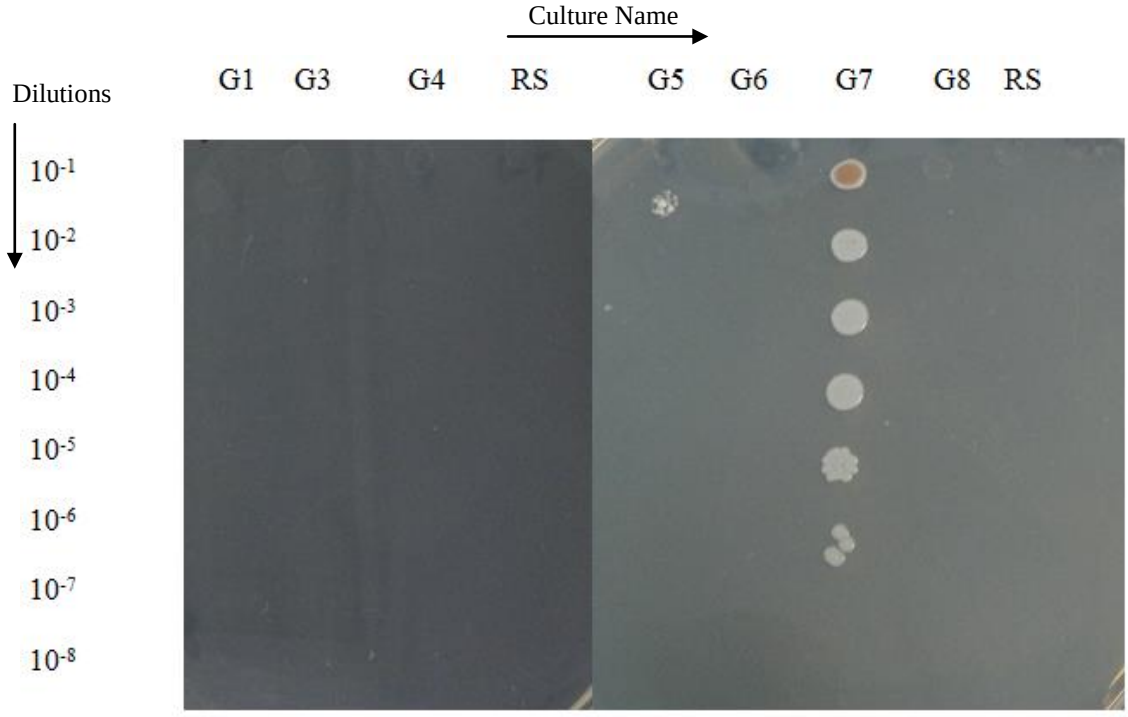

Figure 3.14: Mutant individuals and the RS on LB plate containing 5 mM $AlCl_3$.

It is clear from Figure 3.14 that none of the mutants except G7 had the ability to survive on solid plate containing 5 mM $AlCl_3$.

3.4.5 0.5 mM $CuCl_2$

All of the mutant individuals and also the RS could grow on solid LB plate with 0.3 mM $CuCl_2$. Therefore, concentration was increased to 0.5 mM. Resistance levels of the mutants and the RS were similar (Figure 3.15).

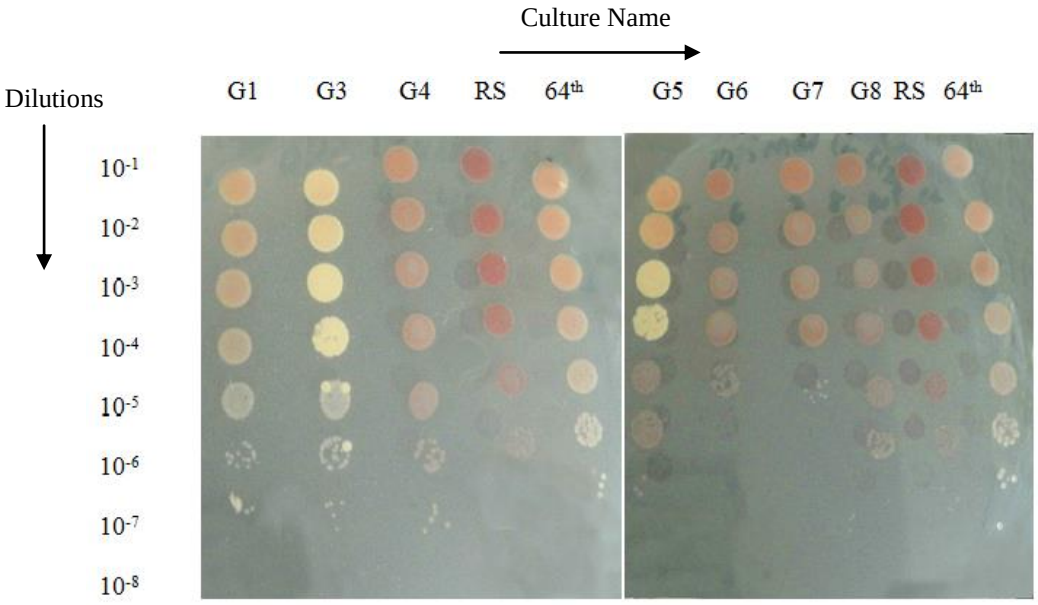

Figure 3.15: Mutant individuals, 64th population and the RS on LB plate containing 0.5 mM $CuCl_2$ after four days of incubation.

3.4.6 2 mM $NiCl_2$

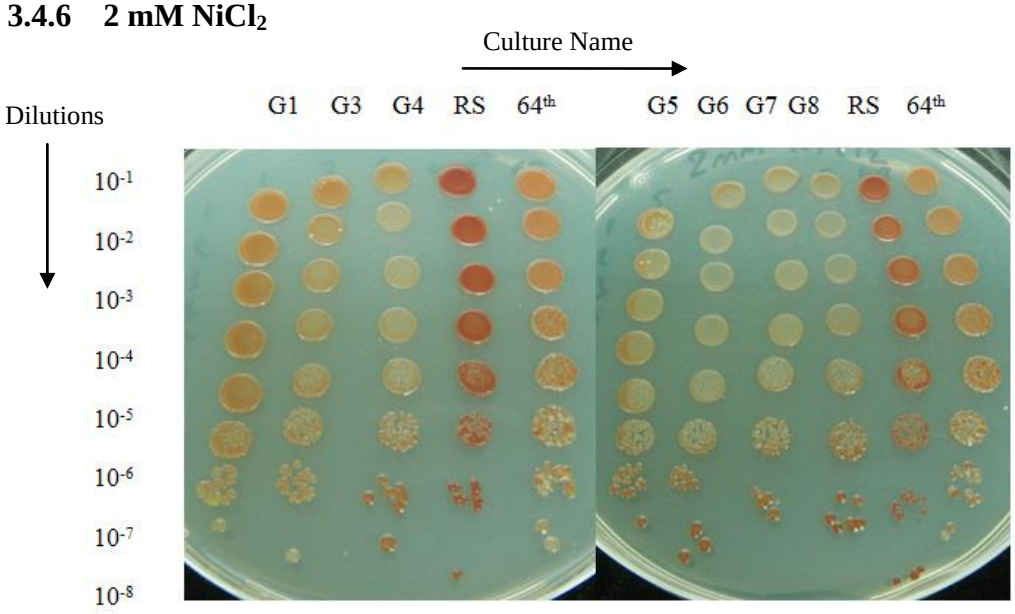

Figure 3.16: Mutant individuals, 64th population and the RS on LB plate containing 2 mM $NiCl_2$.

3.4.7 2.2 mM $NiCl_2$

All dilutions of the RS and the individuals could grow at 2 mM $NiCl_2$ stress. Therefore, 2.2. mM and 2.4 mM $NiCl_2$ concentrations were chosen for nickel stress resistance determination.

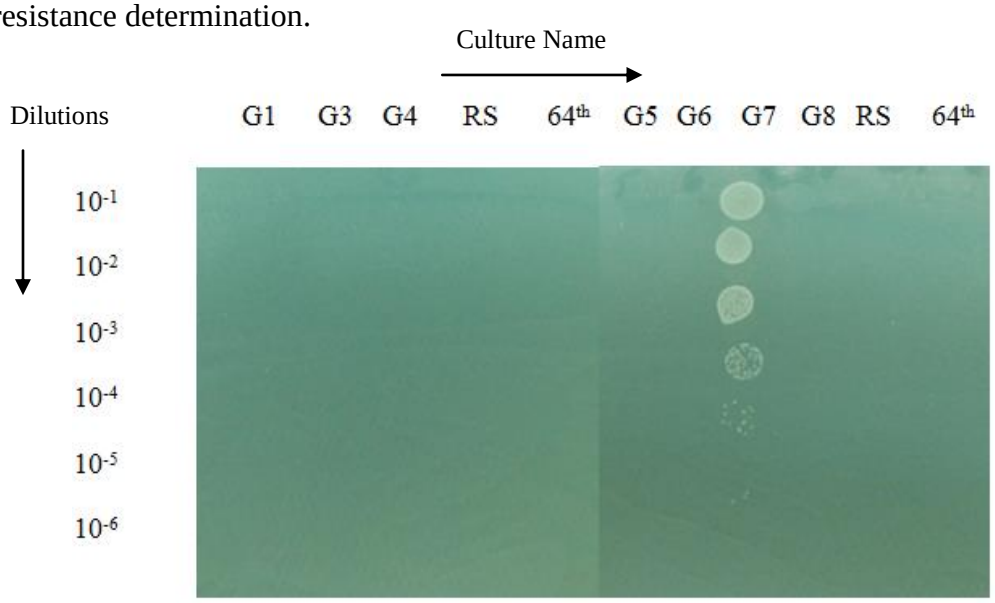

Figure 3.17: Mutant individuals, 64th population and the RS on LB plate containing 2.2 mM $NiCl_2$ after four days of incubation.

3.4.8 2.4 mM $NiCl_2$

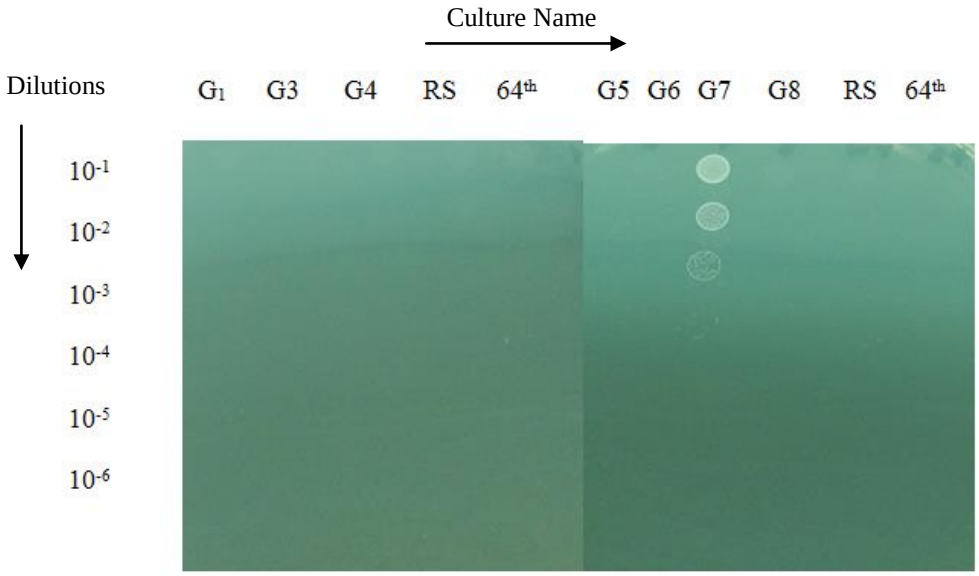

Figure 3.18: 2.4 mM $NiCl_2$ stress was applied to mutants, 64th population and the RS.

Interestingly, while all mutant individuals and the RS showed resistance to 2 mM $NiCl_2$, none of them - except for G7 - were able to survive at 2.2 mM and 2.4 mM $NiCl_2$ (Figure 3.17, Figure 3.18).

3.4.9 500 mM $MgCl_2$

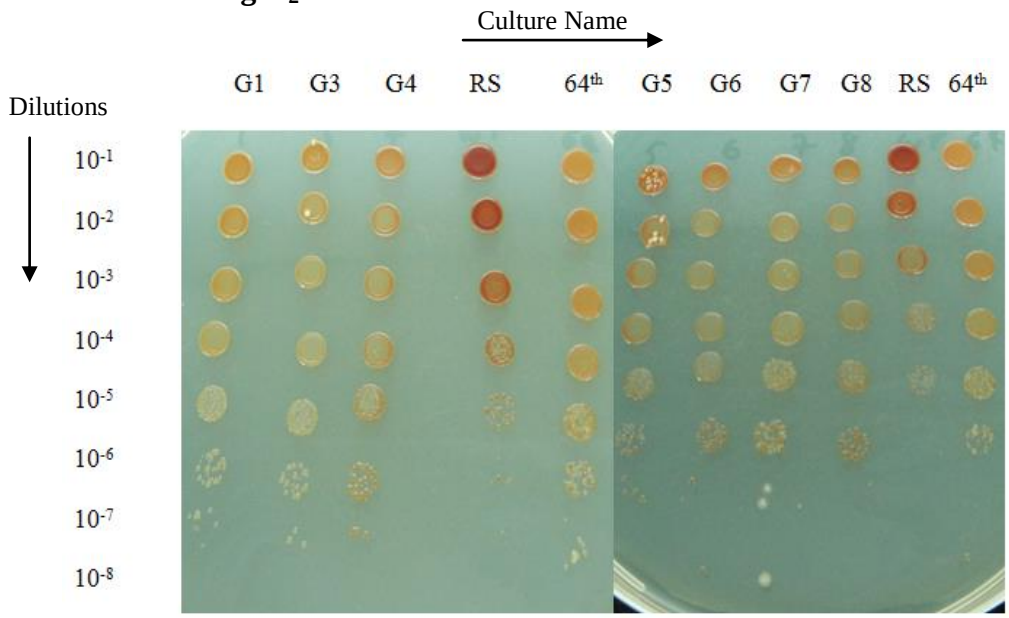

Figure 3.19: Mutant individuals, 64th population and the RS on LB plate containing 500 mM $MgCl_2$.

According to Figure 3.19, mutant individuals were more resistant to magnesium stress, when compared to RS.

3.4.10 750 mM $MgCl_2$

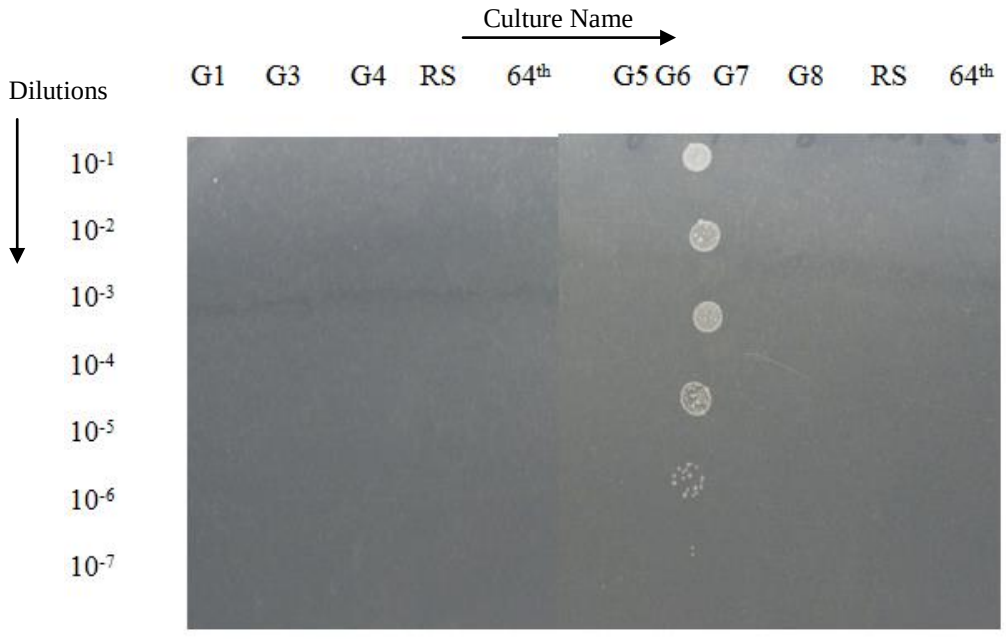

Figure 3.20: 750 mM $MgCl_2$ stress application on mutant individuals, 64th population and the RS.

3.4.11 1 M $MgCl_2$

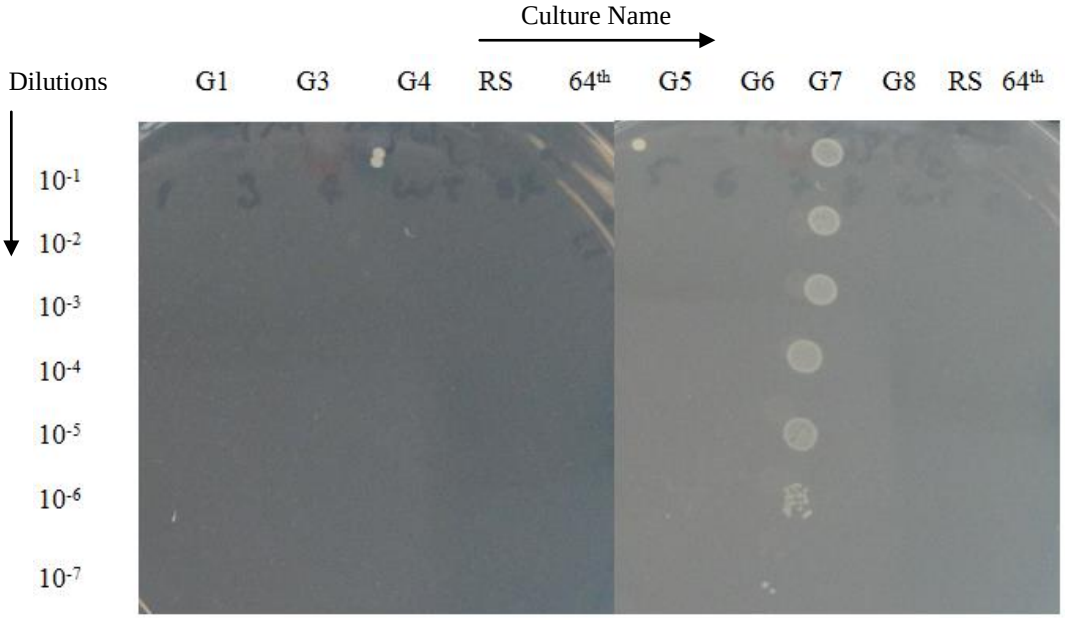

Figure 3.21: 1 M $MgCl_2$ stress was applied to mutant individuals, 64th population and the RS.

G7 showed resistance to 1 M $MgCl_2$. In addition to G7, only 10^1-fold diluted G4 and G5 could grow on this media. Similar to NaCl, $AlCl_3$ and $FeCl_2$ stress test results, G7 also showed resistance to $MgCl_2$.

3.4.12 1 mM H_20_2

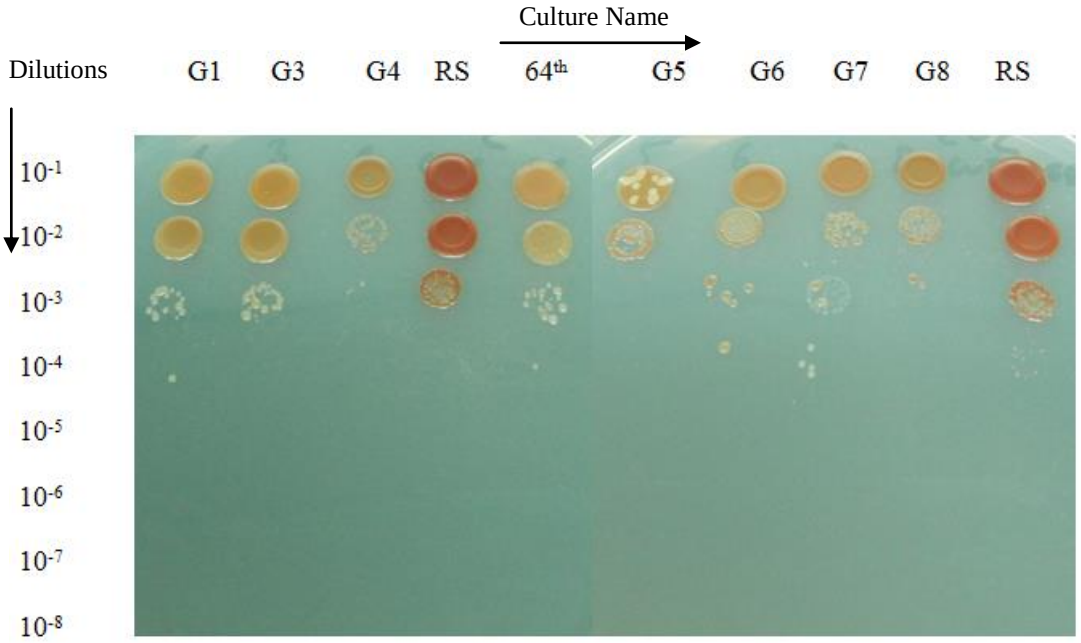

Figure 3.22: Mutant individuals, 64th population and the reference strain on LB plate containing 1 mM H_2O_2 after four days of incubation.

3.4.13 2 mM H_20_2

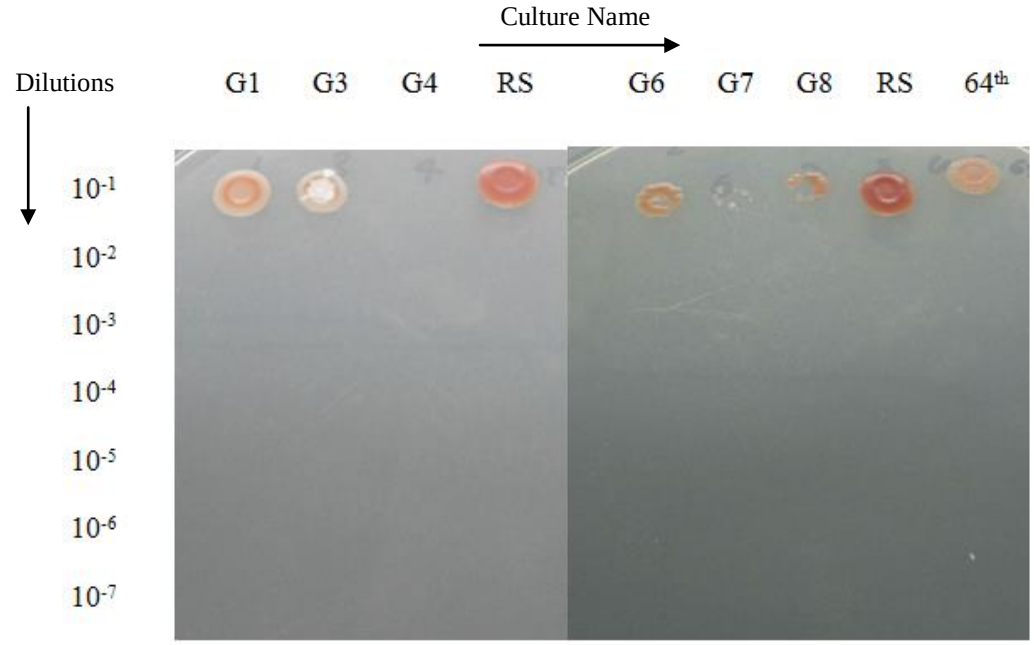

Figure 3.23: Mutant individuals, 64th population and the RS on LB plate containing 2 mM H_2O_2 after four days of incubation.

According to Figure 3.22, resistance leves of the individuals and the RS to 1 mM H_2O_2 were similar.

3.4.14 10 mM $MnCl_2$

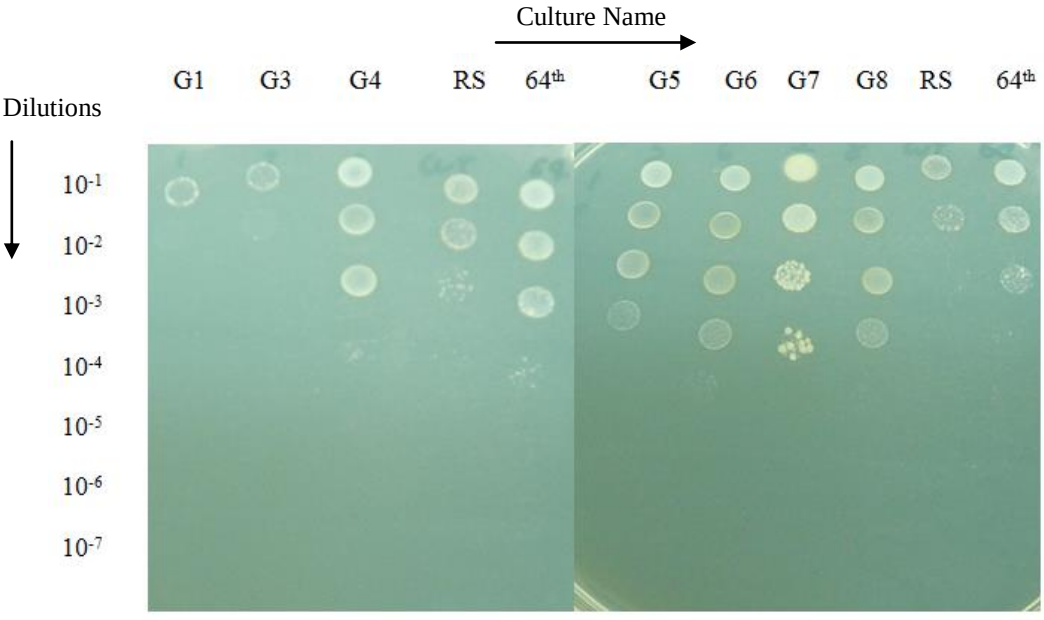

Figure 3.24: Mutant individuals, 64th population and the RS on LB plate 10 mM $MnCl_2$ after four days of incubation.

3.4.15 4 mM $FeCl_2$

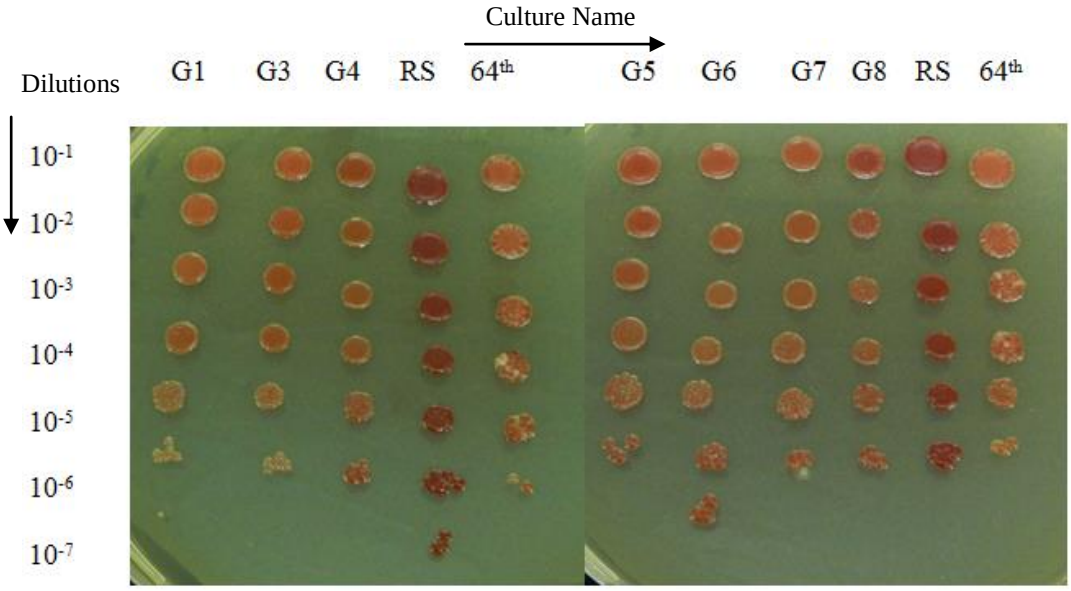

Figure 3.25: Mutant individuals, 64th population and the RS on LB plate containing 4 mM $FeCl_2$ after eight days of incubation.

Normally, images of the plates were taken after four days of incubation, but colonies under $FeCl_2$ stress could not grow in four days. Because of this, $FeCl_2$ stress-applied cells were incubated for eight days, then photographed.

3.4.16 5 mM $FeCl_2$

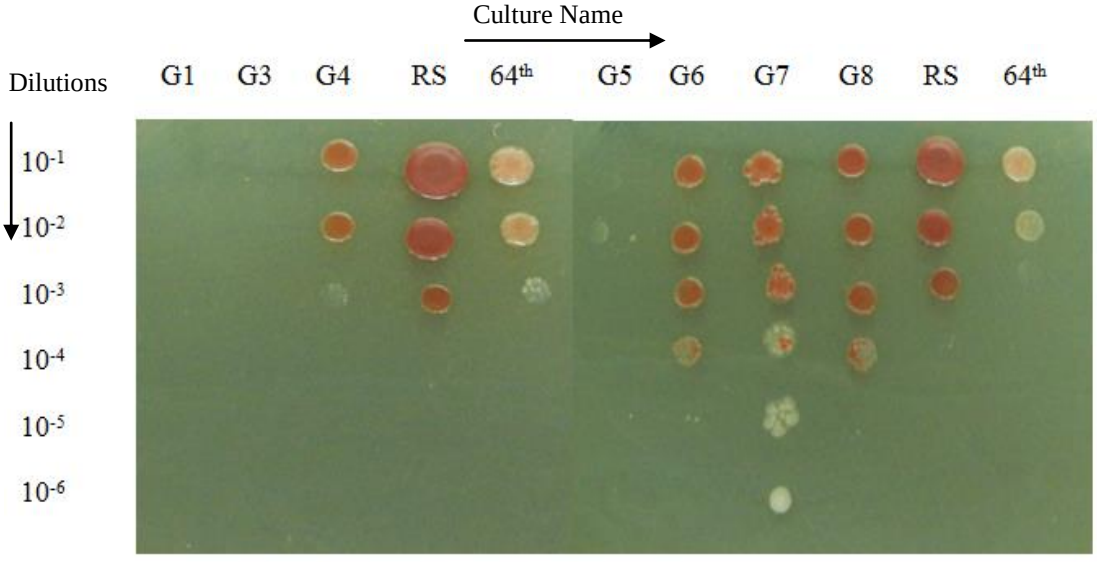

Figure 3.26: Mutant individuals, 64th population and the RS on LB plate with 5 mM $FeCl_2$ after eight days of incubation.

3.4.17 5 mM $(NH_4)_2Fe(SO_4)_2$

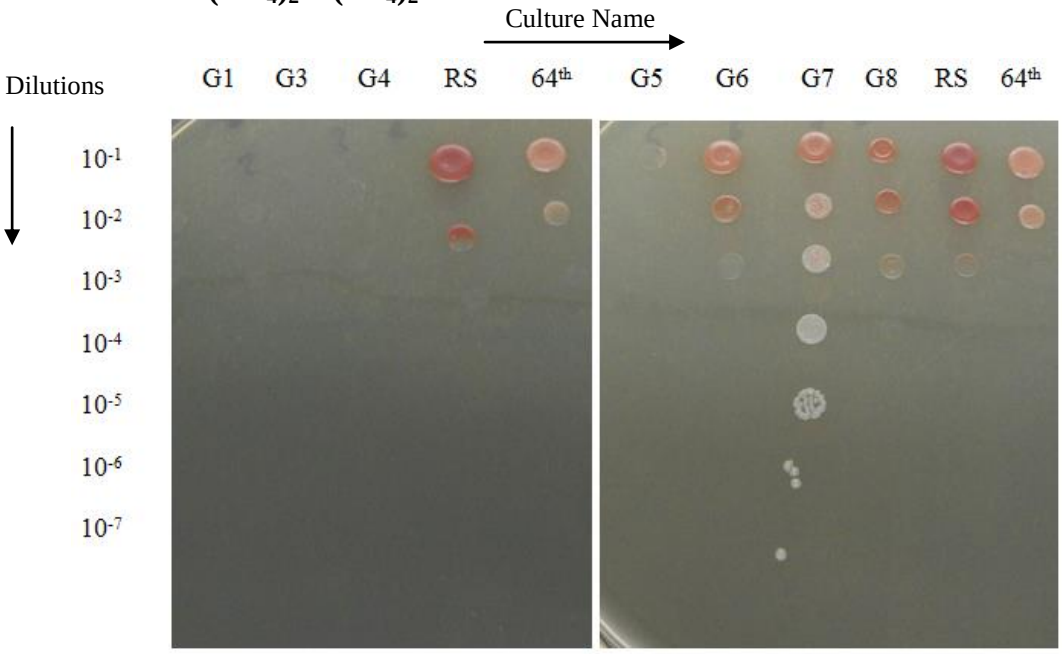

Figure 3.27: Mutant individuals, 64th population and the RS on LB plate containing 5 mM $(NH_4)_2Fe(SO_4)_2$ after four days of incubation.

While the first dilution of the G7 culture had red colour, more diluted spots of G7 became white under Fe^{2+} stress (Figure 3.27).

3.4.18 1 mM $ZnCl_2$

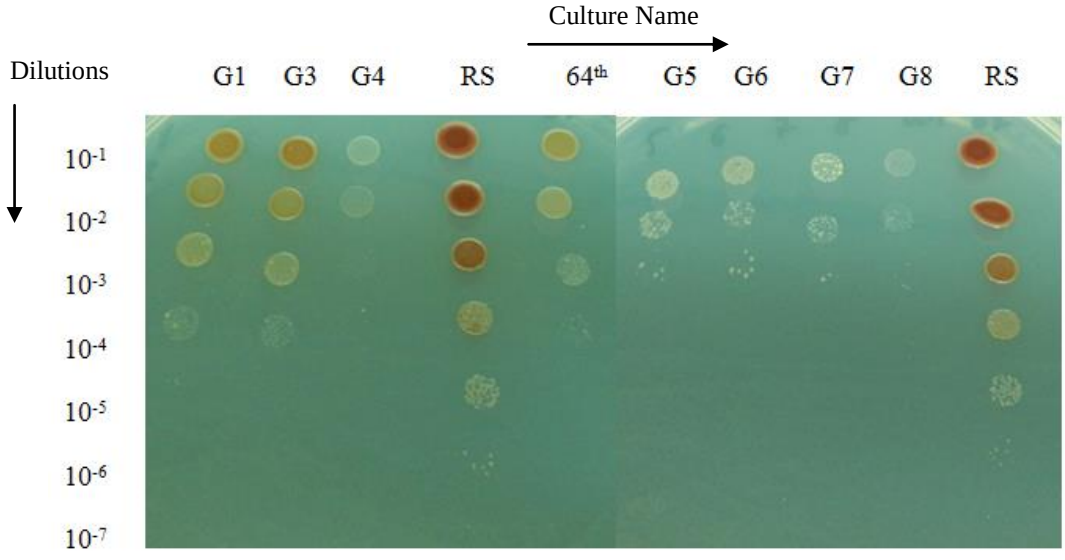

Figure 3.28: 1 mM $ZnCl_2$ stress application on mutant individuals, 64th population and the RS on LB after five days of incubation.

According to Figure 3.28, mutant individuals were sensitive to $ZnCl_2$. It can be observed that G1 and G3 were more resistant, compared to other mutants, but still less resistant than the RS.

3.4.19 30 mM H_3BO_3

10^8-fold diluted mutant individuals and the RS could grow on solid LB plates containing 5 mM, 10 mM, 15 mM and 20 mM H_3BO_3. Therefore, the concentration was increased to 30 mM and 50 mM.

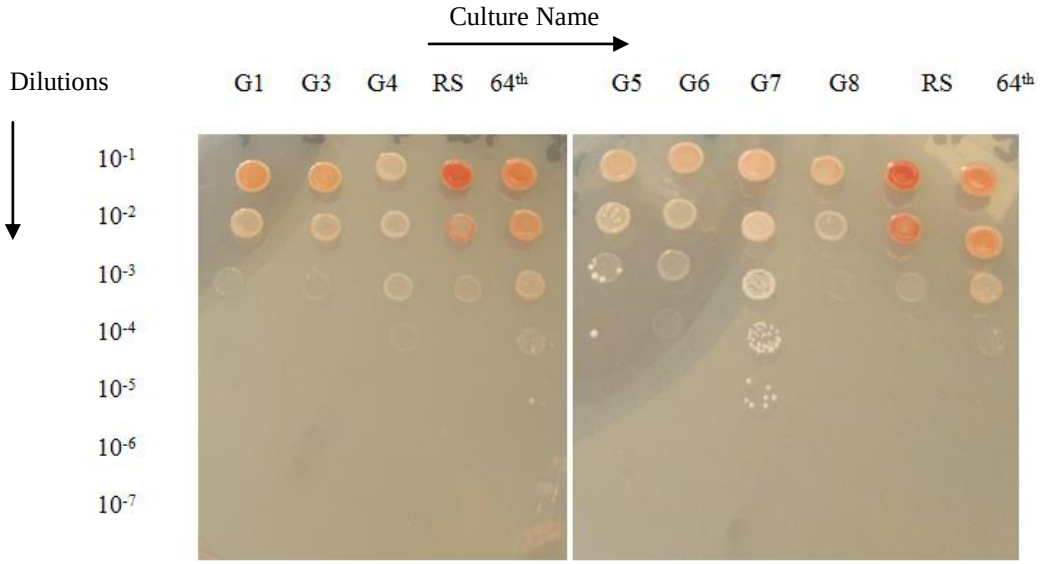

Figure 3.29: Mutant individuals, 64th population and the reference strain on LB plate containing 30 mM H_3BO_3 after four days of incubation.

3.4.20 50 mM H_3BO_3

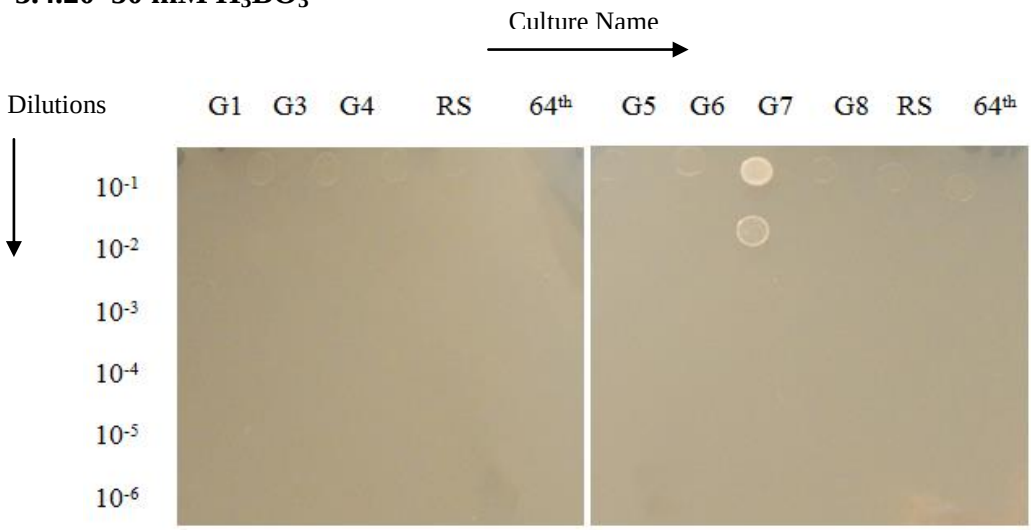

Figure 3.30: Mutant individuals, 64th population and the reference strain on LB plate containing 50 mM H_3BO_3.

Unlike other mutants, G7 also gained H_3BO_3-resistance at high concentrations (Figure 3.30).

3.4.21 20 mM caffeine

10^8-fold diluted mutant colonies and the reference strain could grow on solid LB plates containing 10 mM caffeine; therefore, the concentration was increased to 20 mM.

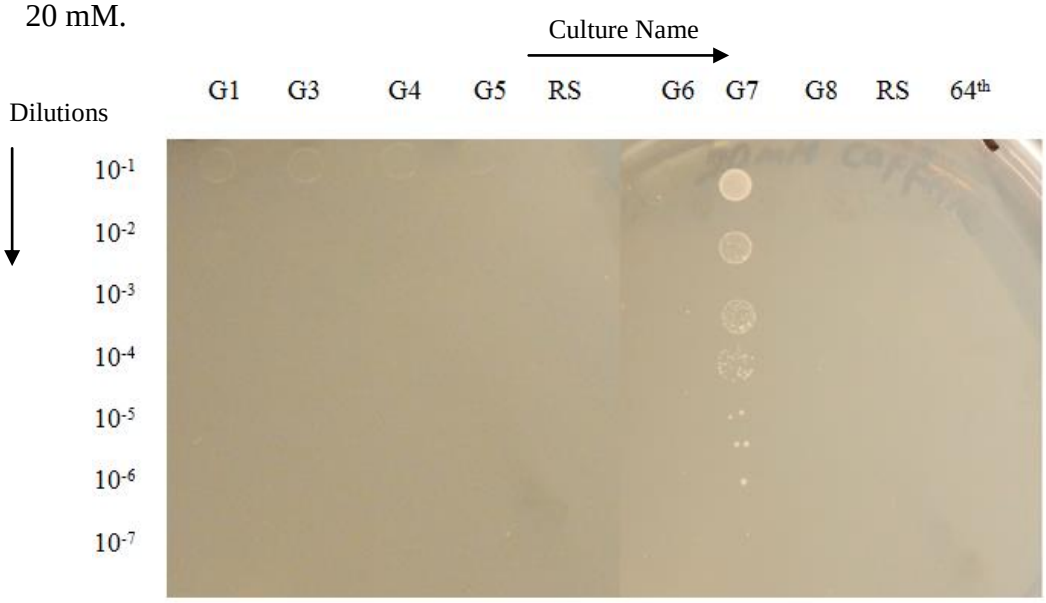

Figure 3.31: Mutant individuals, 64th population and the RS on LB plate with 20 mM caffeine stress after four days of incubation.

Selected seven mutant individuals, 64th population, and the RS could not grow on solid LB media containing zinc chloride (2.5 mM, 5 mM, 10 mM), zinc sulfate (5 mM, 10 mM), aluminium chloride (10 mM), manganese (II) chloride (20 mM, 25 mM), ammonium iron (II) sulfate (10 mM, 25 mM, 50 mM), ethanol (15% v/v), iron (II) chloride (6 mM, 8 mM, 10 mM, 25 mM, 50 mM), nickel (II) chloride (2.75 mM, 5 mM, 10 mM).

3.5 Genetic Stability Analysis of Mutant Individuals

As described in Section 2.2.4, genetic stability test was performed in order to test if the gained cobalt resistance of G4, G6, G7 is permenant or not. Mutant individuals' precultures were inoculated to 10 mL M27 and after incubation at 30°C and at 150 rpm, 1 OD_{535} unit of cells were centrifuged at 13,000 rpm for 5 min. This cultivation was repeated 10 times and MPN method was performed to estimate cell numbers that can survive under different $CoCl_2$ stress.

Mutants were cultured with M27 to control and M27 containing 4 mM, 8 mM and 12 mM $CoCl_2$ to do MPN. To test for potential contamination, G4, G6 and G7 were inoculated into solid LB on the first and sixth day of the genetic stability test.

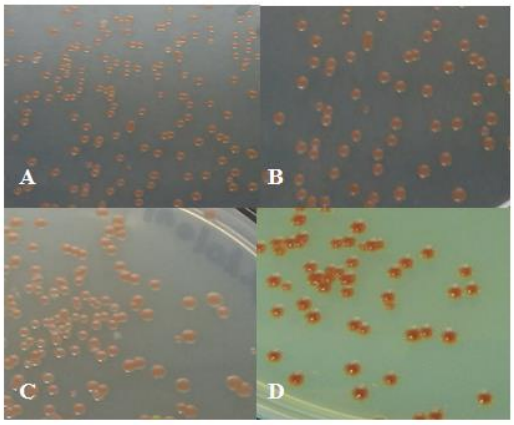

Figure 3.32: 10^6-fold diluted G4 (A), G6 (B) and G7 (C) mutants and the RS (D) spread on solid LB plates on the first day of the genetic stability test.

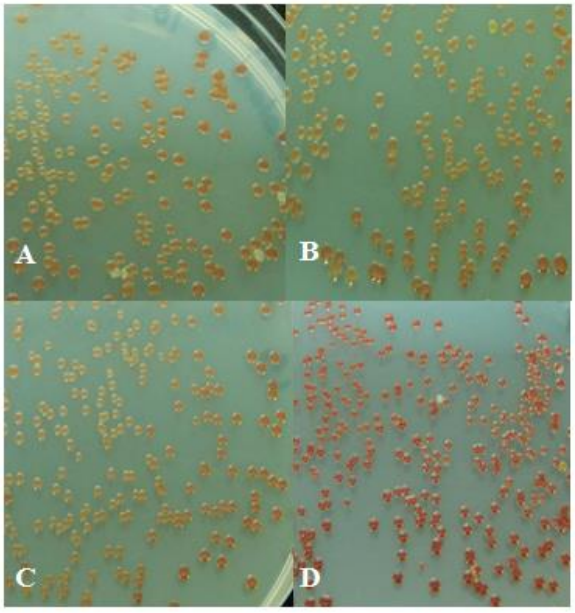

Figure 3.33: 10^6-fold diluted G4 (A), G6 (B), G7 (C) mutants and the RS (D) spread on LB plates on the sixth day of the genetic stability test.

According to Figure 3.32 and Figure 3.33, mutant G4, G6 and G7 were bright red coloured, while colonies of the RS were dark red. In addition, it can be observed that the mutants individuals were morphologically the same on the first and the sixth day.

Table 3.4: Cell numbers and percent survival rates after four days of incubation.

Days	Individual number	Cell Number (cell/mL)			% Survival rate for 4 mM $CoCl_2$	% Survival rate for 8 mM $CoCl_2$
		0 mM	4 mM	8 mM		
1	**4**	$1.1x10^8$	$2.4x10^6$	$5.4x10^5$	2.18	0.49
	6	$1.1x10^8$	$3.5x10^6$	$1.6x10^6$	3.18	1.45
	7	$1.6x10^8$	$2.4x10^7$	$2.4x10^6$	15.00	1.50
	RS	$2.2x10^8$	$2.3x10^2$	$2.3x10^1$	0	0
2	**4**	$2.2x10^8$	$2.4x10^6$	$2.4x10^5$	1.09	0.11
	6	$1.6x10^8$	$2.4x10^6$	$1.6x10^6$	1.50	1.00
	7	$1.7x10^8$	$2.4x10^6$	$1.6x10^6$	1.41	0.94
	RS	$2.2x10^8$	$2.4x10^2$	$2.3x10^1$	0	0
3	**4**	$2.4x10^8$	$2.4x10^6$	$2.4x10^5$	1.00	0.10
	6	$2.4x10^8$	$2.4x10^6$	$3.5x10^5$	1.00	0.15
	7	$1.6x10^8$	$2.4x10^5$	$2.4x10^5$	0.15	0.15
	RS	$5.4x10^7$	$1.3x10^2$	$1.3x10^2$	0	0
4	**4**	$3.5x10^8$	$5.4x10^5$	$3.5x10^4$	0.15	0.01
	6	$1.1x10^8$	$2.4x10^6$	$2.4x10^5$	2.18	0.22
	7	$1.6x10^8$	$2.4x10^6$	$2.4x10^5$	1.50	0.15
	RS	$2.4x10^8$	$1.3x10^2$	$2.3x10^1$	0	0
5	**4**	$2.4x10^8$	$2.4x10^6$	$2.4\ x10^5$	1.00	0.10
	6	$1.6x10^9$	$5.4x10^5$	$2.4x10^5$	0.03	0.02
	7	$1.6x10^8$	$9.4x10^6$	$2.4\ x10^5$	5.88	0.15
	RS	$5.4x10^8$	$1.3x10^2$	$2.3x10^1$	0	0
6	**4**	$7.0x10^7$	$2.4x10^5$	$2.4\ x10^4$	0.34	0.03
	6	$1.6x10^8$	$2.4x10^6$	$3.5x10^5$	1.50	0.22
	7	$2.2x10^8$	$2.4x10^6$	$9.2x10^5$	1.09	0.42
	RS	$1.7x10^8$	$2.3x10^1$	$2.3x10^1$	0	0
7	**4**	$1.8x10^9$	$2.4x10^5$	$2.4x10^4$	0.01	0
	6	$1.7x10^8$	$3.5x10^5$	$2.4x10^5$	0.21	0.14
	7	$1.4x10^8$	$2.4x10^6$	$5.4x10^5$	1.71	0.39
	RS	$3.3x10^8$	$2.4x10^2$	$2.3x10^1$	0	0
8	**4**	$3.5x10^{10}$	$2.4x10^6$	$2.4x10^5$	0.01	0

Table 3.4 (continued): Cell numbers and percent survival rates after four days of incubation.

Days	Individual number	Cell Number (cell/mL)			% Survival rate for 4 mM $CoCl_2$	% Survival rate for 8 mM $CoCl_2$
		0 mM	4 mM	8 mM		
8	**6**	$3.5x10^{10}$	$2.4x10^{6}$	$2.4x10^{5}$	0.01	0
	7	$9.4x10^{8}$	$2.4x10^{6}$	$2.4x10^{6}$	0.26	0.26
	RS	$2.8x10^{9}$	$2.3x10^{1}$	$2.3x10^{1}$	0	0
9	**4**	$3.5x10^{8}$	$9.2x10^{5}$	$1.6x10^{6}$	0.26	0.46
	6	$2.6x10^{8}$	$2.4x10^{6}$	$2.4x10^{5}$	0.92	0.09
	7	$5.4x10^{8}$	$3.5x10^{6}$	$2.4x10^{6}$	0.65	0.44
	RS	$3.5x10^{8}$	$4.9x10^{1}$	$3.3x10^{1}$	0	0
10	**4**	$5.4x10^{7}$	$1.6x10^{6}$	$5.4x10^{5}$	2.96	1.00
	6	$5.4x10^{7}$	$2.4x10^{6}$	$2.4x10^{5}$	4.44	0.44
	7	$9.2x10^{7}$	$2.4x10^{6}$	$2.4x10^{6}$	2.61	2.61
	RS	$3.5x10^{8}$	$2.3x10^{1}$	$2.3x10^{1}$	0	0

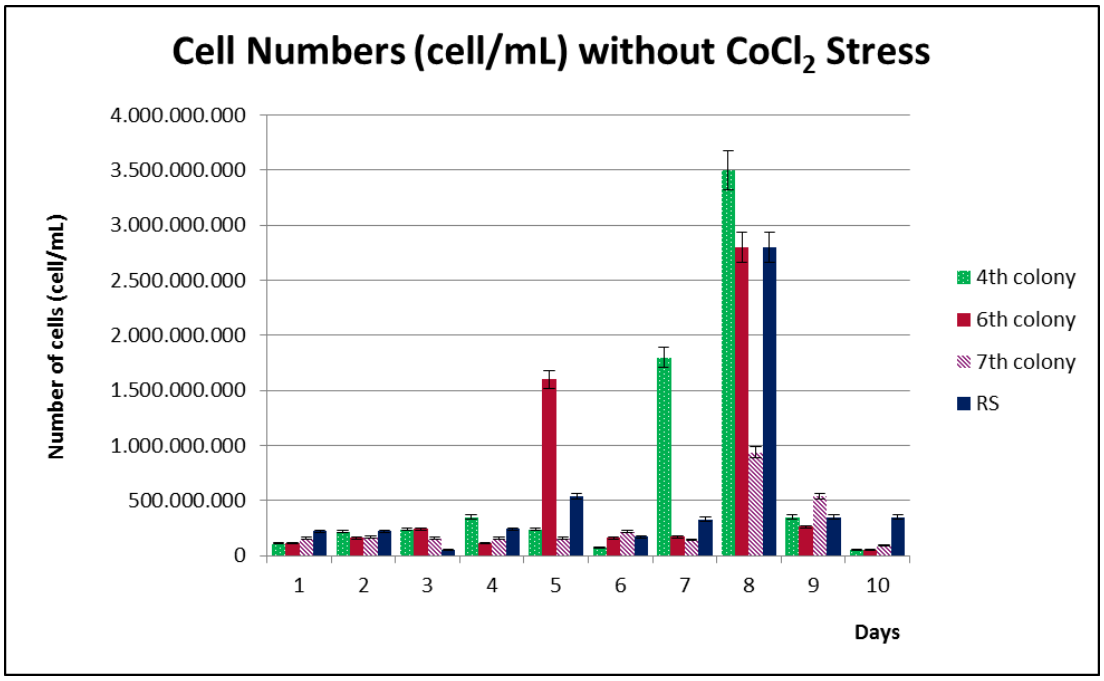

Figure 3.34: Viable cell numbers (cell/mL) of G4, G6, G7 in control media without $CoCl_2$ stress.

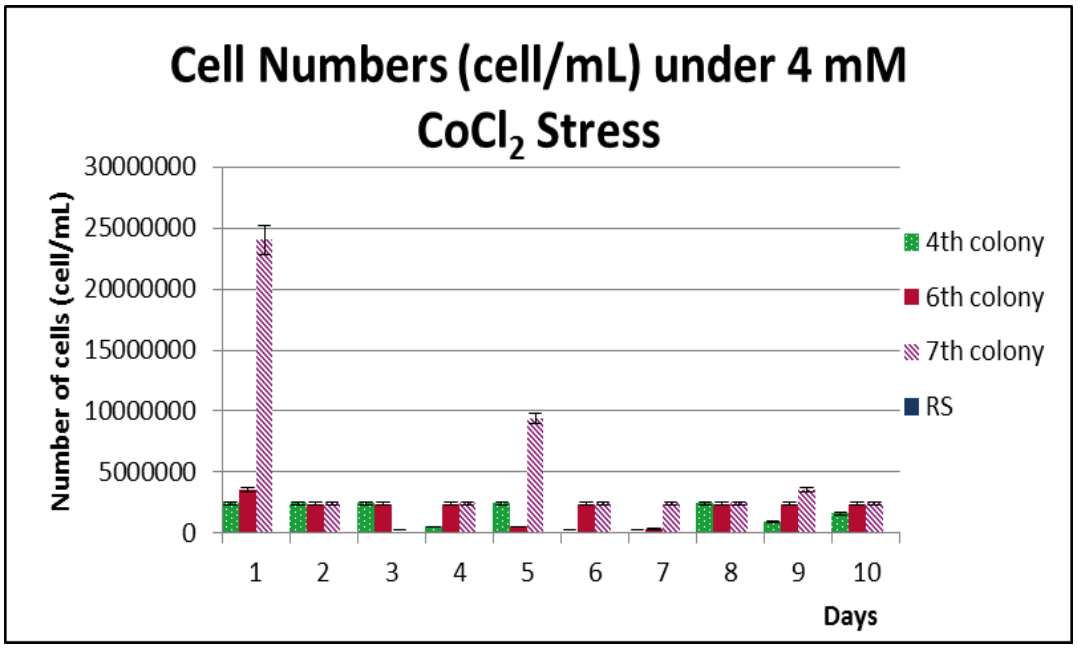

Figure 3.35: Viable cell numbers of G4, G6, G7 and the RS that survived in the presence of 4 mM $CoCl_2$.

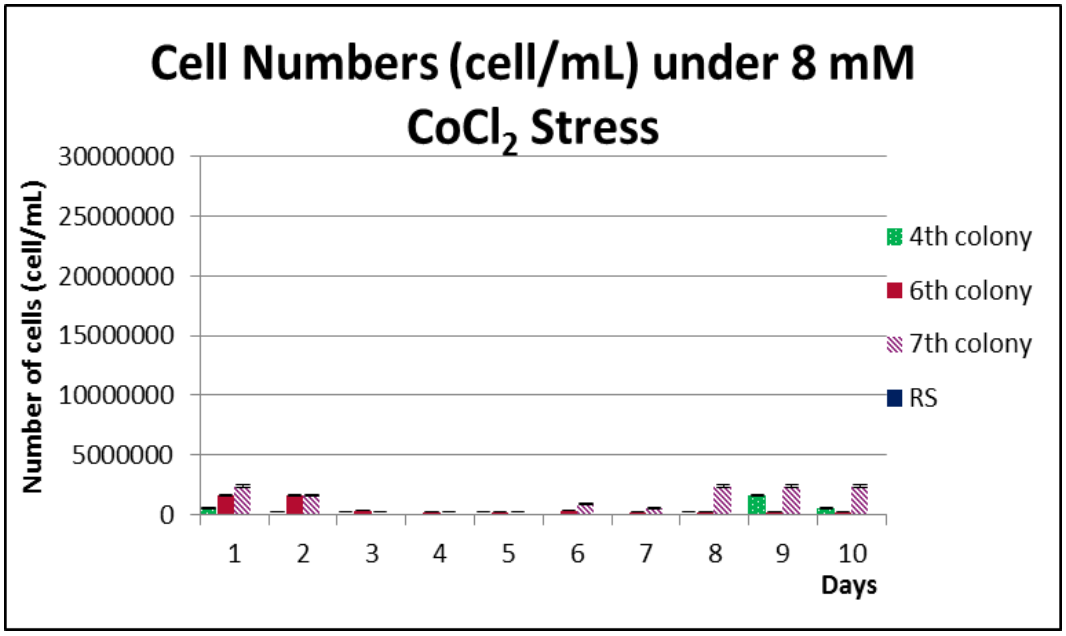

Figure 3.36: Viable cell numbers (cell/mL) of the mutant individuals under 8 mM $CoCl_2$ stress.

All mutants analyzed by genetic stability test showed higher resistance values under 4 mM $CoCl_2$ stress, when compared to RS. However, as indicated in Figure 3.38, cell numbers of the individuals decreased sharply day by day. % survival rate values were calculated by dividing numbers of cells after stress exposure by that of non-treated cells.

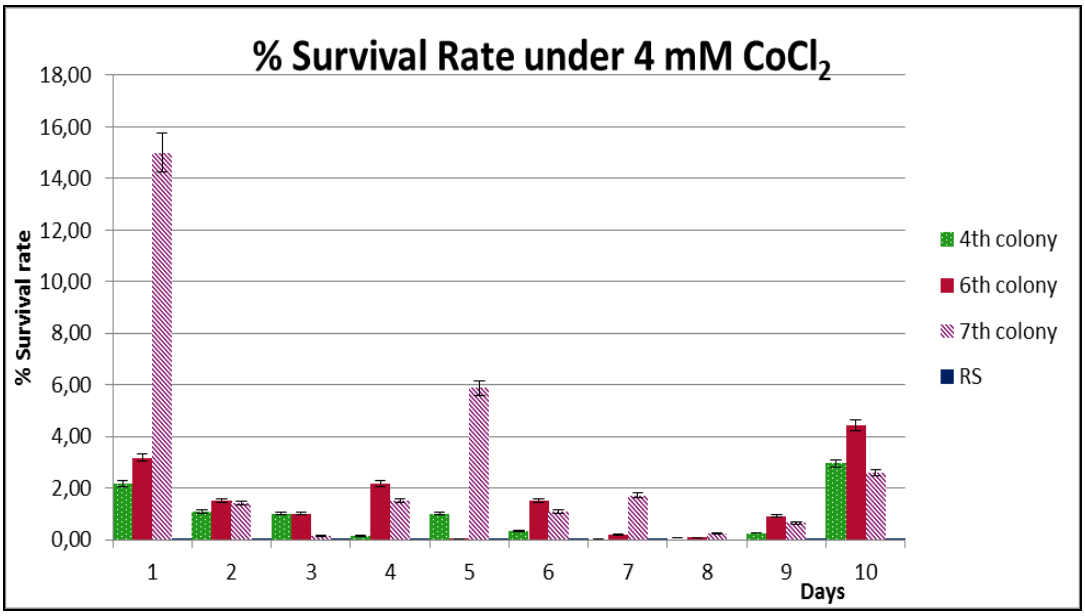

Figure 3.37: Survival rate values upon each following incubation for ten days under 4 mM $CoCl_2$ stress.

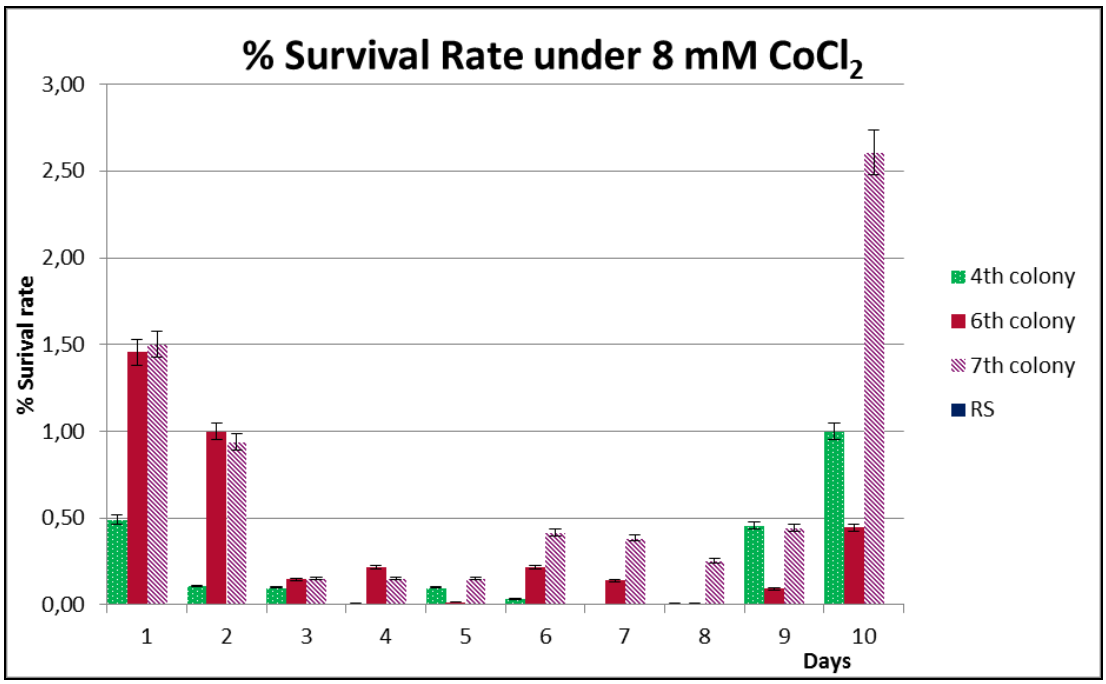

Figure 3.38: Survival rate values upon each following incubation for ten days under 8 mM $CoCl_2$ stress.

According to the Figure 3.37 and 3.38, percent survival values of the individuals decreased during the experiment, which may imply that mutants were not stable under cobalt stress. However, when compared to RS, G4, G6 and G7 were genetically stable, as shown in Figure 3.40 and 3.41. Survival of the mutant

individuals were calculated by dividing the number of the cells (cell/mL) of G4, G6 and G7 to that of the RS, under 4 mM and 8 mM $CoCl_2$ stress.

Table 3.5: Survival of the mutant individuals as fold of RS survival.

Days	Individual number	Cell number (cell/mL) of the colony / cell number (cell/mL) of RS		
		0 mM	4 mM	8 mM
1	**4**	0.5	10435	23478
	6	0.5	15217	69565
	7	0.7	104348	104348
2	**4**	1	10000	10435
	6	0.7	10000	69565
	7	0.8	10000	69565
3	**4**	4.4	18462	1846
	6	4.4	18462	2692
	7	3.0	1846	1846
4	**4**	1.5	4154	1522
	6	0.5	18462	10435
	7	0.7	18462	10435
5	**4**	0.4	18462	10435
	6	3.0	4154	10435
	7	0.3	72308	10435
6	**4**	0.4	10435	1043
	6	0.9	104348	15217
	7	1.3	104348	40000
7	**4**	5.5	1000	1043
	6	0.5	1458	10435
	7	0.4	10000	23478
8	**4**	1.3	104348	10435
	6	1.0	104348	10435
	7	0.3	104348	104348
9	**4**	1.0	18776	48485
	6	0.7	48980	7273
	7	1.5	71429	72727
10	**4**	0.2	69565	23478
	6	0.2	104348	10435
	7	0.3	104348	104348

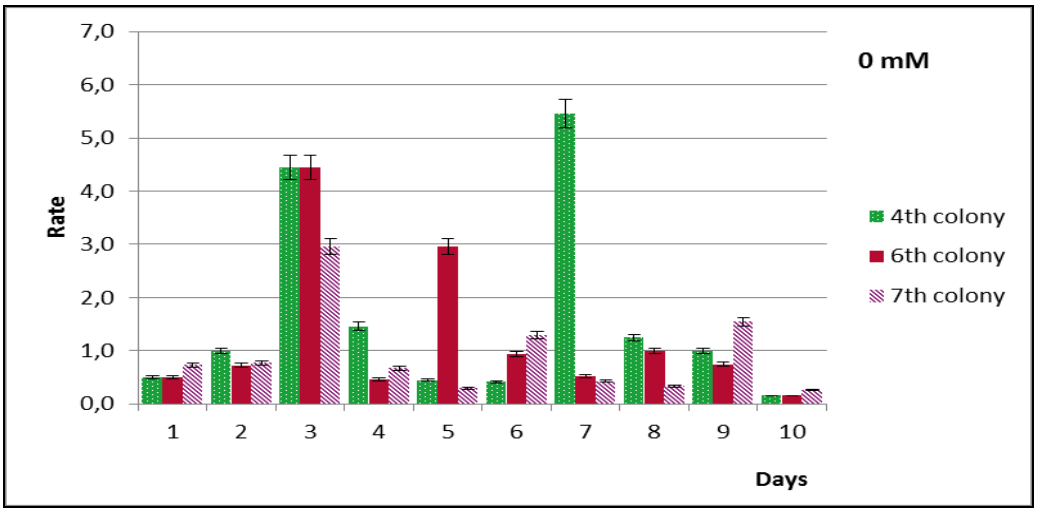

Figure 3.39: Survival as fold of RS in control media without stress.

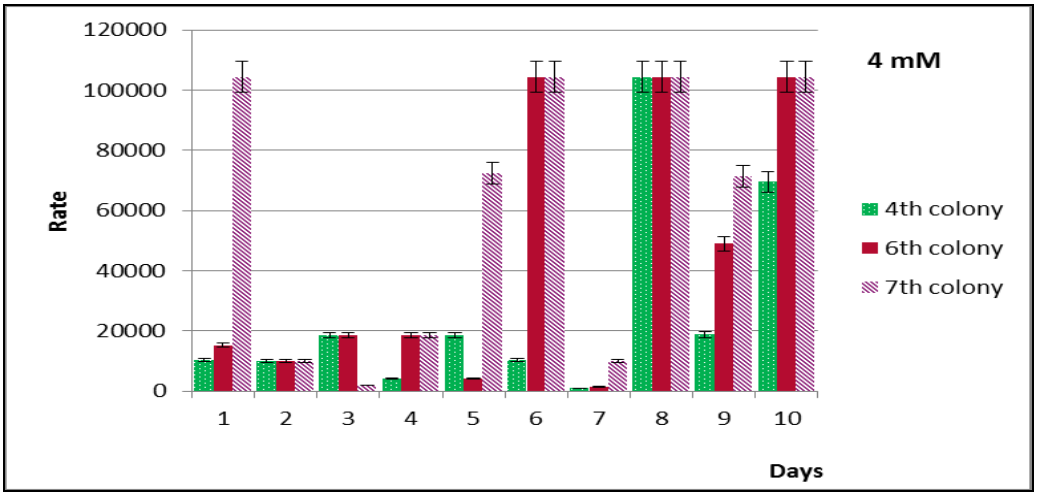

Figure 3.40: Survival as fold of RS under 4 mM $CoCl_2$ stress.

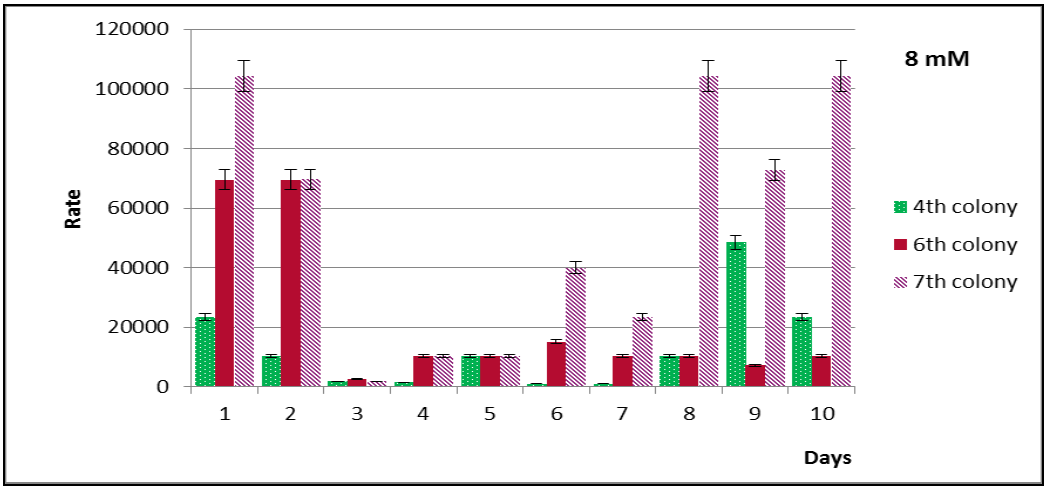

Figure 3.41: Cell numbers (cell/mL) of G4, G6 and G7 was divided to cell number of the RS under 8 mM $CoCl_2$ stress.

The results obtained by this genetic stability test were not satisfactory to decide about the genetic stability. For this reason, continuous $CoCl_2$ stress exposure was applied to G4, G6, G7 and RS as control.

3.6 Continuous $CoCl_2$ Stress Exposure

According to the MPN results, mutants exposed to higher concentrations of $CoCl_2$ than 4 mM had low resistance to cobalt. In spite of this, 4 mM $CoCl_2$ concentration was chosen for the stress exposure test.

G4, G6 and G7 were tested for their genetic stability after 4 mM $CoCl_2$ exposure for five days by spot assay test. Each dilution of the selected mutant was spotted onto LB plates containing 1 mM, 2 mM, 3 mM, 4 mM, 5 mM and 7 mM $CoCl_2$. Plates were incubated at 30°C for four days.

3.6.1 Control plate

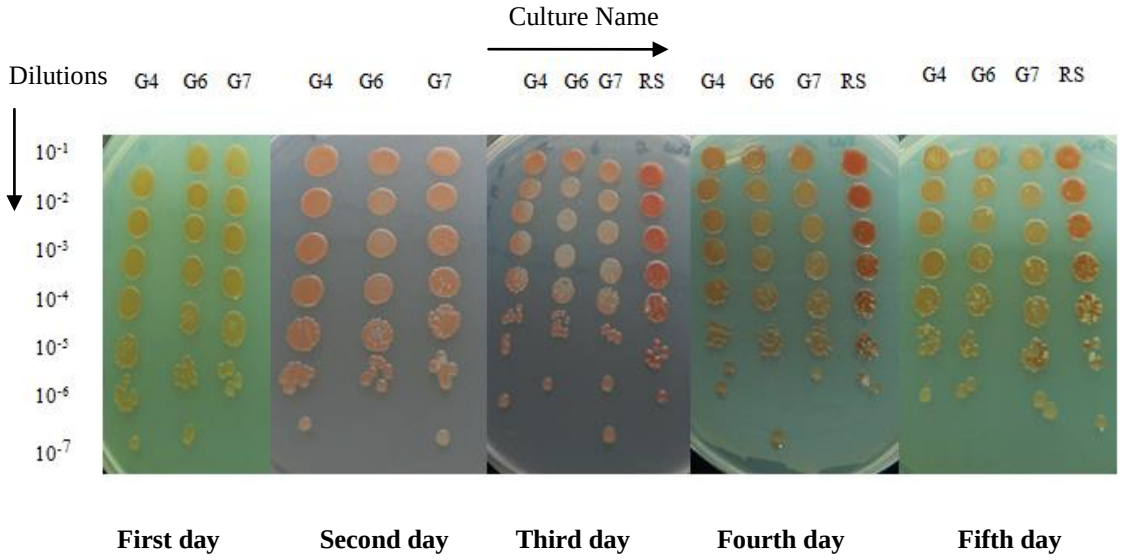

Figure 3.42: Mutant individuals (G4, G6, G7) and the RS plated on solid LB without stress day by day.

The RS could not be used in the spot assay on the first and second days of the experiment, as it did not grow until day three. After two days of incubation at 30°C and 150 rpm, OD_{535} value of RS reached normal levels as the selected mutants, and it was spotted on LB like G4, G6 and G7.

3.6.2 1 mM $CoCl_2$

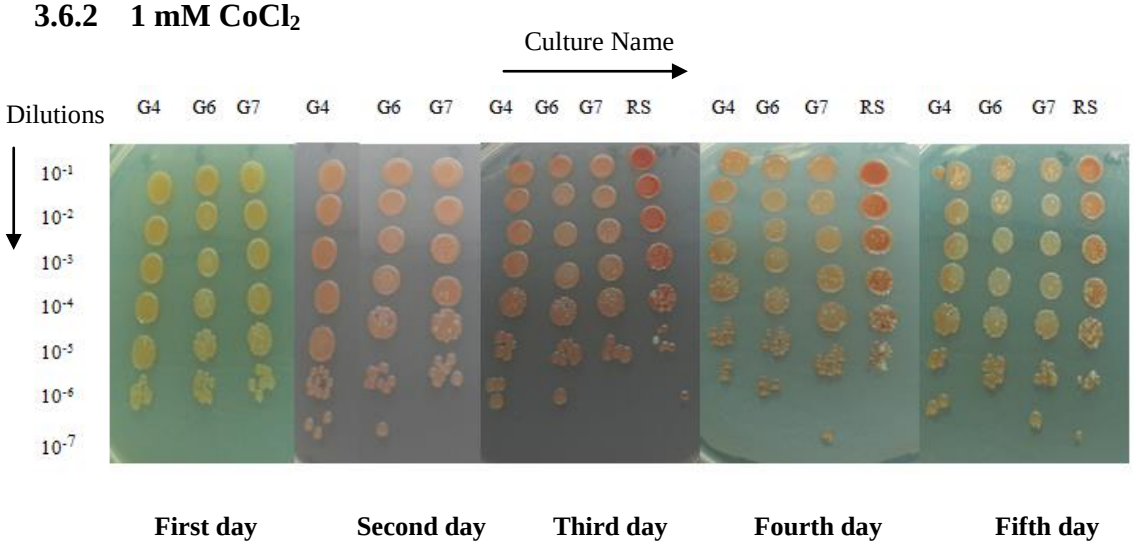

Figure 3.43: Mutant individuals and the RS on LB containing 1 mM $CoCl_2$. Growth was monitored after four days of incubation at 30°C during five days.

Under 1 mM $CoCl_2$ stress, cobalt resistance of selected mutants were similar to that of the RS (Figure 3.43).

3.6.3 2 mM $CoCl_2$

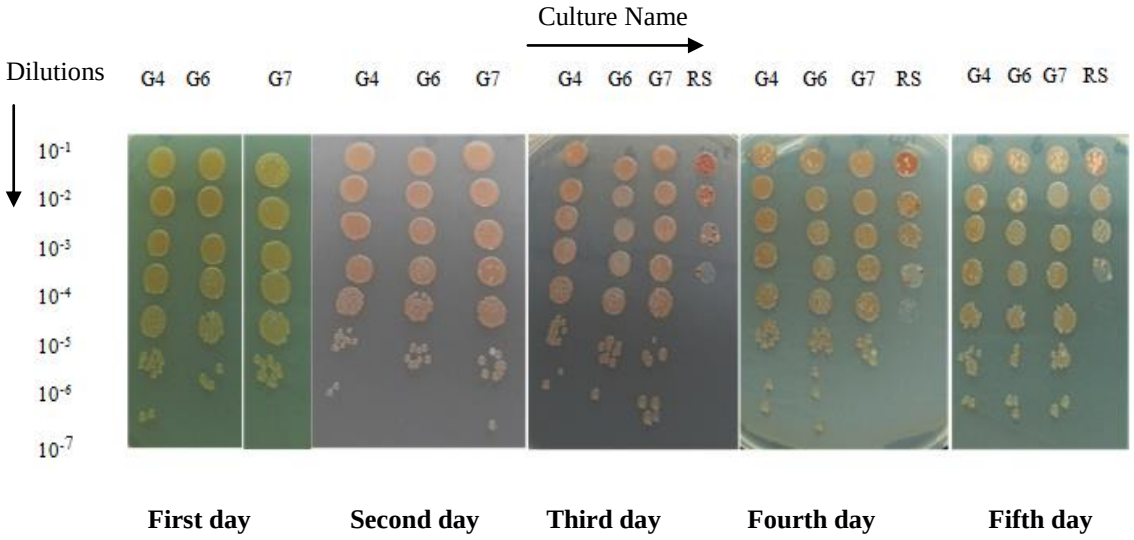

Figure 3.44: Mutant individuals and RS under 2 mM $CoCl_2$ stress after four days of incubation at 30°C.

3.6.4 3 mM $CoCl_2$

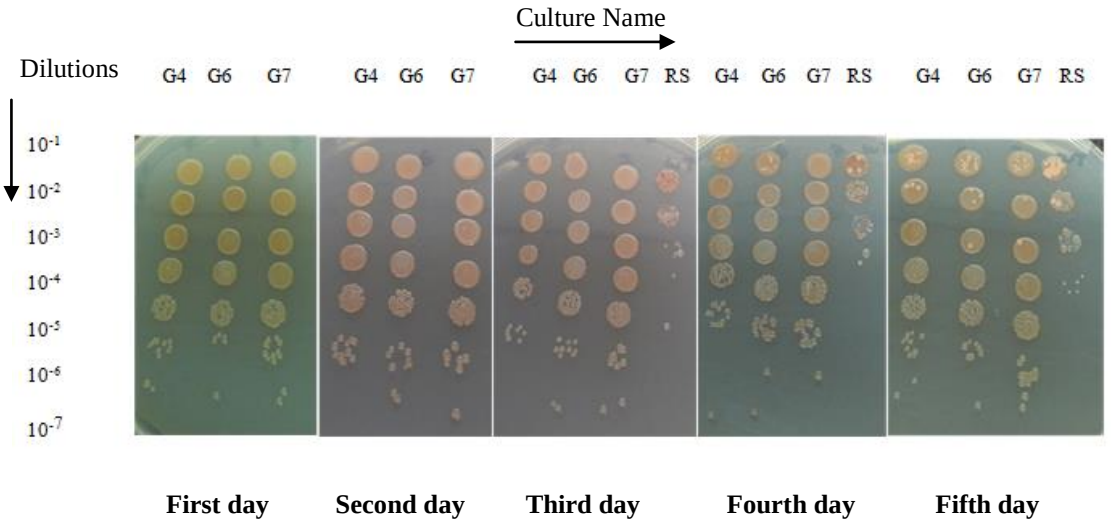

Figure 3.45: Mutant individuals and the RS on LB plate with 3 mM $CoCl_2$ stress. Growth was monitored after four days of incubation.

With regard to Figure 3.45, 10^7-fold diluted mutants could survive on the fifth day, like on the first day. According to this, it can be said that G4, G6 and G7 are genetically stable under 3 mM $CoCl_2$ stress.

3.6.5 4 mM $CoCl_2$

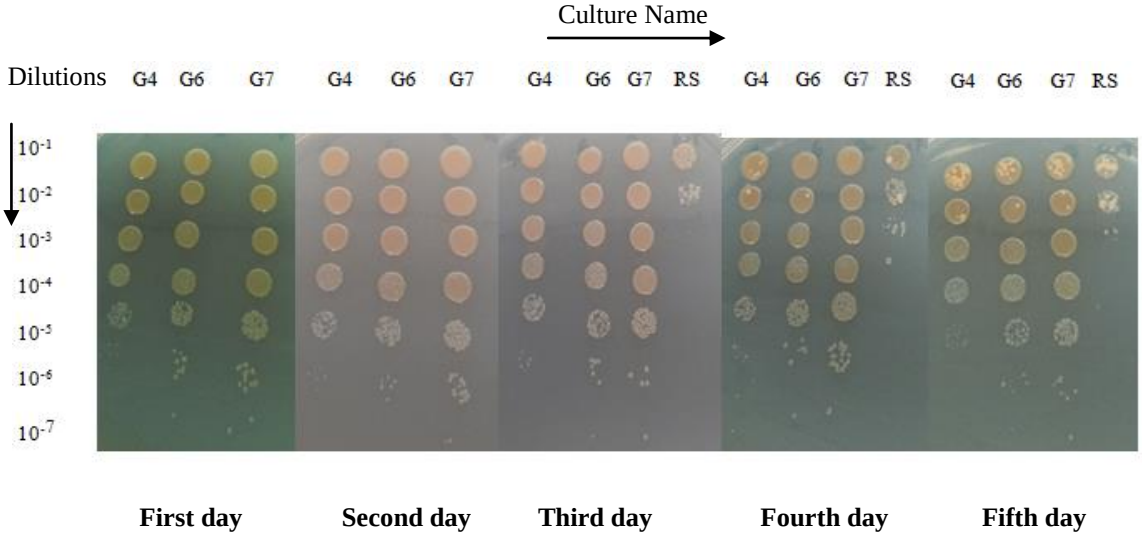

Figure 3.46: G4, G6, G7 and the RS under 4 mM $CoCl_2$ stress after four days of incubation.

3.6.6 5 mM $CoCl_2$

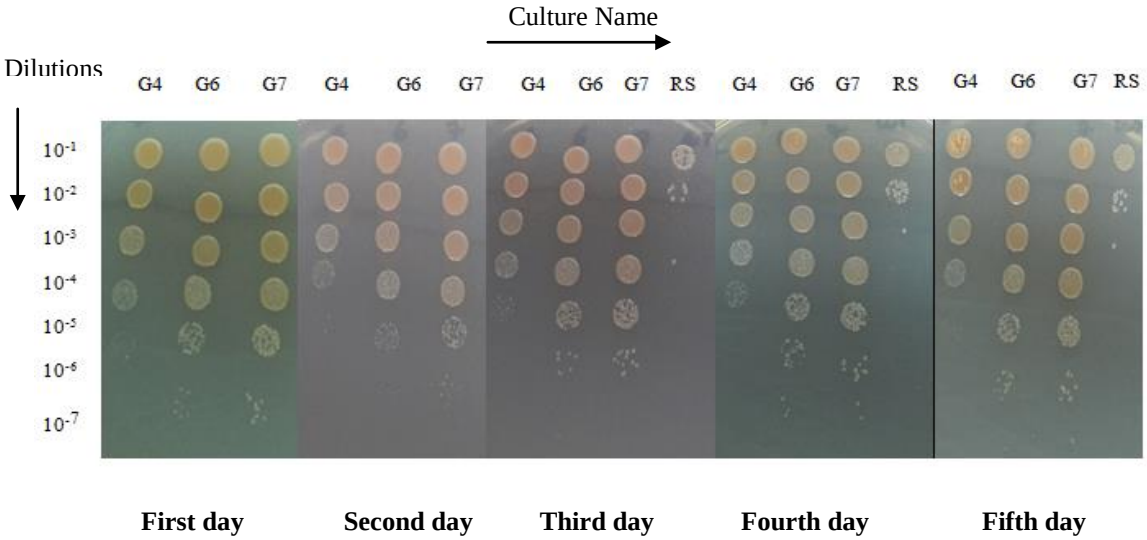

Figure 3.47: Mutant individuals and the RS under 5 mM $CoCl_2$ stress after four days of incubation.

It was observed that G6 and G7 were more resistant to 5 mM $CoCl_2$ stress than G4. RS barely survived under this stress condition.

3.6.7 7 mM $CoCl_2$

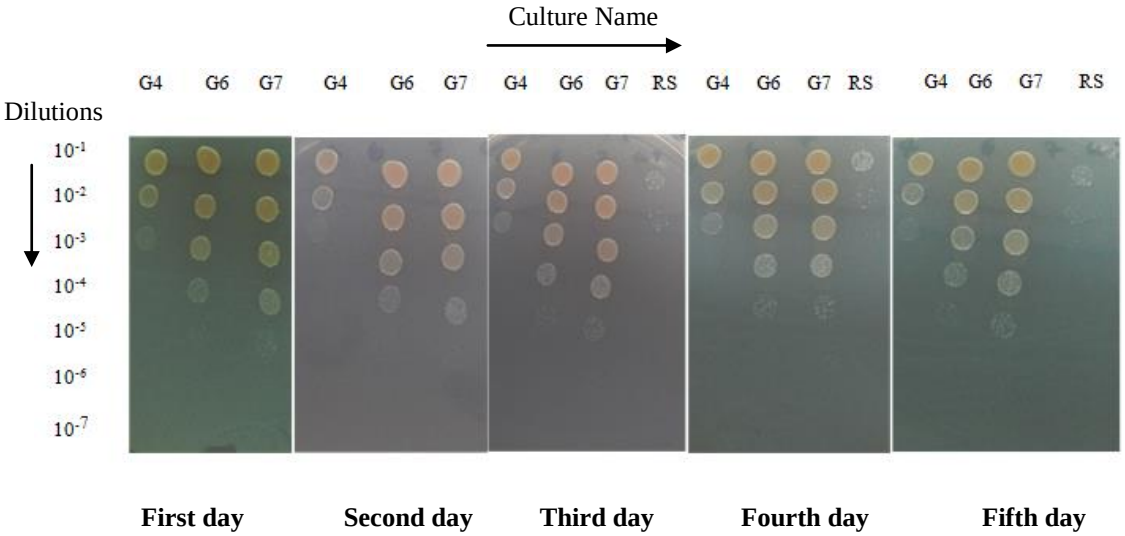

Figure 3.48: Mutant individuals and the RS on LB with 7 mM $CoCl_2$ after four days of incubation.

According to the experimental results, it is clear that the mutant individuals obtained by evolutionary engineering approach were genetically stable. G6 and G7 were more resistant to cobalt stress than G4, and RS spotted on LB with 7 mM $CoCl_2$ could not survive under this condition while the mutant individuals could.

3.7 Growth Curves of RS and G7

Growth curves of the RS and G7 without stress and under 4 mM $CoCl_2$ stress were obtained by measuring OD_{535} at selected time points (Table 3.6). Cultures were incubated at 30°C at 150 rpm for 72 hours.

Table 3.6: OD_{535} values of RS and G7.

Time (hour)	RS OD_{535} AVG	G7 OD_{535} AVG	RS 4 mM $CoCl_2$ OD_{535} AVG	G7 4 mM $CoCl_2$ OD_{535} AVG
2	0.38	0.45	0.09	0.05
3.5	0.42	0.51	0.31	0.38
5	0.79	0.75	0.42	0.55
7	1.38	1.19	0.53	0.79
9	2.18	1.72	0.67	1.12
11	2.55	2.32	0.57	1.54
13.5	2.72	2.59	0.73	1.97
16	2.94	2.87	0.90	2.51
21	3.46	3.66	1.31	3.53
24.5	3.29	3.57	1.18	2.98
28	3.32	3.83	1.53	3.18
38.5	3.24	3.64	1.70	3.21
54.5	3.35	3.20	2.26	3.45
83	3.13	2.93	2.39	2.85

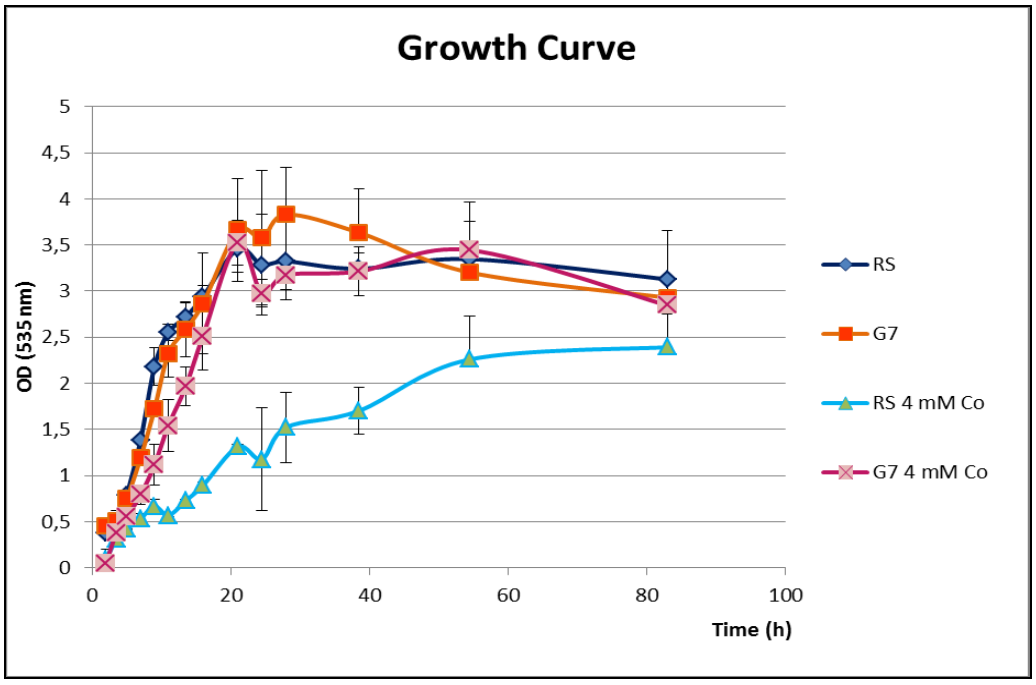

Figure 3.49: Growth curves of RS and G7 in the presence and absence of $CoCl_2$.

As shown in Figure 3.49, it was observed that there was a short lag phase until the 3rd hour both for RS and G7, the cells then entered the exponential phase at the 3rd hour. RS reached the stationary phase at 28 h, similar to G7 in the presence and absence of $CoCl_2$. However, OD_{535} values of G7 without stress were higher than those of RS and G7 with 4 mM $CoCl_2$. Final OD_{535} value of RS in the presence of $CoCl_2$ was the lowest, as expected.

3.8 Determination of Cell Dry Weights (CDWs)

CDWs of RS and G7 were obtained in the presence and absence of $CoCl_2$ in triplicate. Avarage cell dry weights of the cultures are depicted in Figure 3.53.

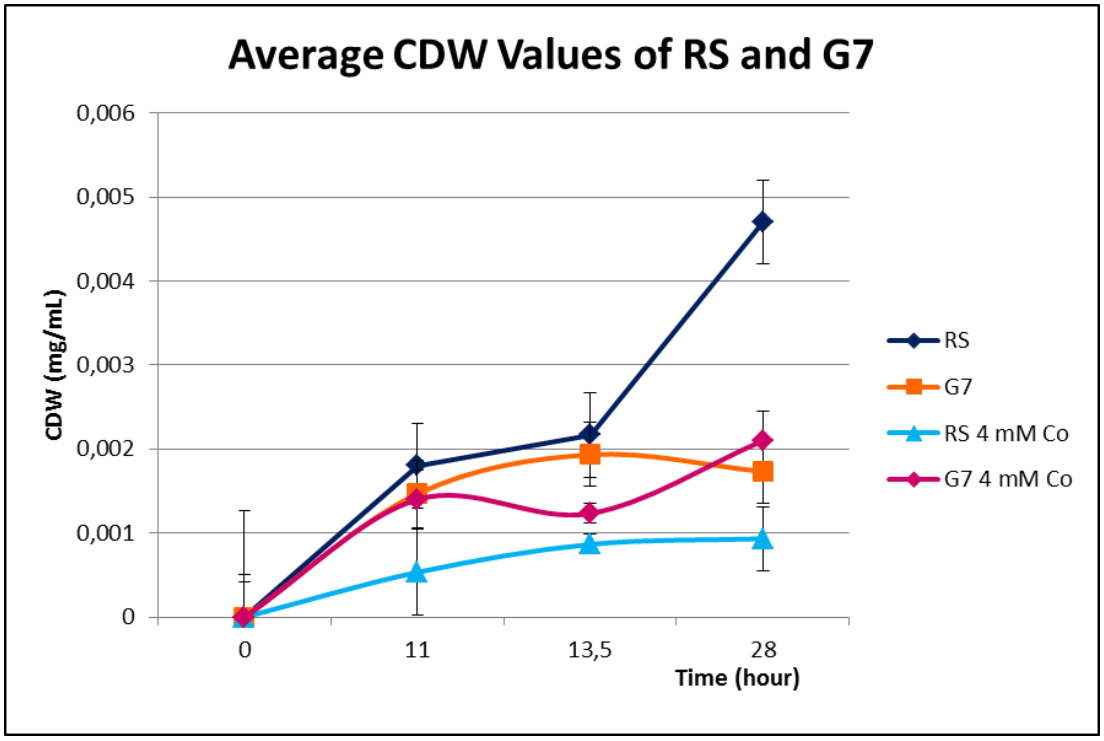

Figure 3.50: Average CDW results of RS and G7 with cobalt stress and without stress.

As shown in Figure 3.50, there is not a good correlation between the growth curve of RS and G7 through OD_{535} measurements and the CDW values. At the 28th hour of incubation, average CDW values for RS and G7 without and with $CoCl_2$ stress were 0.0047, 0.0017, 0.0009, 0.0021 (mg/mL), respectively.

4. DISCUSSION & CONCLUSIONS

In this thesis study, mutant individuals were selected from a cobalt-resistant *R. sphaeroides* population obtained by evolutionary engineering method, and they were physiologically analysed. Eight individuals were selected from the last population and their stress resistances were determined by MPN method, spot assay and cross-resistance tests. In addition, genetic stability analyses were performed to understand whether their resistance is permanent or not.

Screening test was performed by optical density measurements of RS at 535 nm and Viable Cell Counting method (VCC). Percent survival rate values were quite high according to the OD_{535} measurements of the screening test at high concentrations of $CoCl_2$. This was resulting from cobalt sedimentation that occurs during cultivation under high concentrations of cobalt. As a result, OD_{535} measurements were not correlated with VCC values obtained by spreading cultures onto solid LB plates containing cobalt stress. VCC results showed that RS had the highest survival rate under mild cobalt stress (5mM) after 25 hours of incubation.

At the beginning of the evolutionary engineering strategy, the RS was exposed to 0.1 mM $CoCl_2$ concentration and this concentration was increased continuously until 15 mM. The survival ratio of the 64^{th} population was %21, but cobalt sedimentation during incubation of the cultures prevented increasing of $CoCl_2$ stress. The last (64^{th}) population was spread on solid LB plate and 8 mutant individuals (G1, G2, G3, G4, G5, G6, G7, G8) were selected with various levels of red pigmentation. *R. sphaeroides* cultures had a high risk of contamination, thus working with them was difficult. Due to this, in early stages of the study, G2 was contaminated and excluded from the experiments. To estimate cobalt resistance levels of the mutant individuals, spot assay and MPN methods were performed.

According to the MPN results, survival rate of the mutants as fold of RS reached the highest values in the presence of 4 mM $CoCl_2$, compared to results at 2 mM, 6 mM, 8mM $CoCl_2$ concentrations. However, results obtained by the MPN method were not

very satisfactory, because of counting cell numbers based on turbidity differences, and not single colony formation in 96-well plates.

In spot assay, mutant individuals were tested for their cobalt resistance on solid LB plates with different $CoCl_2$ concentrations. Resistance was apparently observed under 3 mM $CoCl_2$ stress and above this concentration. While RS could not grow on plates with this concentrations, 10^6-fold diluted mutants could survive.

To understand whether there is a relationship between cobalt resistance and resistance to other stress types, cross-resistance analyses were performed. According to the results, mutant individuals showed lower resistance than RS only at 1 mM $ZnCl_2$. Also, mutants showed the same or slightly lower resistance at 0.5 mM $CuCl_2$, 2 mM $NiCl_2$,1 mM and 2 mM H_2O_2, 4 mM $FeCl_2$, 8% (v/v) ethanol and 500 mM $MgCl_2$ stress conditions, compared to RS. Mutants on LB with 10 mM $MnCl_2$ were more resistant than RS and appeared as white on media, suggesting that cells might have lost the ability to produce pigments under $MnCl_2$ stress. The most striking result of the cross-resistance test was the high level of resistance of G7 against a wide range of stress types. Except for G7, none of the mutants and the RS could survive at 5 mM $FeCl_2$, 30 mM and 50 mM H_3BO_3, 0.5 M NaCl, 5mM $AlCl_3$, 2.2 mM and 2.4 mM $NiCl_2$, 5 mM $(NH_4)_2Fe(SO_4)_2$, 750 mM and 1 M $MgCl_2$ and 20 mM caffeine. The highest Ni^{2+} concentration (2.4 mM) at which G7 could grow was higher than the inhibitory concentration of Ni^{2+} (1 mM) in *E. coli*. In addition, all individuals and the RS survived at 1 mM $ZnCl_2$ stress, which was the minimal inhibitory concentration of Zn^{2+} in *E. coli* (Nies, 1999).

Nies (1999) suggested that heavy metal ions may interact with physiological cations such as Co^{2+} with Fe^{2+}, Zn^{2+} with Mg^{2+}, by changing the characteristics of the physiological ions. As a result, resistance of the mutants against various metal stresses were possibly gained through evolutionary engineering approach by exposure to gradually increasing $CoCl_2$ concentrations.

Sequence analysis was performed to make sure that the high resistance of G7 was not related to contamination. Therefore, in addition to G7; G4 and G6 were also chosen for sequencing. BLAST programme was used to search for the similarity between sequences of reference strain of the *R. sphaeroides* and the mutants. After sequence

analysis, it was found that the level of 16s rRNA identity of the mutants with the reference strain was 99 % or more with the reference strain.

Genetic stability tests of G4, G6 and G7 were performed by MPN method for 10 days. Stress condition was applied as 4 mM and 8 mM $CoCl_2$ stress. The results obtained after 4 days of incubation via MPN demonstrated that mutants were genetically unstable under $CoCl_2$ stress, but MPN test results of the *R. sphaeroides* mutants were not trusted. Therefore, genetic stability of the mutants was investigated by continuous $CoCl_2$ exposure. For this purpose, G4, G6 and G7 were exposed to 4 mM $CoCl_2$ stress for 5 days, and then adjusted to fresh medium without cobalt during five days. Spot assay test was performed for the mutants and the RS day by day, but the RS that could not grow in 2 days after cobalt stress was spotted on plates on the third day of the experiment. It can be concluded that the resistance of the mutants did not decrease at each day, and as a result selected mutant individuals showed genetic stability for five passages.

Growth curves of RS and G7 were obtained in the presence and absence of 4 mM $CoCl_2$ stress. The growth curve of the RS under control conditions was not the same as but similar to that reported by Giotto et al. (Giotto et al., 2006). They reported the duration of the exponential phase of wild type *R. sphaeroides* as 40 hours, while in this study exponential growth phase of the reference strain lasted for 28 hours. In addition, growth patterns of the mutant G7 with stress and without stress conditions were similar to that of RS. While RS under stress had a similar growth trend as G7, the OD_{535} values of the RS were significantly below that of G7.

To summarize, cobalt-resistant and genetically stable mutant individuals of *R. sphaeroides* were succesfully obtained using evolutionary engineering. Physiological characterization of the mutant strains showed that the mutants were not only resistant to $CoCl_2$, but also cross-resistant to a variety of stress types. Detailed transcriptomic and/or proteomic analyses may help understand the molecular mechanisms of $CoCl_2$-tolerance in the metabolically diverse and biotechnologically important bacterium, *R. sphaeroides.*

5. REFERENCES

Akroum-Amrouche, D., Abdi, N., Lounici, H., Mameri, N. (2011). Effect of physico-chemical parameters on biohydrogen production and growth characteristics by batch culture of *Rhodobacter sphaeroides* CIP 60.6, *Applied Energy*, 88: 2130-2135.

Berry, R. M., Armitage, J. P. (2000). Response kinetics of tethered *Rhodobacter sphaeroides* to changes in light intensity, *Biophysical Journal*, 78 (3): 1207-1215.

Bertani, G. (1951). Studies on lysogenesis. I. The mode of phage liberation by lysogenic *Escherichia coli*, *Journal of Bacteriology*, 62: 293-300.

Borsetti, F., Tremaroli, V., Michelacci, F., Borghese, R., Winterstein, C., Daldal, F., Zannoni, D. (2005). Tellurite effects on *Rhodobacter capsulatus* cell viability and superoxide dismutase activity under oxidative stress conditions, *Research in Microbiology*, 156 (7): 807-13.

Chang, C. H., El-Kabbani, O., Tiede, D., Norris, J., Schiffer, M. (1991). Structure of the membrane-bound protein photosynthetic reaction center from *Rhodobacter sphaeroides*, *Biochemistry*, 30 (22): 5352-5360.

Choudhary, M., Yun-Xin, F., Mackenzie, C., Kaplan, S. (2004). DNA sequence duplication in *Rhodobacter sphaeroides* 2.4.1: Evidence of an ancient partnership between chromosomes I and II, *Journal of Bacteriology* 186 (7): 2019-2027.

Choudhary, M., Zanhua X., Fu, Y. X., Kaplan S. (2007). Genome analyses of three strains of *Rhodobacter sphaeroides*: evidence of rapid evolution of chromosome, *Journal of Bacteriology*, 189 (5): 1914-1921.

Çakar, Z. P., Turanlı-Yıldız, B., Alkım, C., Yılmaz, C. (2012). Evolutionary engineering of *Saccharomyces cerevisiae* for improved industrially important properties, *FEMS Yeast Research*, 12 (2): 171-182.

Çetin, D., Gündüz, U., Eroğlu, İ., Yücel, M., Lemi, T. (2006). Poly-β-hydroxybutyrate accumulation and releasing by hydrogen producing bacteria, *Rhodobacter sphaeroides* O.U.001. A transmission electron microscopic study, *African Journal of Biotechnology*, 5 (22): 2069-2072.

Fabela, S., Domenzain, C., De la Mora, J., Osorio, A., Ramirez-Cabrera, V., Poggio, S., Dreyfus, G., Camarena, L. (2013). A distant homologue of the FlgT protein interacts with MotB and FliL and is essential for flagellar rotation in *Rhodobacter sphaeroides*, *Journal of Bacteriology*, 195 (23): 5285-5296

Feris, K., Ramsey, P., Frazar, C., Moore, J. N., Gannon J. E., Holben, W. E. (2003). Differences in hyporheic-zone microbial community structure

along a heavy-metal contamination gradient, *Applied and Environmental Microbiology*, 69 (9): 5563-5573.

Gabrielyan, L., Sargsyan, H., Hakobyan, L., Trchounian, A. (2014). Regulation of hydrogen photoproduction in *Rhodobacter sphaeroides* batch culture by external oxidizers and reducers, *Applied Energy*, 131: 20-25.

Glaeser, J. and Klug, G. (2005). Photo-oxidative stress in *Rhodobacter sphaeroides*: Protective role of carotenoids and expression of selected genes, *Microbiology*, 151: 1927-1938.

Giotta, L., Agostiano, A., Italiano, F., Milano, F., Trotta, M. (2006). Heavy metal ion influence on the photosynthetic growth of *Rhodobacter sphaeroides*, 62 (9): 1490-1499.

Hunter, C. N., Hundle, B. S., Hearst, J. E., Lang, H. P., Gardiner, A. T., Takaichi, S., Cogdell, R. J. (1994). Introduction of new carotenoids into the bacterial photosynthetic apparatus by combining the carotenoid biosynthetic pathways of *Erwinia herbicola* and *Rhodobacter sphaeroides*, *Journal of Bacteriology*, 176 (12): 3692.

Imam, S., Yilmaz, S., Sohmen, U., Gorzalski, A. S., Reed, J. L., Noguera, D. R., Donohue, T. J. (2011). iRsp1095: A genome-scale reconstruction of the *Rhodobacter sphaeroides* metabolic network, *BMC Systems Biology*, 5:116.

Italiano, F., Pisani, F., De Leo, F., Ceci, L., Gallerani, R., Zolla, L., Rinalducci, S., Giotta, L., Milano, F., Agostiano, A., Trotta, M. (2008). Effect of cobalt ions on the soluble proteome of a *Rhodobacter sphaeroides* carotenoidless mutant, *14th International Congress on Photosynthesis*, 1479-1483.

Italiano, F., Buccolieri, A., Giotta, L., Agostiano A., Valli L., Milano, F., Trotta, M. (2009). Response of the carotenoidless mutant *Rhodobacter sphaeroides* growing cells to cobalt and nickel exposure, *International Biodeterioration & Biodegradation*, 63: 948-957.

Ivanovskii, R. N., Mil'ko, E. S., Mil'ko, D. M. (2013). Isolation of the phase variants of the purple photosynthetic bacterium *Rhodobacter sphaeroides* and investigation of their molecular, physiological, biochemical, and morphological characteristics, *Microbiologiya*, 82 (2): 169–175.

Kamer, H. (2015). Evolutionary engineering of *Rhodobacter sphaeroides* under selective $CoCl_2$ stress, M.Sc. thesis, Institute of Science and Technology, Istanbul Technical University.

Karls, R. K., Brooks, J., Rossmeissl, P., Luedke, J., Donohue, T. J. (1998). Metabolic roles of a *Rhodobacter sphaeroides* member of the σ^{32} family, *Journal of Bacteriology*, 180 (1): 10-19.

Kiley, J. P. and Kaplan, S. (1988). Molecular Genetics of Photosynthetic membrane biosynthesis in *Rhodobacter sphaeroides*, *Microbiological Reviews*, 52 (1): 50-69.

Lang, H. P. and Hunter, C. N. (1994). The relationship between carotenoid biosynthesis and the assembly of the light-harvesting LH2 complex in *Rhodobacter sphaeroides*, *Biochemical Journal*, 298: 197-205.

Levin, B. D., Pitt, L., Love, M. (2004). Biohydrogen production: prospects and limitations to practical application, *International Journal of Hydrogen Energy*, 29: 173–185.

Mil'ko, E. S., Krasil'nikova, E. N., Keppen, O. I., Lebedeva, N. V., Ivanovsky R. N. (2014). Metabolism of the Phase Variants of the Phototrophic Bacterium *Rhodobacter sphaeroides*, *Microbiology*, 83 (4): 411-415.

Molyneux, S. L., Young, J. M., Florkowski, C. M., Lever, M., George P. M. (2008). Coenzyme Q10: Is there a clinical role and a case for measurement?, *Clinical Biochemist Reviews*, 29 (2): 71-82.

Moore, M. D. and Kaplan, S. (1992). Identification of Intrinsic High-Level Resistance to Rare-Earth Oxides and Oxyanions in Members of the Class Proteobacteria: Characterization of Tellurite, Selenite, and Rhodium Sesquioxide Reduction in *Rhodobacter sphaeroides*, *Journal of Bacteriology*, 174 (5): 1505-1514.

Mulvaney, R. L., Khan, S. A., Mulvaney, C. S. (1997). Nitrogen fertilizers promote denitrification, *Biology and Fertility of Soils*, 24: 221-220.

Nepple, B. B. and Bachofen R. (1997). Induction of stress proteins in phototrophic bacterium *Rhodobacter sphaeroides*, *FEMS Microbiology Letters*, 153: 173-180.

Nies, D.H. and Silver, S. (1995). Ion efflux systems involved in bacterial metal resistances, *Journal of Industrial Microbiology*, 14 (2): 186-99.

Nies, D. H. (1999). Microbial heavy-metal resistance, *Applied Microbiology and Biotechnology*, 51: 730-750.

Panwichian, S., Kantachote, D., Wittayaweerasak, B. , Mallavarapu, M. (2011). Removal of heavy metals by exopolymeric substances produced by resistant purple nonsulfur bacteria isolated from contaminated shrimp ponds, *Electronic Journal of Biotechnology*, 14 (4).

Pisani, F., Italiano F., De Leo, F., Gallerani, R., Rinalducci, S., Zolla, L., Agostiano, A., Ceci, L. R., Trotta, M. (2009). Soluble proteome investigation of cobalt effect on the carotenoidless mutant of *Rhodobacter sphaeroides*, *Journal of Applied Microbiology*, 106: 338-349.

Sabaty, M., Gagnon, J., Verméglio, A. (1994). Induction by nitrate of cytoplasmic and periplasmic proteins in the photodenitrifier *Rhodobacter sphaeroides* forma sp. *denitrificans* under anaerobic or aerobic condition, *Archieves of Microbiology*, 162: 335-343.

Sandaa, R. A., Torsvik, V., Enger, Ò., Daae, F. L., Castberg, T., Hahn, D. (1999). Analysis of bacterial communities in heavy metal-contaminated soils at different levels of resolution, *FEMS Microbiology Ecology*, 30: 237-251.

Sasaki, K., Watanabe, M., Tanaka T., Tanaka T. (2002). Biosynthesis, biotechnological production and applications of 5-aminolevulinic acid, *Applied Microbiology and Biotechnology*, 58 (1): 23-29.

Šlouf, V., Chábera, P., Olsen, J. D., Martin, E. C., Qian, P., Hunter, C. N., Polívka, T. (2012). Photoprotection in a purple phototrophic bacterium mediated by oxygen-dependent alteration of carotenoid excited-state properties, *Proceedings of the National Academy of Sciences of the United States of America*, 109 (22): 8570-8575.

Slovak, P. M., Wadhams, G. H., Armitage, J. P. (2005). Localization of MreB in *Rhodobacter sphaeroides* under conditions causing changes in cell shape and membrane structure, *Journal of Bacteriology*, 187 (1): 54-64.

Stephen, J. R., Chang Y. J., Macnaughton, S. J., Kowalchuk, G. A., Leung, K. T., Flemming, C. A., White, D. C. (1999). Effect of toxic metals on indigenous soil b-subgroup proteobacterium ammonia oxidizer community structure and protection against toxicity by inoculated metal resistant bacteria, *Applied and Environmental Microbiology*, 65 (1): 95-101.

Suzuki, T., Tsygankov A. A., Miyake, J., Tokiwa, Y., Asada Y. (1995). Accumulation of poly-(hydroxybutyrate) by a non-sulfur photosynthetic bacterium, *Rhodobacter sphaeroides* RV at different pH, *Biotechnology Letters*, 17 (4): 395-400.

Takaichi, S., Jung, D. O., Madigan, T. M. (2001). Accumulation of unusual carotenoids in the spheroidene pathway, demethylspheroidene and demethylspheroidenone, in an alkaliphilic purple nonsulfur bacterium *Rhodobaca bogoriensis*, *Photosynthesis Research*, 67 (3): 207-214.

Tao, Y., Liu, D., Yan, X., Zhou, Z., Lee, K. J., Yang, C. (2012). Network identification and flux quantification of glucose metabolism in *Rhodobacter sphaeroides* under photoheterotrophic H_2- producing conditions, *Journal of Bacteriology*, 194 (2): 274-283.

Tosques, I. E., Shi, J., Shapleigh, J. P. (1996). Cloning and characterization of *nnrR*, whose product is required for the expression of proteins involved in nitric oxide metabolism in *Rhodobacter sphaeroides* 2.4.3., *Journal of Bacteriology*, 178 (16): 4958-4964.

Tosques, I. E., Shi, J., Shapleigh, J. P. (1997). Characterization and regulation of the gene encoding nitrite reductase in *Rhodobacter sphaeroides* 2.4.3., *Journal of Bacteriology*, 179 (4): 1090-1095.

Vermeglio, A., Joliot, P. (1999). The photosynthetic apparatus of *Rhodobacter sphaeroides* , *Trends in Microbiology*, 7 (11): 435-440.

Yang, M. K., Lin, Y. C., Shen C. H. (2006). Identification of two gene loci involved in poly-betahydroxybutyrate production in *Rhodobacter sphaeroides* FJ1, *Journal of Microbiology, Immunology and Infection*, 39: 18-27.

Yeliseev, A. A. and Kaplan, S. (1997). Anaerobic carotenoid biosynthesis in *Rhodobacter sphaeroides* 2.4.1: H_20 is a source of oxygen for the 1-methoxy group of spheroidene but not for the 2-oxo group of spheroidenone, *FEBS Letters*, 403: 10-14.

Yen, H. W., Shih, T. Y. (2009). Coenzyme Q_{10} production by *Rhodobacter sphaeroides* in stirred tank and in airlift bioreactor, *Bioprocess and Biosystems Engineering*, 32 (6): 711-717.

Zahiri, H. S., Noghabi, K. A., Shin, Y. C. (2006). Biochemical characterization of the decaprenyl diphosphate synthase of *Rhodobacter sphaeroides* for coenzyme Q_{10} production, *Applied Microbiology and Biotechnology*, 73 (4): 796-806.

Zeller, T., Moskvin, O.V., Li K., Klug, G., Gomelsky, M. (2005). Transcriptome and physiological responses to hydrogen peroxide of the facultatively phototrophic Bacterium *Rhodobacter sphaeroides*, *Journal of Bacteriology*, 187 (21): 7232-7242.

6. CURRICULUM VITAE

Name Surname: Güneş ATAY

Place and Date of Birth: Istanbul / 06.03.1990

E-Mail: gunesatay00@gmail.com

B.Sc: Ege University (2008-2012), Biochemistry

M.Sc: Istanbul Technical University (2012-), Molecular Biology-Genetics & Biotechnology